arXiv:0906.4298v1 [nucl-th] 23 Jun 2009

Single Cooper pair transfer in stable and in exotic nuclei

G. Potel[a,b], B. F. Bayman[c], F. Barranco[d], E. Vigezzi[a], R. A. Broglia[*,a,b,e]

[a] *INFN, Sezione di Milano Via Celoria 16, 20133 Milano, Italy.*
[b] *Dipartimento di Fisica, Università di Milano, Via Celoria 16, 20133 Milano, Italy.*
[c] *School of Physics and Astronomy, University of Minnesota, Minneapolis, Minnesota 55455*
[d] *Departamento de Fisica Aplicada III, Universidad de Sevilla, Escuela Superior de Ingenieros, Sevilla, 41092 Camino de los Descubrimientos s/n, Spain.*
[e] *The Niels Bohr Institute, University of Copenhagen, Blegdamsvej 17, 2100 Copenhagen Ø, Denmark.*

Abstract

Arguably, the greatest achievement of many–body physics in the fifties was that of developing the tools for a complete description and a thorough understanding of superconductivity in metals. At the basis of it one finds BCS theory and the Josephson effect. The first recognized the central role played by the appearance of a macroscopic coherent field usually viewed as a condensate of strongly overlapping Cooper pairs, the quasiparticle vacuum. The second made it clear that a true gap is not essential for such a state of matter to exist, but rather a finite expectation value of the pair field. Consequently, the specific probe to study the superconducting state is Cooper pair tunneling.

As forcefully stated by Phil Anderson, tunneling experiments not only gave a measurable physical reality to the phase of the pair wavefunction –the Josephson current is phase–dependent–, they also (essentially) eliminated any uncertainty concerning the mechanisms of electron–electron and electron–phonon interactions which are at the basis of the origin of pairing in metals. This also meant the end of superconductivity as a wide open, speculative field and the beginning of a thoroughly quantitative "exact" era, with uncertainties below the 10% level.

From this vantage point of view it is not difficult to argue that important progress in the understanding of pairing in atomic nuclei –a subject of research started about the time of the BCS papers, but still far from having entered the "exact" era– may arise from the systematic study of two–particle transfer reactions starting from drip line, exotic, halo nuclei (like for example ^{11}Li and ^{12}Be), stabilized by the pairing correlations associated with a single Cooper pair, and

---

[*] Corresponding author. Tel:(+39)3388959875

Email addresses: `gregory.potel@mi.infn.it` (G. Potel), `bayman@physics.umn.edu` (B. F. Bayman), `barranco@us.es` (F. Barranco), `Enrico.Vigezzi@mi.infn.it` (E. Vigezzi), `Ricardo.Broglia@mi.infn.it` (R. A. Broglia)

gradually proceeding to the case of many (but still few)–Cooper pair systems like e.g. Sn–isotopes.

Time seems to be ripe for such a study, in keeping with the fact that one now knows how to describe microscopically the structure of these systems taking properly into account the interplay between bare and medium polarization (induced) pairing interaction between Cooper pair partners. Also, how to calculate the absolute two–particle transfer cross sections taking properly into account the full non–locality of the Cooper pairs (correlation length much larger than nuclear dimensions). While much of what is necessary to carry out the research program needed to enter the "exact" era of nuclear pairing making use of Cooper pair transfer is to a large extent known, a unified picture to implement it is still lacking.

To remedy this situation and eventually help at starting the new rigorous era of pairing studies in nuclei we discuss in this paper both the past and the present of two–nucleon transfer reactions, as well as try to foresee the near future of such studies in nuclei, induced by light as well as by heavy ion reactions.

Key words: pairing, finite many–body systems, two–nucleon transfer, tunneling
PACS: 25.40.Hs, 25.70.Hi, 74.20.Fg, 74.50.+r

1. Introduction

Two years ago physicists celebrated all around the world the 50th anniversary of BCS theory (Bardeen et al. (1957a), Bardeen et al. (1957b)). The success of such a theory is not so much, or better not only, the fact that it provided the definitive solution to one of the most spectacular phenomenon of all of physics – permanent (super)currents estimated to be stable for $10^{10^{10}}$ y– , but that it provided a paradigm for the phenomenon of spontaneous symmetry breaking and associated emergent properties (Anderson (1994)). This paradigm demonstrated to be successful in a variety of fields starting from solid state physics and extending to nuclear and particle physics, field theory and astrophysics.

Bohr, Mottelson and Pines developed, in the summer of 1957 (Bohr et al. (1958)), the basis of the theory of nuclear superfluidity which was eventually applied to the description of the nuclear structure, in particular to the calculation of the moment of inertia of deformed nuclei (Belyaev (1959)) and of quadrupole vibrations of spherical and of deformed nuclei (Bayman (1960a), Bayman (1960b), Kisslinger and Sorensen (1963), Bès (1963), Soloviev (1965), Bès and Sorensen (1969), see also (Ring and Schuck (1980)).

In subsequent years the consequences of the phenomenon of spontaneous breaking of gauge symmetry in nuclei was investigated. In keeping with the fact that generalized rigidity in gauge space constitutes the most basic of the associated emergent properties, two-particle transfer reactions are the specific probe to study the individual members of the associated pairing rotational and vibrational bands (Bohr (1964), Bès and Broglia (1966), Bohr and Mottelson (1975)), a feat which is totally out of reach in the case of tunneling between two superconductors in condensed matter (Josephson (1962)).

Due to the fact that the number of Cooper pairs participating in the nuclear condensate is small, one can study the phenomenon in terms of specific orbitals, some of which play an essential role in the transfer process (hot orbitals). For this purpose, absolute differential cross sections $d\sigma((A+a) \longrightarrow ((A+2)+(a-2)))/d\Omega$ must be measured as well as calculated (Yoshida (1962), Ascuitto et al. (1971), Glendenning (1963), Glendenning (1965), Glendenning (1968), Bjerregaard et al. (1966), Bayman (1971), Broglia et al. (1973), Broglia (1973), Hashimoto and Kawai (1978), Charlton (1976), Takemasa et al. (1979), Bayman and Chen (1982), Maglione et al. (1985), Igarashi et al. (1991)).

Much have been learned concerning pairing correlations in many–body systems by studying metallic grains at low temperatures (c.f. Farine and Schuck (2002), Farine and Schuck (1999), Perenboom et al. (1981), Anderson (1959), Lauritzen et al. (1993)) as well as by using semiclassical approximations (see e.g. Bengtsson and Schuck (1980), Kucharek et al. (1989), Broglia and Winther (2004) and references therein). New perspectives in the study of pairing correlations among nucleons are being opened through the study of exotic nuclei lying along the drip lines in general (Dobaczewski et al. (1996)), and of halo nuclei in particular. Insight into these systems through two-particle transfer reactions (Lenske and Schrieder (1998), Khan et al. (2004)), and also with high–energy knock–out reactions (Hansen and Tostevin (2003), Tostevin et al. (2004), Tostevin (2007)) is expected to shed light on the relative role the bare and the induced pairing interactions play in regions of very low density (see e.g. Fig. 2 of Richter (1993), and Fig. 3.21 of Heyde (1998), Broglia, private communication), but also on BEC of dilute Fermi gases (see e.g. Pethick and Smith (2008) and references therein), where single–pair transfer experiments are not possible.

The two–particle transfer reactions carried out at Ganil (Chatterjee et al. (2008), Keeley et al. (2007)), TRIUMF (Tanihata et al. (2008)) and Dubna (Golovkov et al. (2008)) as well as those in the planning stage which eventually will be studied, are expected to expand the frontiers of our knowledge concerning quasispin pair alignment (Anderson (1958)) and dynamical pair correlations in nuclei to an extent unthinkable only few years ago.

In keeping with the insight provided by the results of tunneling experiments concerning pairing in metals(Anderson (1969), Josephson (1969), Scalapino (1969), Mc Millan and Rowell (1969), Esaki (1973), Giaver (1973), Josephson (1973), Nambu (1991)), much is expected to be learned concerning the effective, strongly renormalized interaction responsible for the presence of Cooper pairs in the nuclear medium, by measuring the two–particle strength functions (energy dependence of the tunneling phenomenon).

To be prepared to meet the challenge we remind, in the present paper, the basic experimental findings as well as the theory which is at the basis of the unified description of nuclear structure and two–particle transfer reactions developed through the years, and draw the grand picture which is slowly emerging from the exploration of pairing in finite many–body systems, to the limit of a single Cooper pair.

2. Basic experimental findings

In this section we present some of the basic results obtained probing the atomic nucleus through two–particle transfer reactions. The information arising from both light and heavy ion reactions is briefly summarized. The bias towards light ion reactions reflects the experimental situation.

Under the influence of Coulomb and of nuclear external fields which change angular momentum by two units (or by studying the γ–decay of compound nuclei with high angular momentum content), nuclei respond collectively in terms of rotations and of vibration, as testified by spectra of the type shown in Figs. 1 and 2. Not only the spectrum displays a simple behavior with angular momentum as shown in these figures (quadratic in the first case, linear in the second), but also a large enhancement of the quadrupole matrix elements (as measured in terms of single particle units) connecting two successive states.

In keeping with the fact that, as a rule, physical theories are based on the analogy which one can establish between unknown things and simple phenomena (Weil (1966), Weil (1999)) is that the results displayed in Figs. 3 and 4 are to be considered compared with those shown in Figs. 1 and 2. From this analogy it emerges that two–particle transfer data provide the experimental confirmation of the soundness of the concepts of pairing rotational and pairing vibrational bands (Bès and Broglia (1966)), see also Ring and Schuck (1980), Ch. 11, in particular p. 449. Measuring the associated cross sections in terms of pure two-particle configurations – equivalent to Weisskopf units in the case of Coulomb excitation and inelastic scattering– one obtains values of $\approx 5-10$ and $\approx 25-50$ in the case of pairing vibrational and pairing rotational excitations respectively (Broglia et al. (1972), Broglia et al. (1978)) (cf. Figs. 3, 4, 5 and 6).

While two-particle transfer reactions induced by light ions at energies of $\approx 5-10$ MeV/nucleon, like (t,p) reactions, provide detailed spectroscopic information in terms of highly structured L–dependent angular distributions associated with the excitation of *single nuclear states* (see below), the two neutrons in the triton do not display the same correlations as a Cooper pair in nuclei. Among other things, this is the origin of the overlap factor $\Omega_n \lesssim 1$ appearing in the two particle form factor (Glendenning (1968), Broglia et al. (1973)). This limitation can be overcome by means of two–particle reactions induced by heavy ions. By appropriately choosing target and projectile one can prepare the Cooper pair to be transferred to have the desired properties, and tune the two-particle process to be the specific tool to probe nuclear pairing correlations.

Arguably, the main drawback displayed by heavy ion reactions when used for nuclear structure studies is connected with the non–specificity of the angular distributions (bell shaped), associated with the very short wavelength of the relative motion of the two ions (semiclassical behavior) (Broglia and Winther (2004)). Transfer essentially occurs at grazing conditions. For large relative distances the exponential decay of the Cooper pair wavefunction prevents transfer from occurring. At small distances many channels open up and the flux of the elastic and quasielastic channels is drained out (strong absorption). Thus the uncharacteristic shape of the angular distributions.

The second major drawback of heavy ion reactions is the difficulty to observe *single final states*. The large Coulomb and hadronic fields induced by the mutual interaction of the two colliding ions makes transfer from and to inelastic and Coulomb excited states quite likely.

In any case, experimental ingenuity combined with new technical developments have made it possible to obtain precious information from these reactions.

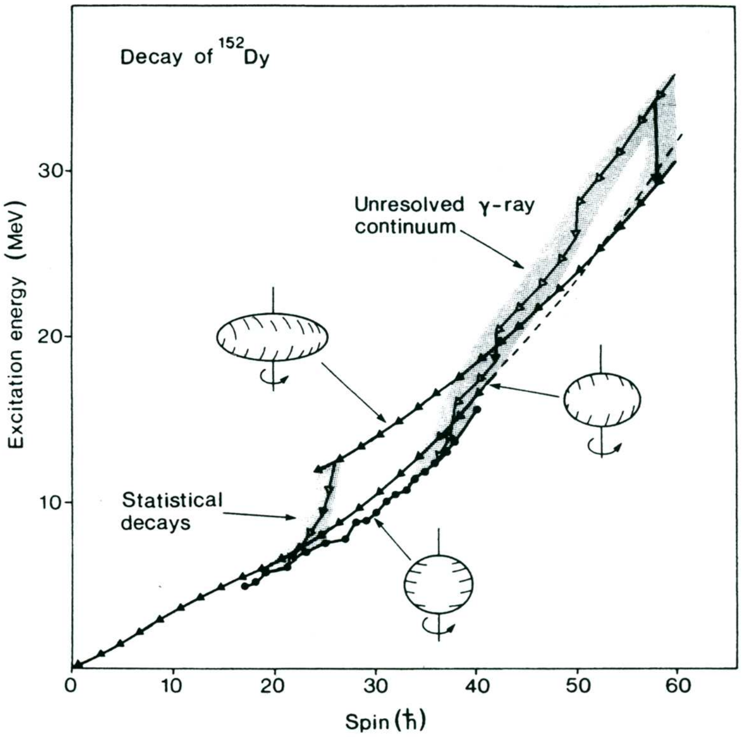

Figure 1: A schematic representation of the proposed γ–ray decay paths from a high–spin entry point in ^{152}Dy. The major initial decay flow occurs mainly via $E2$ transitions in the unresolved γ–ray continuum and reaches the oblate yrast structure between spins $30\hbar$ and $40\hbar$. A small 1% branch feeds the superdeformed band, which is assumed to become yrast at spin $50\hbar$– $55\hbar$. The de–excitation of the superdeformed band around $26\hbar$ occurs when the band is 3–5 MeV above yrast, and a statistical type of decay takes into the oblate states between spin $19\hbar$ and $20\hbar$. The diagram also shows the low–deformation prolate band (after Nolan and Twin (1988))

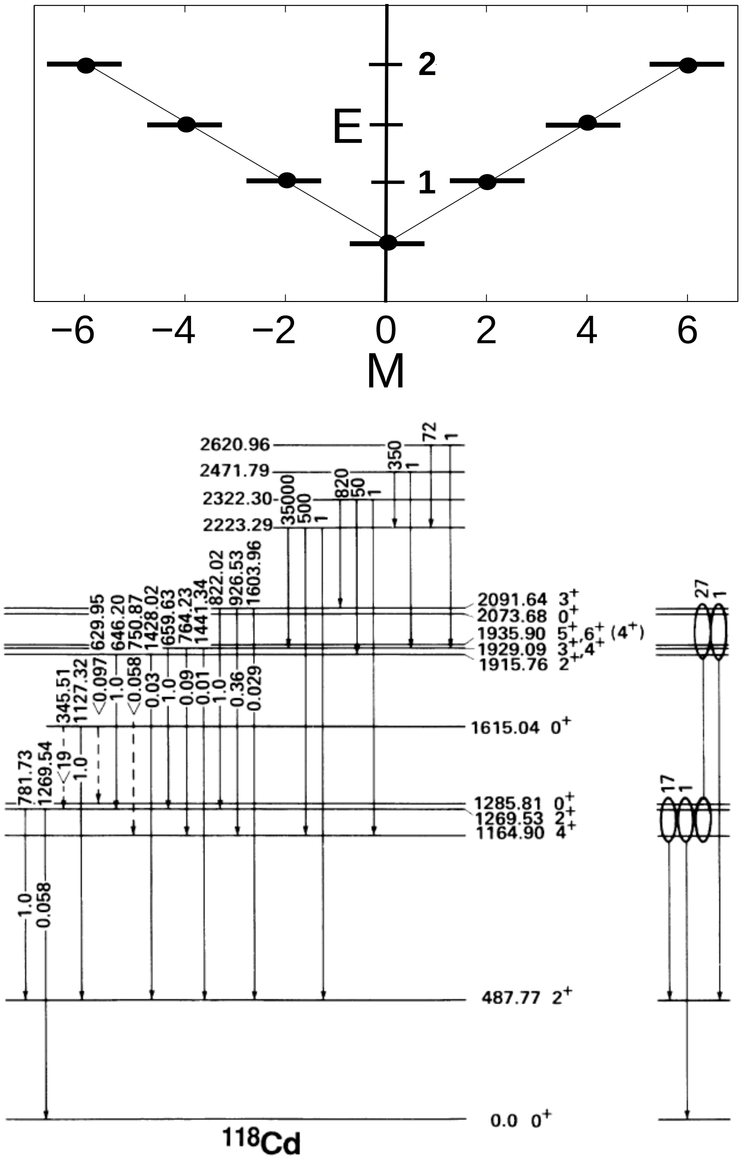

Figure 2: Partial level scheme of ^{118}Cd associated with the quadrupole vibrational band containing up to three phonons (After Aprahamian et al. (1987)). In the inset (upper framed picture), a schematic representation of the energy spectrum of harmonic quadrupole vibrations as a function of the magnetic quantum number M is shown.

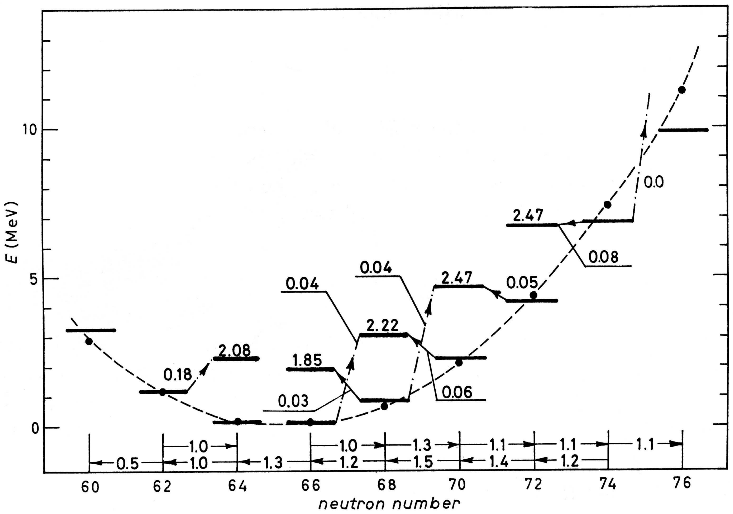

Figure 3: **Pairing rotational band in even Sn–nuclei**. Experimental energies of the $J^\pi = 0^+$ states of the even Sn isotopes. The heavy drawn lines represent the values of the expression $E = -B(S_n) + E_{exc} + 8.58N + 45.3$ (MeV), where the binding energies $B(A)$ (in MeV) are taken from Wapstra and Gove (1971). The dashed line represents the parabola $0.10(N - 65.4)^2$. Also displayed is the excited pairing rotational band associated with the pairing vibrational mode. In all cases where more than one $J^\pi = 0^+$ state has been excited below 3 MeV in two-neutron transfer processes, the energy $\sum_i \sigma(0_i)E(0_i^+)/\sum_i \sigma(0_i^+)$ of the centroid is quoted, as well as the corresponding cross section $\sum_i \sigma(0_i^+)$. The quantity $\sigma(0_i^+)$ is the relative cross-section with respect to the ground state cross-section. The numbers along the abscissa are the ground-state (p, t) and (t, p) cross-sections normalized to the ^{116}Sn $\leftrightarrow ^{118}$Sn(gs) cross-section. The (t, p) and (p, t) data utilizing in constructing this figure were taken from refs. (Bjerregaard et al. (1968), Bjerregaard et al. (1969), Flynn et al. (1970), Fleming et al. (1970)). (After Bès and Broglia (1977), and Brink and Broglia (2005)).

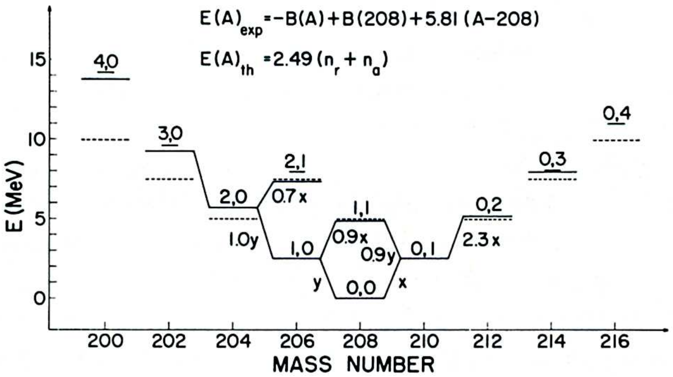

Figure 4: **Pairing vibrations in even Pb nuclei**. The ground state binding energies $B(A)$ were used to evaluate the energies $E(A)_{\text{exp}}$ as defined in the figure. The constant in front of the linear term, was determined so that $E(210)_{\text{exp}} = E(206)_{\text{exp}}$. Excited states were placed at the measured excitation energy above the relevant ground state. Experimental levels are shown as full lines, states predicted from the harmonic vibrational model are shown as broken lines at an energy $E(A)_{\text{th}}$, whereas the short lines indicate the level position including a phenomenological anharmonic term. The two–particle transfer cross sections are given in terms of the pair–addition and pair–substraction cross sections denoted x and y respectively (After Brink and Broglia (2005))

In particular, based on the experience with light projectiles, an enhancement factor (EF) due to pairing correlations for two–nucleon transfer between heavy nuclei can be defined (von Oertzen and Vitturi (2001), Wu et al. (1990)). This quantity is particularly simple to be extracted from the experimental data, provided the single–nucleon transfer probability P_{1n} is used as the appropriate unit: $P_{2n} = EFP_{1n}^2$ (see Figs. 5, 6). In the independent particle picture this factor is just unity. Values of $EF \gg 1$ imply correlations among pairs of nucleons transferred between the two heavy ions (see also Broglia et al. (1972)).

Using particle–γ coincidence techniques, well defined binary channels with final states of known quantum numbers can be selected. One- and two-nucleon transfer cross sections in the collision of ^{206}Pb+^{118}Sn have been measured in this way (von Oertzen and Vitturi (2001)). Large enhancement factors have been observed, suggesting a strong contribution arising from superfluid pair transfer, as predicted (Dietrich et al. (1971), Dietrich and Hara (1973), Broglia et al. (1978), see also Lotti et al. (1991)).

3. The Josephson effect

It is well–known that the phase of the wavefunction and the number of nucleons are conjugated variables. Gauge invariance, that is, invariance under phase changes, implies particle number conservation in the same way in which rotational

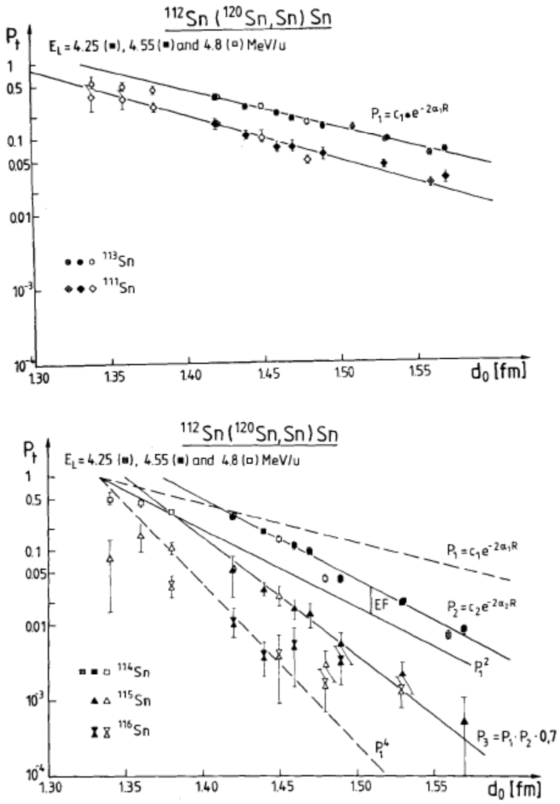

Figure 5: Measured transfer probabilities (transfer function) for one–(*top*) up to four–neutron (*bottom*) transfer in the system ^{112}Sn+^{120}Sn, as a function of the overlap parameter $d_0 = R_{min}/(A_a^{1/3} + A_A^{1/3})$, R_{min} being extracted in a unique way from the reaction angle for reactions at energies below or close to the Coulomb barrier E_c. Data at three energies (4.25, 4.55 and 4.8 MeV/nucleon) are shown. After Wu et al. (1990).

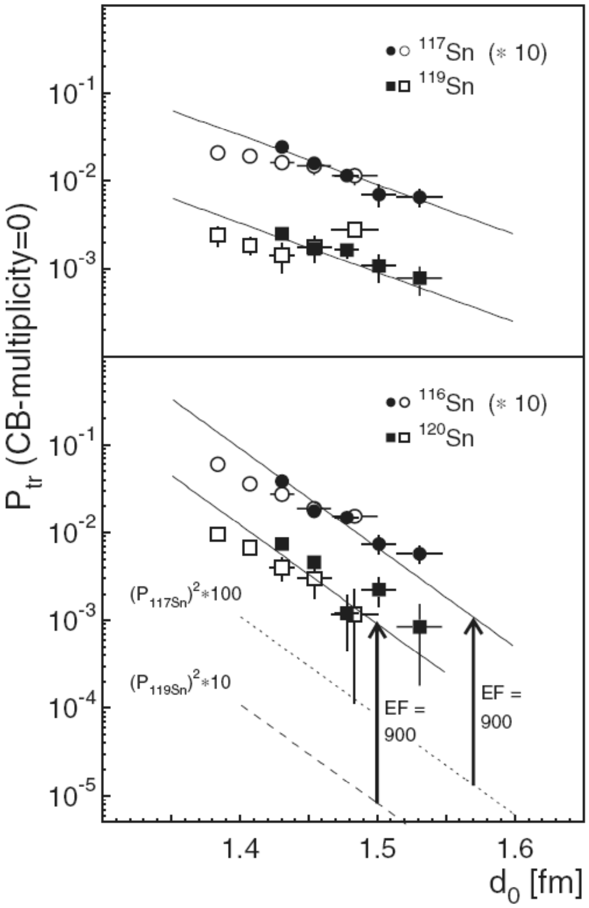

Figure 6: One–neutron (above) and two–neutron (lower part) transfer probabilities in ^{206}Pb+^{118}Sn collisions as a function of the overlap parameter d_0 measured in particle–γ coincidences, with the Crystal Ball in anticoincidence. Filled symbols refer to a bombarding energy of 5.14 MeV/u, and open symbols to 5.32 MeV/u. The nuclei are identified by their characteristic γ–transitions. The squared value of the measured $1n$–transition probabilities are drawn as broken lines in the lower part. The shift between the squared of the $1n$–transfer probability and the corresponding $2n$–transfer probability defines the enhancement factor *EF* (after von Oertzen and Vitturi (2001)). Values of the order of 10^3 are observed in keeping with the fact that both target and projectile can be viewed as superfluid nuclei, their respective gs → gs transitions being enhanced by a factor of the order 25–30 as mentioned in the text (Broglia et al. (1978)).

invariance implies angular momentum conservation. A simple demonstration is the following: take a wavefunction with a fixed number of particles,

$$\Psi = a_1^\dagger a_2^\dagger \cdots a_N^\dagger |0\rangle. \tag{1}$$

Multiply the field operator by a phase factor

$$\Psi' = (e^{i\phi} a_1^\dagger)(e^{i\phi} a_2^\dagger)\cdots(e^{i\phi} a_N^\dagger)|0\rangle = e^{iN\phi}\Psi. \tag{2}$$

Clearly $-i\partial/\partial\phi \ \Psi' = N\Psi'$. Thus

$$\hat{N} \equiv -i\frac{\partial}{\partial\phi}, \tag{3a}$$

$$i\frac{\partial}{\partial N} \equiv \hat{\phi}, \tag{3b}$$

and

$$[\hat{\phi}, \hat{N}] = i. \tag{4}$$

Correspondingly, there is an uncertainty principle $\Delta N \Delta\phi = 1$. In keeping with this fact, the BCS solution of the pairing Hamiltonian

$$|BCS\rangle = \prod_{\nu>0}(U_\nu + V_\nu e^{2i\phi} a_\nu^\dagger a_{\bar{\nu}}^\dagger)|0\rangle, \tag{5}$$

violates gauge invariance, and $|BCS\rangle$ describes a deformed state which defines a privileged orientation in gauge space (see Fig. 7). The magnitude of the deformation is measured by $e^{i\phi}\alpha_0 = \langle BCS|P^\dagger|BCS\rangle$, where $P^\dagger = e^{2i\phi}\sum_{\nu>0} a_\nu^\dagger a_{\bar{\nu}}^\dagger$ is the pair creation operator. Of notice that the $|BCS\rangle$ state can be viewed as a Bose–Einstein condensate of strongly overlapping Cooper pairs [1] . Josephson proposed in 1962 (Josephson (1962)) that there should be a contribution to the current through an insulating barrier between two superconductors which would behave like direct tunneling of condensed pairs at the Fermi surface from one superconductor to another.

---

[1] Quoting from Anderson (1969) commenting on the original BCS papers:

> . . . The idea that $P_\nu^\dagger = a_\nu^\dagger a_{\bar{\nu}}^\dagger$, the pair field, has a finite mean value is there, although oddly enough the statement that Bose–Einstein condensation of the pairs is irrelevant is also there. The reason is that at the time Bose–Einstein condensation was thought as, of necessity, a condensation of preexisting particles, not as the appearance of a macroscopic coherent field, as we should understand it . . .

Each of the superconductors can be thought as a rotor in gauge space (see Fig.7), weakly coupled to each other. The rate at which quanta are exchanged between the two superconductors is given by

$$\dot{N}_1 = (-\dot{N}_2) = \frac{i}{\hbar}[H_{coup}, N_1] = -\frac{1}{\hbar}\frac{\partial H_{coup}}{\partial \phi} \sim \sin(2(\phi_1 - \phi_2) + 2d), \tag{6}$$

where $H_{coup}(\sim P^{\dagger}P \sim e^{2i\phi_1}e^{2i\phi_2}e^{id}$, (see e.g. Brink and Broglia (2005), Appendix L) is the coupling Hamiltonian, d a phase related to the insulating barrier, while the rotational frequency of the rotors corresponds to the chemical potential of the superconductors ($\dot{\phi} = \frac{1}{\hbar}\partial H/\partial N = \frac{1}{\hbar}\lambda$). This means that if there is a difference in chemical potential between the two superconductors, which can be obtained by applying an external voltage, there will be an oscillating current running between the two superconductors (DC–Josephson effect). In terms of the voltage differential $V_1 - V_2$, one can write

$$\dot{N}_1 \sim \sin(\frac{2e}{\hbar}(V_1 - V_2)t + 2d). \tag{7}$$

This shows that the frequency of the oscillating current is determined by the applied voltage, the carriers having a charge $2e$.

One can thus subsume superconductivity (as well as superfluidity) under the general theory of spontaneous symmetry breaking phenomena if one lets the order parameter be $\delta = e^{2i\phi}\alpha_0$ (note that $\Delta = G\delta$; see however next section) and fix it in phase (ϕ) as well as in amplitude (α_0). Because of the long–range–order (10^2Å $\lesssim \xi = \hbar v_F/2\Delta \lesssim 10^3 - 10^4$Å), only a very small external force is necessary to fix the order parameter, and a direct observation of the phenomenon (experiments) can be carried out.

The importance of the Josephson effect, then, is that it provides an instrument which can act in a similar way as a clamp for a solid or a coercive field for a ferromagnet: it can pin down the (relative) gauge phase through correlated pair transfer, the specific probe of dynamic (pairing vibrations) and static (pairing rotations) spontaneous symmetry violation of gauge invariance (Anderson (1984)).

Within this context we take issue at the otherwise superb monograph Quantum Liquids of Tony Leggett (Oxford University Press, Oxford (2007)). In the introduction Professor Leggett writes

> . . . it is neither necessary nor desirable to introduce the idea of "spontaneous broken $U(1)$ symmetry", that is to consider (alleged) quantum superpositions of states containing different total numbers of particles; rather, I take from the start the viewpoint first enunciated explicitly by C.N. Yang, namely that one should simply think, in non–technical terms, about the behaviour of single particles, or pairs of particles, averaged over the behaviour of all others . . .

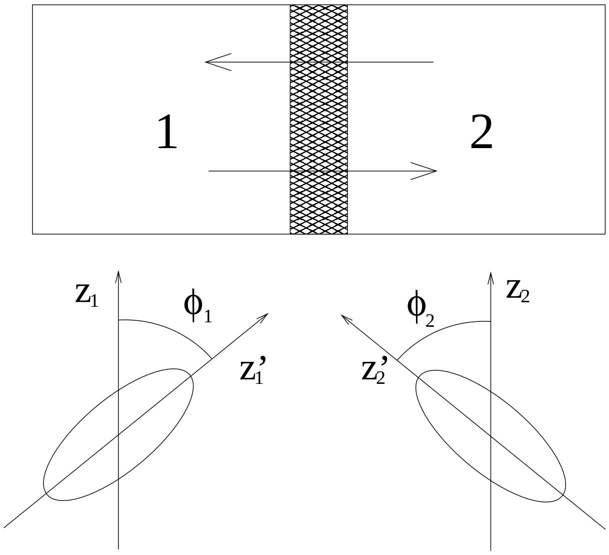

Figure 7: Schematic representation of a Josephson junction

In fact, it is this non technical thinking which tells us that in most nuclei, nucleons feel the average effect of all other nucleons in terms of a potential displaying a finite average value of the quadrupole operator (Nilsson potential). Rotational bands (see Fig. 1) observed up to the limits of the centrifugal force which the nuclear liquid drop can sustain ($I \approx 60\hbar$) before fissioning, are some of the clearest evidence of the physical insight provided by such a picture. J. P. Elliott correctly argued, based on the results of his SU_3 model that he could get rotational bands without the need of a deformed rotating body (Elliot (1958a), Elliot (1958b), Elliot (1962), Elliot and Harvey (1963), Broglia and Maqueda (1966)). This is in principle correct, and applies also to the Interacting Boson Model (Iachello and Arima (1988), see also Bès and Broglia (1979)) as well as to full shell model diagonalizations (see e.g Rowe (1970) and references therein).

The power of the spontaneous symmetry breaking picture (see also Laughlin (2006)) is that it can be used to systematically predict the collective degrees of freedom of many–body systems, (in particular of finite many–body systems of which the atomic nucleus is a much studied example) as well as to individuate the specific experimental probes to study them. The associated steps to be taken to implement this strategy are: a) find the variety of mean (constrained) fields which violate each of the different symmetries of the nuclear Hamiltonian (rotational, specular (parity), Galilean,isospin, gauge, etc.) b) restore symmetry by averaging out the alignment –privileged orientation in the different (abstract) spaces– thus giving rise to the variety of nuclear collective motions and associated generalized rigidities. Examples of such an approach are given by: 1) quadrupole and octupole rotations and vibrations (degeneracy of positive and negative parity states), 2) dipole and 3) Gamow–Teller giant resonances, 4) pairing rotational (and vibrational) bands [2], etc (see e.g. Anderson (1964), Anderson (1972), Anderson (1958), Bohr and Mottelson (1975), Bès and Broglia (1966)) .

The ground state wavefunctions associated with the variety of mean fields determined in step a) display a finite value of the: 1) quadrupole– and octupole–, 2) center of mass–, 3)isospin– and 4) pair transfer–operator. These operators identify the experiments which specifically excite the corresponding collective nuclear modes, e.g. quadrupole or octupole Coulomb excitation in case 1) and two–particle transfer in case 4).

The ratio between the energy of the pairing rotational transitions and of the intrinsic excitations (two–quasiparticle states) is much smaller than one (see Fig. 3), the ratio approaching zero as the phase space available to correlate the nucleons, and thus the number of particles approaches the thermodynamic limit. In this connection, it is illuminating to quote part of the discussion in Weinberg (1996) on spontaneously broken global symmetries, where he uses a chair as an example of a macroscopic system:

> spontaneous symmetry breaking actually occurs only for idealized systems that are infinitely large. The appearance of broken symmetry for a chair arises because it has a macroscopic moment of inertia $\Im$, so that its ground state is part of a tower of rotationally excited states whose energies are separated by only tiny amounts, of the order of $\hbar^2/\Im$. This gives the state vector of a chair an exquisite sensitivity to external perturbations; even very weak external fields will shift the energy much more than the energy difference of these rotational levels. In consequence, any rotationally asymmetric external field will cause the ground state or any other state of the chair with definite angular momentum rapidly to develop components with other angular

---

[2] In other words, spontaneous symmetry breaking (2nd order phase transitions) is always associated with emergent properties, in particular generalized rigidity. In fact, if one subjects a quadrupole deformed spheroidal nucleus to a torque, by pushing one pole (e.g. through an inelastic (p, p') experiment), the opposite pole will react immediately as if the system was a rigid body, although the strong force through which the nucleons interact does not propagate instantaneously. The moment of inertia of the associated rotational band (see Fig. 1) gives a measure of this rigidity. The same applies to the tilting of one side of a domain wall defining a spin domain in a paramagnetic metal below the Curie temperature. In the phenomenon of spontaneous symmetry breaking, certain elements play a central role. For example, high angular momentum (hot) orbitals in the case of deformed nuclei and magnetic impurities in the case of spin domains in paramagnetic metals. In fact, the polarization effects of hot orbitals in inducing nuclear deformation (as a rule intruder states) can be studied in model calculations by artificially changing the value of spin–orbit potential, or simply by mutating (substituting) artificially the hot orbital by a low l–orbital.

> momentum quantum numbers. The states of the chair that are relatively stable with respect to small external perturbations are not those with definite angular momentum quantum numbers, but rather those with a definite orientation, in which the rotational symmetry of the underlying theory is broken.

Weinberg's arguments are true for an atomic nucleus only when $N \to \infty$. Nevertheless, when one observes a (pairing) rotational band one can talk about a privileged direction in gauge space, which can be clamped down by the transfer of Cooper pairs from another superfluid nucleus in a heavy ion collision (Broglia and Winther (2004), von Oertzen and Vitturi (2001)). Because the total energy of the pairing rotational band is to be calculated in the laboratory frame, one has to add to the BCS Hamiltonian (Routhian) a term linear in N, equal to λN, and associated with the Coriolis term in gauge space (equivalent to e.g. ωI_x in the case of rotation of quadrupole deformed nuclei based on the intrinsic Nilsson state) to obtain it. The resulting energy of the pairing rotational band band $\lambda N + \hbar^2 N^2/2\Im$ contains thus a linear term in N and can consequently be viewed as the Anderson–Goldstone–Nambu mode (massless particle) of the associated gauge symmetry (Anderson (1958), Goldstone (1961), Nambu (1960), Broglia et al. (2000)).

Of notice is that the same concepts have been instrumental to shed light into other fields of physics (see e.g. Nambu and Jona-Lasinio (1961), Weise (1994), Klimt et al. (1990), Vogl et al. (1990), Vogl and Weise (1991)) and of natural research at large. In particular, into protein evolution and protein folding (Broglia (2002) and Broglia (2005)) and as a result, in the design of drugs which do not create resistance (Lo Cicero et al. (2007), Ferramosca et al. (2008), Broglia (2009a), Broglia (2009b), Broglia et al. (2009)). In this case the second order phase transition (Shakhnovich and Gutin (1993), Ramanathan and Shakhnovich (1994)) takes place under evolutionary pressure (lowering the temperature in sequence space) and results in the becoming of proteins taking place when the "hot" amino acids of the protein are set in place. The most conspicuous emergent property is folding which is at the basis of metabolism and thus life on earth. Mutation of amino acids on cold sites of a protein gives rise to families of proteins, the associated native states displaying very similar energies (stability). They can thus be viewed as members of a rotational band in sequence space. The 2nd order phase transition and thus one of its associated emergent properties, namely folding can be blocked by mutating hot amino acids (protein denaturation) (Broglia (2009b), cf. also footnote 2 of present section).

4. Successive and simultaneous transfer

Because the correlation length ξ of Cooper pairs in nuclei is of the order of 30–40 fm, that is much larger than nuclear dimension (5–7 fm), one expects that successive transfer of nucleon pairs does not destroy the correlation existing between the nucleons forming the Cooper pair and contribute similarly than simultaneous transfer to the associated two–particle transfer process . Furthermore, because the single–particle bases used to describe the transferred nucleons in entrance and exit channels are, as a rule, different, non–orthogonal contributions are also expected to be important in the calculation of the absolute two–particle transfer cross section. It is of notice that only in the case of the two center shell model basis, two–nucleon transfer is tantamount to successive transfer, aside from the (very small) simultaneous contribution arising from transfer through the pairing force.

Within this context one can mention that because the nuclear pairing interaction has matrix elements which are considerably smaller than the value of the single-particle potential $U(r)$ at grazing distances, the pair transfer potential looks much like $(U(r))^2$ (Broglia and Winther (2004)). Within this context it is of interest to mention the discussion between John Bardeen (Bardeen (1962)) and Brian Josephson (Josephson (1962)) (see also Cohen et al. (1962)) concerning the fact that in a Josephson junction the gap vanishes at the surface of the insulating dioxide layer and its implication concerning the possibility of a supercurrent across the barrier.

Let us remind that in Gorkov's formulation of superconductivity, $F(x,x')(\sim \sum_\nu U_\nu V_\nu \varphi_\nu(x)\varphi_{\bar{\nu}}(x')$ related to $\delta)$ is the amplitude for two electrons, at x and x', to belong to a Cooper pair. The gap function $\Delta(x)$ is given by $V(x)F(x,x)$, where $V(x)$ is a local two–body interaction at the point x. In the insulating barrier $V(x)$ is zero and thus $\Delta(x)$ is also zero. The crucial point, however, is that vanishing Δ does not imply vanishing F (expectation value of the pair transfer operator). In fact, $F(x,x')$ can have large amplitudes for electrons separated by distances $|x-x'|$ up to the coherence length. Hence, for barriers thin compared to that length, two electrons on opposite sides of the barrier can still be correlated. Consequently, the pair current is substantial, even if the mechanism of transfer is through a single–particle mean field potential.

While in the nuclear case one would not observe supercurrents, one can study the consequences of dynamic and static deformation in gauge space in terms of the tunneling (transfer) of single Cooper pairs. Particularly illustrative is the case of the exotic nucleus ^{11}Li, embodiment of a single Cooper pair system.

If neutrons are progressively added to a normal, stable nucleus lying along the stability valley, the Pauli principle forces them into states of higher momentum. When the core becomes neutron–saturated, the nucleus expels most of the wavefunction of the last neutrons outside to form a halo, which because of its large size can have lower momentum. In the case of ^{11}Li, one of the best studied halo nucleus, the last two neutrons are very weakly bound (by $\approx$ 300keV). Consequently, these neutrons need very little energy to move away from the nucleus.

There they can remain in the "stratospheric" orbits, spreading out and forming a tenuous halo. If one neutron is taken away from ^{11}Li, a second neutron will come out immediately (in keeping with the fact that ^{10}Li decays into ^{9}Li as fast as it is formed), leaving behind the core of the system, the ordinary ^{9}Li. This result testifies to the fact that pairing plays a central role in the stability of ^{11}Li. In fact, essentially all of the experimental findings characterizing ^{11}Li can be explained, even quantitatively, in terms of the following scenario: the formation of one Cooper pair which is held together to the ^{9}Li core essentially by the coupling to low–frequency phonons corresponding to long–wavelength vibrations of the core and of the halo (Barranco et al. (2001), see also Vinh Mau (1995)). A similar picture accounts also for the nuclear structure of ^{12}Be (Gori et al. (2004)). Of notice, is that the extended shell model results of this halo nucleus are consistent with the above picture (Sagawa et al. (1993), Navin et al. (2000)), as well as the dipole recoil model developed by Esbensen et al. (1997) (see also Broglia et al. (2002)).

In the case of the Sn–isotopes, typical superfluid nuclei lying along the stability valley, the condensate is made out of about 5–10 Cooper pairs correlated half through the bare nucleon–nucleon interaction, the remaining glue being provided by medium polarization effects (Barranco et al. (2004)).

The above picture of halo and of superfluid nuclei can be experimentally tested, in particular through processes of Cooper pair transfer induced by nuclear reactions. A particular exciting possibility is that of making ^{11}Li interact with e.g. ^{120}Sn, and measure the associated two–nucleon transfer cross section. Less spectacular, but equally interesting and simpler to analyze, is to measure reactions between ^{11}Li and protons to determine the probability that a proton picks–up the two halo neutrons and form a tritium ($t \equiv ^3_1H_2$ (Tanihata et al. (2008)), see below). The correlation between the halo neutrons influences this probability, since it brings the two neutron which have to combine with the proton closer, as compared to the situation in which the two neutrons are assumed to be uncorrelated (see Figs. 8 and 9 respectively). Of notice also the two–neutron transfer experiments from ^{6}He in the reaction ^{6}He+^{65}Cu (Chatterjee et al. (2008)). By analyzing such reactions, one would be able to obtain a measure of pairing correlations, and of the associated pairing gap in low–density drops of nuclear stuff (halo nuclei), in a similar way in which (t, p) and (p, t) reactions on Sn– and Pb–isotopes have allowed to microscopically test the different contributions to the two–particle transfer cross–sections in stable, "spherical" and "deformed" nuclei in gauge space.

In particular, changing the energy of the proton beam (in a (p, t) reaction), that is by measuring the two–particle transfer strength function one can, in principle, match the frequency associated with the collective modes exchanged between Cooper pair partners (medium polarization effects). A resonant effect on the two–particle transfer cross section is thus expected (as observed in tunneling experi-

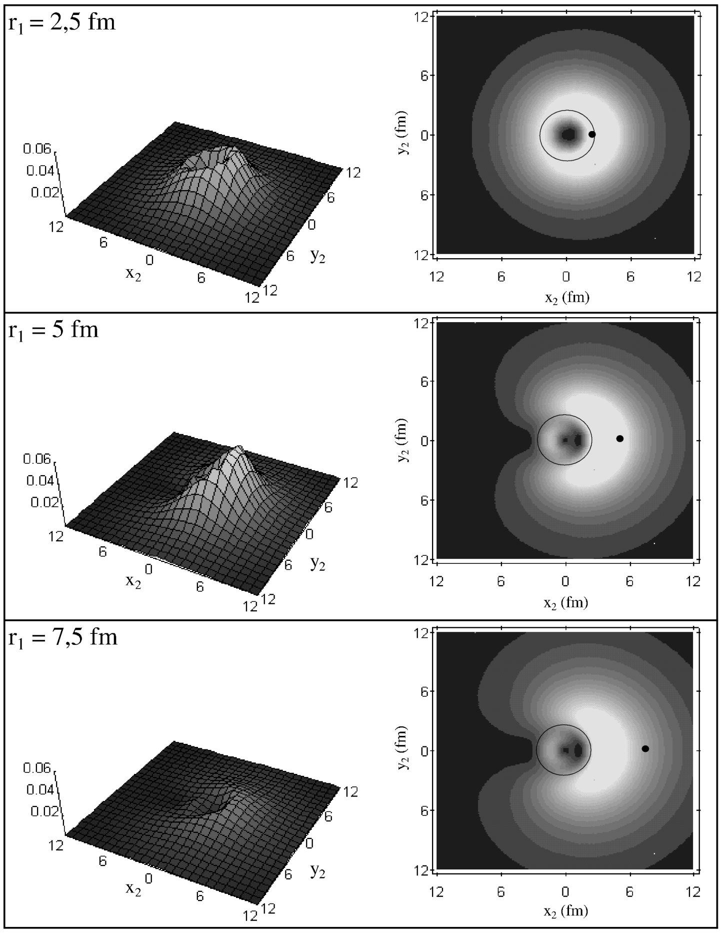

Figure 8: Spatial structure of two–neutron Cooper pair. The modulus squared wave function $|\Psi(\vec{r}_1, \vec{r}_2)|^2 = |\langle \vec{r}_1, \vec{r}_2 | 0^+ \rangle|^2$ describing the motion of the two halo neutrons around the ^{9}Li core (normalized to unity and multiplied by $16\pi^2 r_1^2 r_2^2$) is displayed as a function of the cartesian coordinates $x_2 = r_2 \cos(\theta_{12})$ and $y_2 = r_2 \sin(\theta_{12})$ of particle 2, for fixed values of particle 1 ($r_1 = 2.5, 5, 7.5$ fm) represented in the right panels by a solid dot, while the core ^{9}Li is shown as a black circle. The numbers appearing on the z-axis of the three dimensional plots displayed on the left side of the figure are in units of fm^{-2} (after Barranco et al. (2001)).

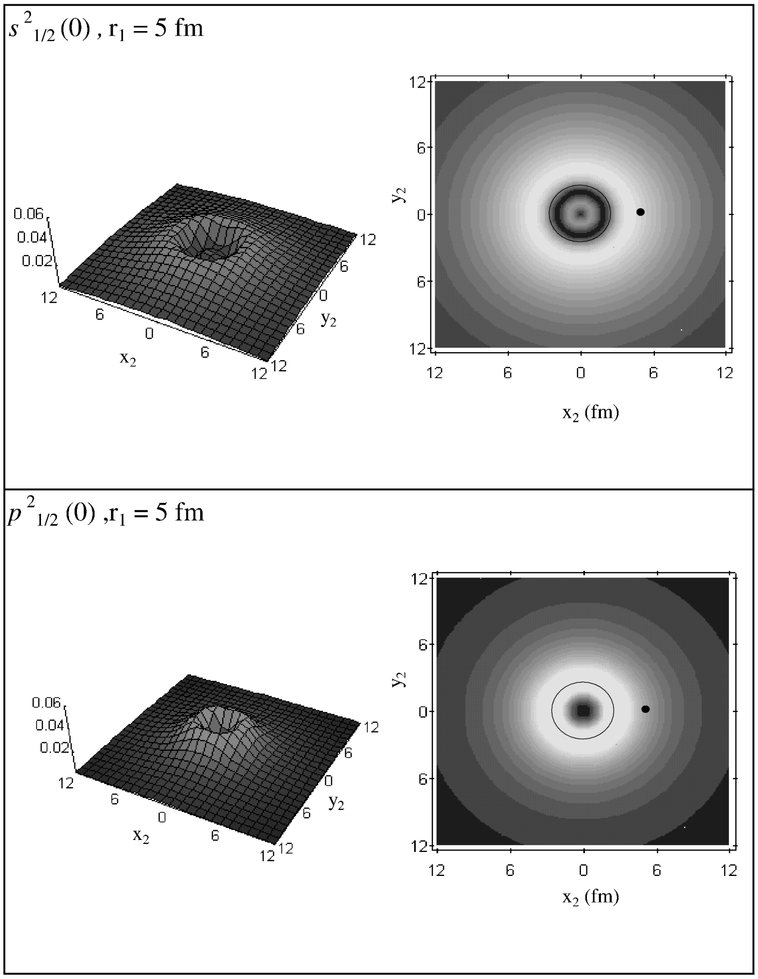

Figure 9: Spatial distribution of the pure two-particle configurations $\boldsymbol{s^2_{1/2}}$ (0) and $\boldsymbol{p^2_{1/2}}$(0) as a function of the *x*- and *y*-coordinates of particle 2, for a fixed value of the coordinate of particle 1 (r_1=5 fm). (after Barranco et al. (2001)).

ments between superconductors (see e.g. Figs 32 and 33 of Scalapino (1969)). Of notice, that such an effect although not directly observed, has already received important circumstantial evidence from transfer experiments in stable nuclei. In particular, through the observation by means of one particle transfer reactions (as well as inelastic scattering), of the septuplet of states $(h_{9/2}(\pi) \otimes 3^-)_J$ resulting from the coupling of the $h_{9/2}$ proton (ground state of ^{209}Bi) and the octupole vibration of the ^{208}Pb core, see e.g. Bortignon et al. (1977) and refs. therein. The ^{208}Pb(^{3}He,d)^{209}Bi experiments populating this septuplet can be viewed as the process equivalent to photoemission of e.g. C_{60} fullerene and providing the electron–phonon coupling constants g_ν used to calculate the induced electron–electron interaction arising from the coupling of the t_{14} electron to A_g and H_g modes (see Gunnarsson (1997), Gunnarsson (2004), Broglia et al. (2004)).

In the case of the reaction $^{210}\text{Po}(t,\alpha)^{209}\text{Pb}((h_{9/2}(\pi) \otimes 3^-))$ one obtains direct evidence of the renormalization of the single–particle state $h_{9/2}(\pi)$ by the 3^- vibration of the Pb core (see Fig. 10 (c)).

Before concluding this section, let us remind some very general facts which are at the basis of nuclear superfluidity. The origin of the BCS many–body solution of superconductivity can be traced to Cooper's solution of the two–electron problem in which all the other electrons play a role only through the exclusion principle. The ground state of ^{210}Pb and of ^{11}Li, in which two neutrons move around the core of ^{208}Pb and of ^{9}Li respectively, provide nuclear realizations of Cooper's model.

Much is known concerning two–nucleon pairing correlations of $|^{210}\text{Pb (gs)}\rangle$. In keeping with the fact that this state can be viewed as the pair addition mode of ^{208}Pb (see Figs. 4 and 10), it has been studied in detail in terms of two–nucleon transfer reactions. In this mode the two nucleon are correlated over a distance $\xi = \hbar v_F/2E_{corr}$, where E_{corr} plays the role of the pairing gap for open shell, superfluid, nuclei. In the case of ^{210}Pb, $E_{corr} \approx 1.2$ MeV. Thus $\xi = 25$ fm. Of course, if the two nucleons are subject to an external field (the central potential generated by e.g. the ^{208}Pb core), they cannot move away from each other more than 14 fm (see Fig. 10), in keeping with the fact that the radius of ^{208}Pb is ≈ 7 fm. On the other hand, in a heavy ion reaction with e.g. impact parameter 17 fm (see Fig. 11 (a) and (b)), the central single–particle potential acting on one of the two nucleons to be transferred is much stronger than typical values of the pairing field. It will thus be this potential responsible for the transfer of one partner of the Cooper pair at time t_1 and of the second one at time t_2 (see Fig. 11 (d)). And this two–step process will take place without loose of (pairing) correlation between the two nucleons. In other words, the Cooper pair is equally well formed at $t < t_1$ and $t > t_2$ (where the relative distance between the two neutrons is always less than 15 fm), than at $t_1 < t < t_2$ where this distance can be much larger (≈ 24) fm. A similar argument applies for the non–orthogonality contribution (see Fig. 11 (c)).

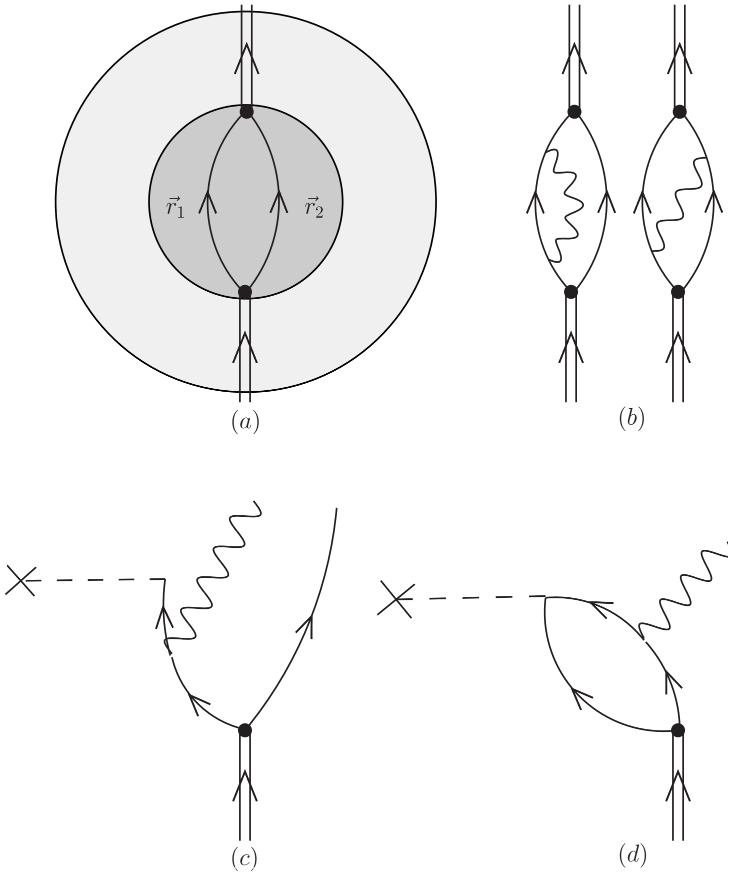

Figure 10: (a) Schematic representation of a two–particle correlated state (pair vibration: pair addition mode) This object (Cooper pair) is highly non–local, the fermions participating in it feeling the presence of the partner within distances inversely proportional to their correlation energy (light grey area) a fact which, in the case of halo exotic nuclei, leads to an increase of the effective nuclear radius of the systems by factors of about 50%. This may not sound much, if it was not for the fact that nuclear matter is highly incompressible and that small changes in the nuclear radius may imply nuclear instability. The mean single–particle field (dark grey area) can be viewed as an external field confining each of the member of Cooper pairs individually, (b) Pairing vibrations can be renormalized through the particle–vibration coupling mechanism in terms of self–energy and vertex corrections, (c) direct one–particle pick–up can excite a $2p$–$1h$ like state while (d) two–particle pick–up may lead to a collective $1p$–$1h$ excited final state.

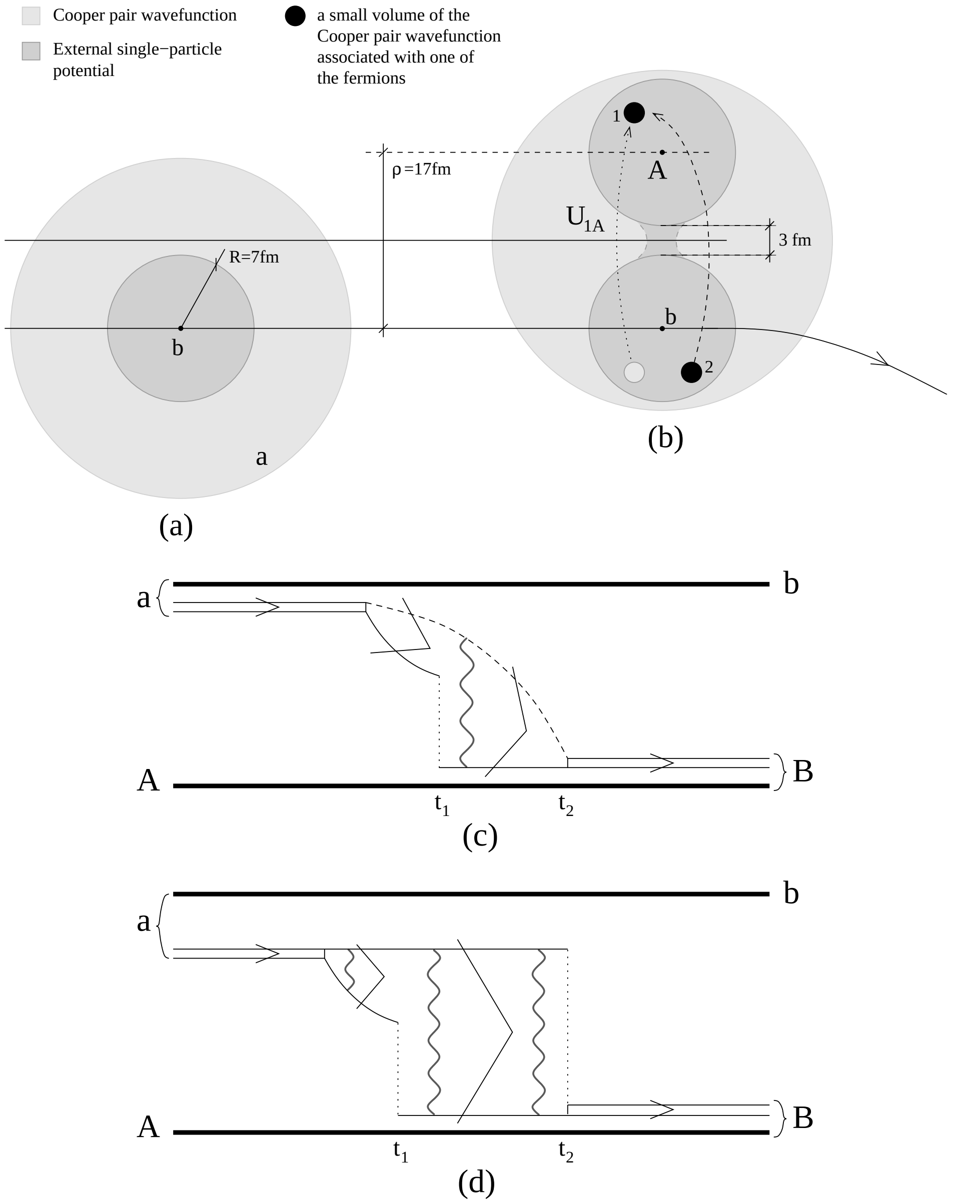
Cooper pair wavefunction
External single−particle potential
a small volume of the Cooper pair wavefunction associated with one of the fermions
ρ =17fm
R=7fm
b
a
(a)
1
A
U1A
3 fm
b
2
(b)
a
b
A
B
t1
t2
(c)
a
b
A
B
t1
t2
(d)

Figure 11: Schematic representation of the transfer of two correlated nucleons in first–order (c) and in second–order perturbation theory (d). In the first case a nucleon is transferred through the single–particle potential U_{1A} acting at time t_1 (dotted vertical line). The second nucleon follows suit (dashed curve) through the non–orthogonality of the wavefunctions belonging to different nuclei and, at time t_2, it can be considered as a nucleon belonging to the nucleus B. In the second case, one nucleon is acted upon at $t = t_1$ by the single–particle field generated by the core A (U_{1A}, dotted vertical line), and upon the second one at $t = t_2$. In all cases the correlation between the two nucleons is maintained throughout in keeping with the fact that $\xi \approx 30$ fm. The wavy lines in both (c) and (d) indicate the correlations existing between the members of the Cooper pair, entity which is represented by two–particle arrowed lines. The light grey area in (a) indicates the (virtual) extension of the Cooper pair wavefunction, the darker one the actual extension of the single–particle wavefunctions in the external single–particle field U_{1b}. When the ion a comes to the closest distance of approach from the target ion A (see (b)), the Cooper pair wavefunction turns from virtual to real extending now over essentially a length equal to ξ. Transfer will receive (important) contributions over distances of ξ , as schematically shown with the help of a small volume of the Cooper pair wavefunction (solid circle). Of course, the transfer integral $\langle \varphi^{(A)}_{Cooper} | U_{1A} | \varphi^{(b)}_{Cooper} \rangle$ receives contributions also from small distances, namely from all the dark grey area.

If we now concentrate our attention on ^{11}Li, arguably the best embodiment of a single Cooper pair fermionic system, in the intermediate, virtual state, the two neutrons can be as far apart as 6-8 fm from each other, and their center of mass displays a mean square radius $\langle r^2_{cm}\rangle^{1/2} \approx 5-6$ fm (cf. Figs. 8, 9 and 10). This in spite of the fact that the systematics of nuclear radii ($R = 1.2A^{1/3}$) adscribes a value of ≈ 2.7 fm to $A = 11$. How does the system manage to extend so far away from the core? The answer is by binding very weakly the last two neutrons (two–neutron separation energy $S_{2n} \approx 300$ keV). Of notice that a *gedanken experiment* in which S_{2n} is set to 20-30 keV would give rise to a Cooper pair which extends over tens of fm. This is consistent with the fact that the phonons (vibrational modes) which, exchanged between the two neutrons bind them to the ^{9}Li core, are vibrations of the same mean field produced by this glue. If one knocks one neutron out, the other will follow suit, even if it is very far away (tens of fermis) from the other. There is nothing strange in this exquisitely non–classical quantum behavior. This is one of the reasons which makes Cooper pairs to be one of the most fascinating quantal objects found in nature (if nothing else because it changes the statistics of the particles involved, from Fermi–Dirac to Bose–Einstein). In the nuclear case, these fragile objects can be studied singly, through tunneling experiments (transfer reactions). Also at energies below that of the Coulomb barrier where they also give rise to strong enhancements of the fusion cross sections (Dasso et al. (1983), Jacobs and Smilansky (1983), Broglia et al. (1981), Broglia et al. (1983), Broglia (1985)). Pairs of nucleon separated by distances much larger than nuclear radii help each other in the (Cooper) tunneling through classical forbidden regions.

Recently the (p, t) reaction on ^{11}Li has been measured with the help of inverse kinematics (Tanihata et al. (2008)). The differential cross section have been determined for transitions to the ^{9}Li ground state and to the first excited 2^+ state. Analysis of data has been carried out with success making use of correlated three–body wavefunctions.

While final channel inelastic scattering events are likely to play a role in the ^{11}Li$(p, t)^9$Li(2^+) reaction, a direct two–particle contribution is expected within the model leading to the Cooper pair wavefunction shown in Fig. 8 (see Fig. 10 (d) as well as Brink and Broglia (2005), Ch. 11). Within this context, it will be extremely illuminating to calculate the absolute two–particle transfer cross section describing the Cooper pair wavefunction in terms of Nuclear Field Theory (NFT, see Bortignon et al. (1977) and refs. therein), taking all possible renormalization effects into account (c.f. Figs. 8, 10 and Barranco et al. (2001)), and the reaction process, within the framework of a quantal calculation (including successive, simultaneous and non–orthogonality contributions, see Sect. 7), and compare the results with both theory and experiment as reported in Tanihata et al. (2008). Of notice is that NFT studies carried out on ^{12}Be (Gori et al. (2004)) provide, through the analysis of single–particle spectroscopic factors, circumstantial evidence of the central role the particle–vibration coupling mechanism plays in the structure of halo nuclei.

5. Two–particle transfer reactions and time–reversal response function

The fact that at the basis of BCS theory was not the pairing gap as initially thought, but the appearance of a coherent particle field which is distinct from it, is at the heart of the majority of results about superconductors. This can be seen by rewriting the pair transfer operator $P^\dagger$ in the form

$$P^\dagger = \sum_{\nu_\alpha,\nu_\beta>0} \langle \tilde{\nu}_\beta | \tau | \nu_\alpha \rangle a^\dagger_{\nu_\alpha} a^\dagger_{\tilde{\nu}_\beta} \tag{8}$$

where τ is the time–reversal operator and $|\tilde{\nu}_\beta\rangle = \tau|\nu_\beta\rangle$. Equation (8) implies that the response of a superconductor to a time–reversal invariant perturbation is dramatically different from the response of the system to a time–reversal noninvariant (pair–breaking or magnetic) one. Furthermore (8) explains why magnetic impurities reduce the transition temperature and non magnetic ones do not.

In the nuclear case magnetic impurities correspond to the intruder states (high j–values) lying close to the Fermi level and coming down in energy from the upper shell due to the spin–orbit effect. Backbending (Stephens and Simon (1972)) is associated with the breaking of pairs built on these states (typically $i_{13/2}(\nu)$ and $h_{11/2}(\pi)$).

Let us study the case of a nucleus under the effect of an external noninvariant time–reversal magnetic field (rotation). The model Routhian (Hamiltonian referred to the intrinsic, body–fixed reference frame) used to describe such a situation can be written as

$$H^\omega = H^\omega_{sp} + H_p. \tag{9}$$

The first term describes the average rotating potential,

$$H^\omega_{sp} = H^N_{sp} - \omega j_x, \tag{10}$$

with

$$H^N_{sp} = Q j_x^2, \tag{11}$$

(Nilsson Hamiltonian) Q being a quantity proportional to the quadrupole moment of the system (see e.g. Bès and Broglia (1979)).

The Hamiltonian H^ω_{sp} is invariant under space reflection (parity) and under rotations through 180° about the x–axis, i.e., rotations induced by the operator

$$\mathcal{R}_x = \exp(-i\pi j_x), \tag{12}$$

but not under time reversal, with exception of the case in which $\omega = 0$. Consequently, the eigenstates $|K\rangle$ of H^ω_{sp} can be labeled by the parity ($\pi = \pm 1$) and the signature ($\alpha = \pm 1/2$) quantum numbers (Bohr and Mottelson (1974)). Let us for simplicity consider particles moving in a single j–shell, e.g. a cranked $i_{13/2}$ orbital displaying axial symmetry. The eigenstates of (9) can be written as

$$|j\rangle \;=\; |\pi, \alpha = 1/2\rangle = \sum_K G^j_K(\omega)|K\rangle \qquad (13)$$

$$|\hat{j}\rangle \;=\; |\pi, \alpha = -1/2\rangle = \sum_K G^{\hat{j}}_{\tilde{K}}(\omega)|\tilde{K}\rangle \qquad (14)$$

where the states $|K\rangle$ and $\tau|K\rangle = |\tilde{K}\rangle$ are linear combinations of the two–fold degenerate Nilsson states.

Of notice that the states $|j\rangle$ and $|\hat{j}\rangle$ are related by the operation of time reversal only at $\omega = 0$. The violation of this symmetry is measured by the deviation from 1 of the pair matrix element (coherent field)

$$M_{j\hat{j}'} = \langle j\hat{j}|P^{\dagger}|0\rangle = \sum_K G^j_K(\omega)H^{\hat{j}}_{\tilde{K}}. \qquad (15)$$

The square of these matrix elements, in the case of a single j–shell ($i_{13/2}$) model, are shown in Figure 12 . While at $\omega = 0$ $|\hat{j}\rangle = \tau|j\rangle = |\tilde{j}\rangle$ (Cooper pairs), at $\omega = 1.0$ MeV all orbitals have become aligned with the rotation, leading to a complete violation of time reversal invariance. The critical rotational separating the two extreme regimes is about $\omega_{rot} \approx 0.5$ MeV. For a detailed discussion of these issues c.f. Nikam and Ring (1987), Nikam et al. (1986), Nikam et al. (1987), Vigezzi et al. (1988), Brink and Broglia (2005), and references therein.

Making use of the language of linear response theory, we can view $P^{\dagger}$ as an external field which adds to the system a pair of particles in time reversal states (see Eq. (8)). One can study such a process as a function of ω as shown in Fig. 13 where we display a schematic representation of a heavy ion collision in which a deformed superfluid (target) nucleus is set in strong rotation by the Coulomb field of the projectile before the two–particle transfer process takes place. If the symmetry axis of the target nucleus is oriented at 45° or 135° the projectile exerts a maximum torque on the system. Oriented it at 0° or 90° with respect to the beam direction, essentially no angular momentum would be transferred to the deformed nucleus. Assuming that in the first situation $\omega \approx \omega_{cr}$ at the distance of closest approach, while $\omega \approx 0$ in the second case, will lead to a well defined pattern in the $d^2\sigma(A \to A+2)/dId\Omega$ double differential cross section eventually determined making use of γ–coincidence (Broglia and Winther (2004)). For $\omega \approx 0$, only the yrast → yrast transition will be observed, the *yrast* (dizziest) band being the *loci* of the states of lower energy for a given angular momentum. For $\omega \gtrsim \omega_{cr}$, that is after the superfluid → normal transition takes place, one can distinguish between particle and hole states (see Fig.14). In this case, we are dealing with an extension

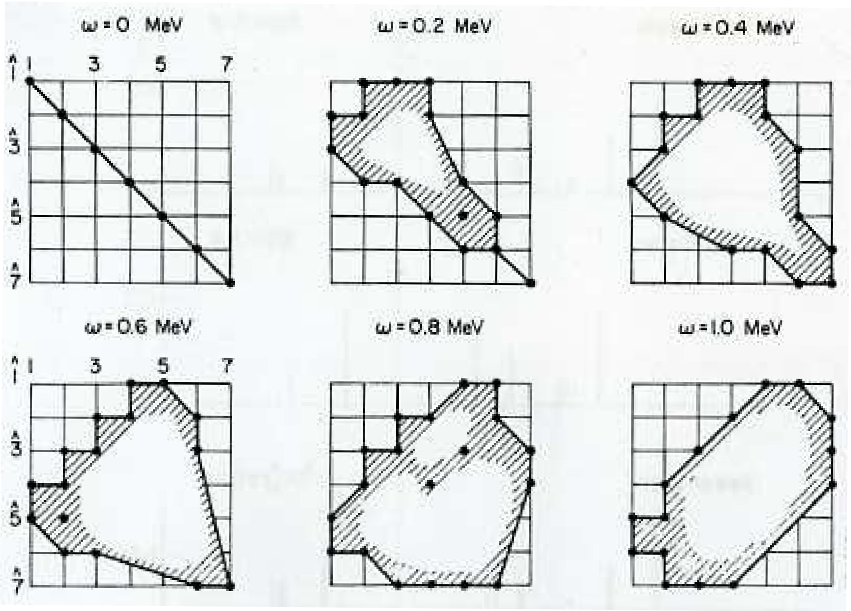

Figure 12: Contour plots for different values of ω of the two dimensional 7×7 pairing matrices $M^2_{j\hat{j}'}$ connecting all the negative signature j'–states with those of positive signature j. The solid circles represent the square of matrix elements larger than 0.2. Consequently, the dashed zones indicate the region where pairing correlations are about one–half of the value displayed by the diagonal configurations at $\omega = 0$.

of the experiments exciting pair vibration bands to the case of finite ω, that is, a combination of Figs. 1,3 and Fig. 4.

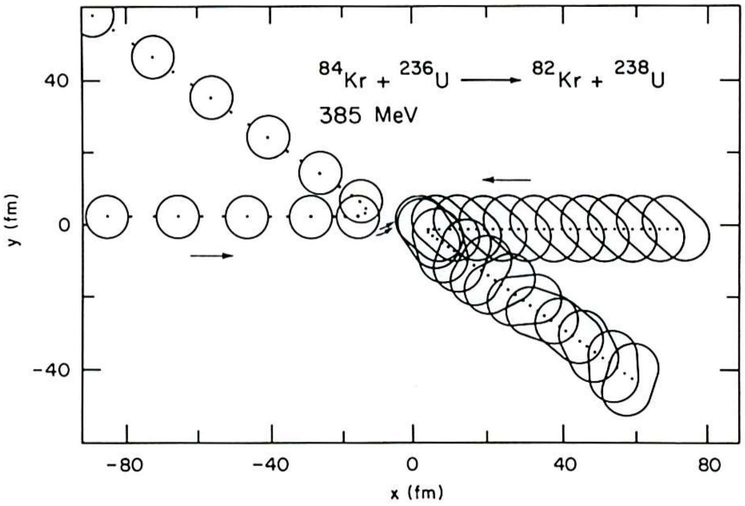

Figure 13: Snapshots of a trajectory of the reaction ^{84}Kr+^{236}U. The target nucleus is started with an orientation of 45° of the symmetry axis with respect to the incoming beam so as to maximize the transfer of angular momenta (see Broglia and Winther (2004)). After Dasso et al. (1984) and Dasso et al. (1982).

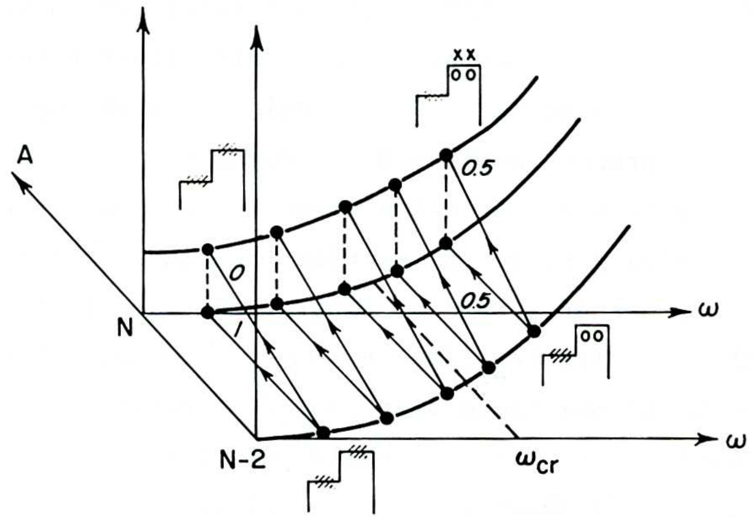

Figure 14: Schematic representation of the two–nucleon transfer processes exciting the one– and two–phonon pairing modes in the N system starting from the corresponding yrast state of the $N-2$ system. The yrast → yrast transition corresponds to the distinction of a pair removal mode, while the yrast → (two–phonon) state corresponds to the creation of a pair addition mode.

6. Testing the tools

6.1. Tunneling processes

In connection with the microscopic description of the tunneling process associated with the Josephson effect, (Cohen et al. (1962)) one can use the Hamiltonian

$$H = H_1 + H_2 + \sum_{k,q} T_{kq}(a^{\dagger}_{k\uparrow} a_{q\uparrow} + a^{\dagger}_{-q\downarrow} a_{-k\uparrow}) + h.c. \tag{16}$$

H_1 and H_2 are the separate Hamiltonians of the two superconductors on each side of the barrier; T_{kq} is the exponentially small tunneling matrix element from state k on one side to state q on the other, and the relationship of phases shown is required by time reversal symmetry.

One of the many procedures for arriving at (16) is to find sets of single–particle functions for each side of the barrier separately, in the absence of the potential of the other metal: then one eliminates the nonorthogonality effect by perturbation theory.

It is however necessary to be careful in using BCS perturbation theory in this case. This is because in a single, continuous block of superconductor it is quite correct to carry out the calculations using perfectly defined values of the relative phases of the energy gaps associated with the different states k and q, since the superconducting condensation energy actually results entirely from the precise coherence of these phases. It is however generally assumed that the total phase of the sample as a whole is meaningless. It is, on the other hand, not necessarily meaningless to discuss the relative phase of the two blocks of superconductors separated by an insulating barrier sufficiently thin for tunneling to occur. Clearly, again,the total phase of the assembly as a whole is not physical, but the relative phases can be given a meaning when we observe that electrons can pass back and forth between the two blocks by jumping across the barrier. Such a process leads to the possibility of coherence between states in which the total number of electrons is differently partitioned between the two sides -just as the phase coherence within the single block means that the number of electrons is not fixed locally (remember that $\Delta N \Delta\phi \lesssim 2\pi$) and, for instance, there is a coherence between the state with $N/2$ electrons in one half of the block and $N/2$ in the other, and that with $(N/2) + 2$ on one side and $(N/2) - 2$ on the other. The same is true when referring to the left and right hand side superconductors in a Josephson junction.

6.2. Two–nucleon transfer reactions

Let us see how the above considerations translate in the case of the transfer of pairs of nucleons in a nuclear reaction, for example in a heavy ion reaction.

A very accurate picture of heavy ion reactions, in particular a two–particle transfer reaction,

$$a(= b + 2) + A \longrightarrow b + B(= A + 2), \tag{17}$$

described by the total hamiltonian

$$\begin{aligned} H &= T_{aA} + H_a + H_A + V_{aA}, \\ &= T_{bB} + H_b + H_B + V_{bB}, \end{aligned} \tag{18}$$

is obtained by assuming that the relative motion of the centers of mass of the two ions can be described, in both entrance $\alpha(\equiv (a, A))$ and exit $\beta(\equiv (b, B))$ channels, classically (Broglia and Winther (2004)).

In (18) T_{aA} is the kinetic energy of relative motion, H_a and H_A the Hamiltonians describing the intrinsic degrees of freedom of nuclei a and A respectively, while V_{aA} is the effective interaction between the nucleons in a and the nucleons in A. Similar notation has been used to describe the corresponding ions in the exit channel.

All the information concerning the process (17) is obtained by solving the time–dependent Schrödinger equation

$$i\hbar\frac{\partial\psi}{\partial t} = H\psi, \tag{19}$$

with the initial condition that the nuclei a and A are in their ground states, and that the relative motion is described by a narrow wavepacket $\chi(\vec{r}_\beta - \vec{R}_\beta(t))$ of rather well–defined impact parameter and velocity. Expanding ψ on the channel wavefunctions $\psi_\beta = \psi^b_m(\xi_b)\psi^B_n(\xi_B)\exp(i\delta_\beta)$, according to

$$\begin{aligned} \psi &= \sum_\beta c((r_\beta - R_\beta), t)\psi_\beta(t)e^{-iE_\beta t/\hbar}, \\ &= \sum_\beta a_\beta(t)\chi(\vec{r}_\beta - \vec{R}_\beta(t), t)\psi_\beta(t)e^{-iE_\beta t/\hbar}. \end{aligned} \tag{20}$$

Upon inserting (20) in (19), one obtains the coupled equations

$$i\hbar\sum_\beta \dot{a}_\beta(t)\langle\psi_\xi|\psi_\beta\rangle_{\vec{R}_{\xi\gamma}}e^{-iE_\beta t/\hbar} = \sum_\gamma\langle\psi_\xi|V_\gamma - U_\gamma(r_\gamma)|\psi_\gamma\rangle_{\vec{R}_{\xi\gamma}}a_\gamma(t)e^{-iE_\beta t/\hbar}, \tag{21}$$

which, together with the condition $a_\gamma(-\infty) = \delta(\gamma, \alpha)$ allows to calculate a_β and thus the transfer reaction cross section, proportional to $|a_\beta|^2$. The sub–index on the matrix elements indicate that in the integration over the degrees of freedom of the two nuclei, the average center–of–mass coordinate $\vec{r}_{\beta\gamma} = \frac{1}{2}(\vec{r}_\beta + \vec{r}_\gamma)$ should be identified with the average classical coordinate, that is,

$$\vec{r}_{\beta\gamma} \rightarrow \vec{R}_{\beta\gamma} = \tfrac{1}{2}(\vec{R}_\beta + \vec{R}_\gamma). \tag{22}$$

Of notice that

$$\langle \psi_\gamma | V_\gamma - U_\gamma | \psi_\gamma \rangle = 0, \tag{23}$$

defines the ion–ion potential U_γ to be the expectation value of the interaction V_γ in the γ–channel.

A characteristic feature of the coupled equations (21) is the presence of the overlap $\langle \psi_\xi | \psi_\beta \rangle$ on the left hand side. If ξ and β describe two channels of the same partition, e.g. $\xi = \beta'$, the prime indicating excited states of the nuclei b and B, the overlap matrix is diagonal, namely,

$$g(\vec{R}) = \langle \psi'_\beta | \psi_\beta \rangle_{\vec{R}} = \delta(\beta', \beta). \tag{24}$$

If ξ and β describe different partitions, the overlap $\langle \psi_\xi | \psi_\beta \rangle$ is different from zero in the region where the densities of the two nuclei overlap.

The coupled equations (21) can be written in a more compact way by introducing the adjoint channel wavefunction

$$\omega_\xi = \sum_\gamma g^{-1}_{\xi\gamma} \psi_\gamma, \tag{25}$$

fulfilling the orthogonality relation

$$(\omega_\xi, \psi_\beta) = \delta(\xi, \beta). \tag{26}$$

Solving (21) in second order perturbation theory one obtains

$$a_\beta(t) = (a_\beta(t))_{(0)} + (a_\beta(t))_{(1)} + (a_\beta(t))_{(2)}, \tag{27}$$

where

$$(a_\beta(t))_{(0)} = \delta(\beta, \alpha), \tag{28}$$

$$(a_\beta(t))_{(1)} = \frac{1}{i\hbar} \int_{-\infty}^{t} \langle \omega_\beta | V_\alpha - U_\alpha | \psi_\alpha \rangle_{\vec{R}_{\alpha\beta}} e^{i(E_\beta - E_\alpha)t'/\hbar} dt', \tag{29}$$

and

$$\begin{aligned}(a_\beta(t))_{(2)} = \left(\frac{1}{i\hbar}\right)^2 \sum_\gamma \int_{-\infty}^{t} \langle \omega_\beta | V_\gamma - U_\gamma | \psi_\gamma \rangle_{\vec{R}_{\beta\gamma}(t')} e^{i(E_\beta - E_\gamma)t'/\hbar} dt' \\ \times \int_{-\infty}^{t'} \langle \omega_\gamma | V_\alpha - U_\alpha | \psi_\alpha \rangle_{\vec{R}_{\gamma\alpha}(t'')} e^{i(E_\gamma - E_\alpha)t''/\hbar} dt''.\end{aligned} \tag{30}$$

The state vectors $|\omega\rangle$ have to include the non–orthogonality effects between channels β, γ and α. To second order one finds

$$\begin{aligned}\omega_\beta =& \psi_\beta - \sum_{\gamma \neq \beta} \langle \psi_\gamma | \psi_\beta \rangle_{\vec{R}_{\gamma\beta}} \psi_\gamma \\ &+ \sum_{\gamma \neq \beta, \alpha} \langle \psi_\alpha | \psi_\gamma \rangle_{\vec{R}_{\alpha\gamma}} \langle \psi_\gamma | \psi_\beta \rangle_{\vec{R}_{\gamma\beta}} \psi_\alpha.\end{aligned} \tag{31}$$

Out of the very many second–order processes, we shall here only discuss the second–order effects in the two nucleon transfer reaction $A+a(=b+2\,\text{nucleons}) \rightarrow B(=A+2\,\text{nucleons})+b$, where the intermediate channel γ corresponds to the one–nucleon transfer channel $F(=A+1\,\text{nucleons})+f(=b+1\,\text{nucleons})$.

Inserting ω_β in (29) and in (30) one finds that the two–nucleon transfer amplitudes can be written as

$$a(\infty) = (a_\beta)_{(1)} + (a_\beta)_{orth} + (a_\beta)_{succ} \tag{32}$$

up to second order of perturbation theory. The different quantities appearing in this equation are

$$(a_\beta)_{(1)} = \frac{1}{i\hbar}\int_{-\infty}^{\infty} dt \langle\psi_\beta|V_\alpha - U_\alpha|\psi_\alpha\rangle_{\vec{R}_{\beta\alpha}} e^{i(E_\beta - E_\alpha)t/\hbar}, \tag{33}$$

$$\begin{aligned}(a_\beta)_{succ} =& \left(\frac{1}{i\hbar}\right)^2 \sum_{\gamma\neq(\beta,\alpha)} \int_{-\infty}^{\infty} dt \langle\psi_\beta|V_\gamma - U_\gamma|\psi_\gamma\rangle_{\vec{R}_{\beta\gamma}(t)} e^{i(E_\beta - E_\gamma)t/\hbar} \\ &\times \int_{-\infty}^{t} dt' \langle\psi_\gamma|V_\alpha - U_\alpha|\psi_\alpha\rangle_{\vec{R}_{\gamma\alpha}(t')} e^{i(E_\gamma - E_\alpha)t'/\hbar},\end{aligned} \tag{34}$$

and

$$\begin{aligned}(a_\beta)_{orth} =& -\frac{1}{i\hbar} \sum_{\gamma\neq(\beta,\alpha)} \int_{-\infty}^{\infty} dt \langle\psi_\beta|\psi_\gamma\rangle_{\vec{R}_{\beta\gamma}(t)} \\ &\times \langle\psi_\gamma|V_\alpha - U_\alpha|\psi_\alpha\rangle_{\vec{R}_{\gamma\alpha}} e^{i(E_\beta - E_\alpha)t/\hbar}.\end{aligned} \tag{35}$$

The first term $(a_\beta)_{(1)}$ describes the simultaneous transfer of two nucleons. The two–step successive transfer is described by $(a_\beta)_{succ}$, while $(a_\beta)_{orth}$ is a second–order contribution arising from the non–orthogonality of the wavefunctions associated with the different channels considered.

Of notice is that the main contribution to (33) arises from the single particle potential in channel α and the overlap between the single–particle wave functions of a nucleon in $a(=b+2)$ and in $B(=A+2)$. The contribution of the two–body pairing interaction, also present in (33) leads to a very small contribution.

In keeping with the above discussion, in the independent particle model, that is in the case in which there are no correlation between nucleons $\sum_\gamma |\psi_\gamma\rangle\langle\psi_\gamma| = 1$, (35) cancels exactly (33). The transfer reaction is then described as a purely successive transfer by the amplitude (34), as expected. In the opposite limit of very strong correlations between nucleons one expects that two–particle transfer occurs essentially as a simultaneous transfer process. This can be seen rewriting (33)–(35) in the post–prior representation. In this representation, at variance from the prior–prior representation of (34), the non–orthogonality term gets absorbed in the successive term which now reads

$$(\overline{a})_{(2)} = \left(\frac{1}{i\hbar}\right)^2 \sum_{\gamma} \int_{-\infty}^{\infty} dt \langle \psi_\beta | V_\beta - U_\beta | \psi_\gamma \rangle_{\vec{R}_{\beta\gamma}} e^{i(E_\beta - E_\gamma)t/\hbar} \\ \times \int_{-\infty}^{t} dt' \langle \psi_\gamma | V_\alpha - U_\alpha | \psi_\alpha \rangle_{\vec{R}_{\gamma\alpha}} e^{i(E_\gamma - E_\alpha)t'/\hbar}. \tag{36}$$

The expression (33) remains identical because of the post–prior symmetry. In the case in which the two particles to be transferred have a very strong mutual interaction V_{12}, $(\overline{a})_2$ become very small. This is because in the intermediate state one has to break a pair, an event which becomes less and less likely as V_{12} increases. Because in (35) the transfer potential does not contain V_{12}, the effect mentioned above implies that $(\overline{a}_\beta)_{(2)} \to 0$ as $V_{12} \to \infty$. Now, in actual situations $V_{12} \ll \langle V \rangle$, the first picture (i.e. $a_{(1)} \approx -(a)_{orth}$) applies, and two–particle transfer process can be essentially viewed as a successive transfer process.

7. Results

7.1. Heavy ion reactions

We now turn our attention to the results obtained in the analysis of the heavy–ion reaction ^{208}Pb(^{16}O, ^{18}O)^{206}Pb at 86 MeV. As the wavelength of the relative motion is relatively short at this energy ($\lambda \simeq 0.8$ fm), the semiclassical scheme sketched above is expected to be well suited. In Fig. 15 we display the results of the semiclassical calculation for this reaction, in comparison with the calculation carried out within the framework of a fully quantal theory, (second order DWBA formalism) and the experimental data.

In second order DWBA we need to calculate the simultaneous ($T^{(1)}$), successive ($T^{(2)}_{succ}$) and non–orthogonal ($T^{(2)}_{NO}$) contributions to the transition amplitude between the initial $(j_i)^2$ and final $(j_f)^2$ single–particle states (Bayman and Chen (1982)),

$$T^{(1)}(j_i, j_f) = 2 \sum_{\sigma_1\sigma_2} \int d\mathbf{r}_{fF} d\mathbf{r}_{b1} d\mathbf{r}_{A2} [\Psi^{j_f}(\mathbf{r}_{A1}, \sigma_1)\Psi^{j_f}(\mathbf{r}_{A2}, \sigma_2)]^{0*}_0 \chi^{(-)*}_{bB}(\mathbf{r}_{bB}) \\ \times v(\mathbf{r}_{b1}) [\Psi^{j_i}(\mathbf{r}_{b1}, \sigma_1)\Psi^{j_i}(\mathbf{r}_{b2}, \sigma_2)]^0_0 \chi^{(+)}_{aA}(\mathbf{r}_{aA}), \tag{37a}$$

$$
\begin{aligned}
T^{(2)}_{succ}(j_i, j_f) = 2 \sum_{K,M} \sum_{\substack{\sigma_1\sigma_2 \\ \sigma'_1\sigma'_2}} \int & d\mathbf{r}_{fF} d\mathbf{r}_{b1} d\mathbf{r}_{A2} [\Psi^{j_f}(\mathbf{r}_{A1}, \sigma_1)\Psi^{j_f}(\mathbf{r}_{A2}, \sigma_2)]^{0*}_0 \\
& \times \chi^{(-)*}_{bB}(\mathbf{r}_{bB}) v(\mathbf{r}_{b1}) [\Psi^{j_f}(\mathbf{r}_{A2}, \sigma_2)\Psi^{j_i}(\mathbf{r}_{b1}, \sigma_1)]^K_M \\
& \times \int d\mathbf{r}'_{fF} d\mathbf{r}'_{b1} d\mathbf{r}'_{A2} G(\mathbf{r}_{fF}, \mathbf{r}'_{fF}) [\Psi^{j_f}(\mathbf{r}'_{A2}, \sigma'_2)\Psi^{j_i}(\mathbf{r}'_{b1}, \sigma'_1)]^K_M \\
& \times \frac{2\mu_{cC}}{\hbar^2} v(\mathbf{r}'_{c2}) [\Psi^{j_i}(\mathbf{r}'_{A2}, \sigma'_2)\Psi^{j_i}(\mathbf{r}'_{b1}, \sigma'_1)]^0_0 \chi^{(+)}_{aA}(\mathbf{r}'_{aA}),
\end{aligned} \tag{37b}
$$

$$
\begin{aligned}
T^{(2)}_{NO}(j_i, j_f) = 2 \sum_{K,M} \sum_{\substack{\sigma_1\sigma_2 \\ \sigma'_1\sigma'_2}} \int & d\mathbf{r}_{fF} d\mathbf{r}_{b1} d\mathbf{r}_{A2} [\Psi^{j_f}(\mathbf{r}_{A1}, \sigma_1)\Psi^{j_f}(\mathbf{r}_{A2}, \sigma_2)]^{0*}_0 \\
& \times \chi^{(-)*}_{bB}(\mathbf{r}_{bB}) v(\mathbf{r}_{b1}) [\Psi^{j_f}(\mathbf{r}_{A2}, \sigma_2)\Psi^{j_i}(\mathbf{r}_{b1}, \sigma_1)]^K_M \\
& \times \int d\mathbf{r}'_{b1} d\mathbf{r}'_{A2} [\Psi^{j_f}(\mathbf{r}'_{A2}, \sigma'_2)\Psi^{j_i}(\mathbf{r}'_{b1}, \sigma'_1)]^K_M \\
& \times [\Psi^{j_i}(\mathbf{r}'_{A2}, \sigma'_2)\Psi^{j_i}(\mathbf{r}'_{b1}, \sigma'_1)]^0_0 \chi^{(+)}_{aA}(\mathbf{r}'_{aA}).
\end{aligned} \tag{37c}
$$

In these expressions, the spatial and spin coordinates of the two transferred nucleons are explicitly referred to with the subscripts 1 and 2. The subscripts A and b indicate the core to which the position of each of the nucleons are referred to. The vectors $\mathbf{r}_{aA}$, $\mathbf{r}_{bB}$ and $\mathbf{r}_{fF}$ are the relative motion coordinates in the initial, final and intermediate channels respectively (note difference with Appendix B, where the intermediate–channel coordinate is denoted $\mathbf{r}_{cC}$).

The single–particle wavefunctions $\Psi^j(\mathbf{r}, \sigma)$ with total angular momentum j are generated using a Woods–Saxon potential (see Table 1)

$$
U(r) = -\frac{V_0}{1 + \exp\left[\frac{r - R_0}{a}\right]}, \tag{38}
$$

where

$$
R_0 = r_0 A^{1/3}. \tag{39}
$$

The depth V_0 is adjusted for each level to reproduce the corresponding experimental energy. The positive–energy wavefunctions $\chi^{(+)}_{aA}(\mathbf{r}_{aA})$ and $\chi^{(-)}_{bB}(\mathbf{r}_{bB})$ are the ingoing distorted wave in the initial channel and the outgoing distorted wave in the final channel respectively. They are continuum solutions of the Schrödinger equation associated with the corresponding elastic scattering optical potentials. In Table 2 we show the (Woods–Saxon) parameters for these potentials.

The transition potential responsible for the transfer of the pair is, in the *post* representation,

$$
V_\beta = v_{bB} - U_\beta, \tag{40}
$$

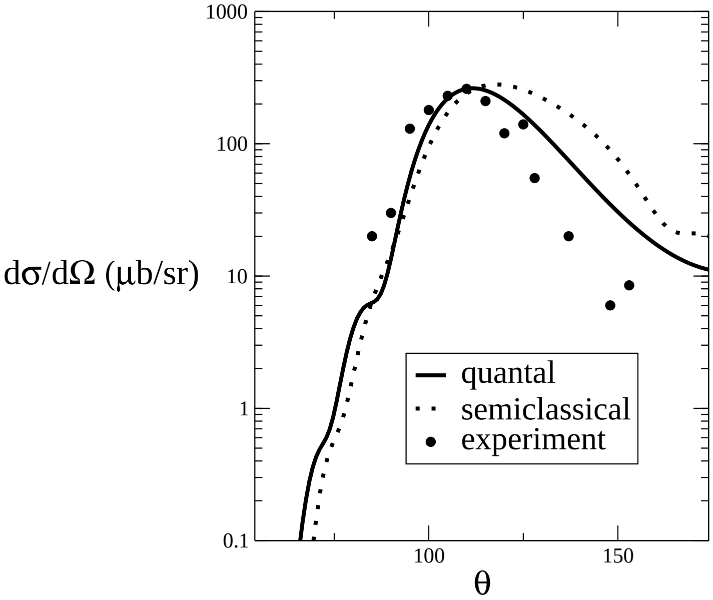

Figure 15: Differential cross section for the reaction ^{208}Pb(^{16}O, ^{18}O)^{206}Pb at an energy of 86 MeV in the laboratory frame, expressed in μb. We present the results of the quantal and semiclassical calculations, along with the experimental data, see also Bayman and Chen (1982).

	r_0	a
Pb	1.3	0.65
O	1.24	0.65

Table 1: Parameters used for the single particle potentials associated with the reaction ^{208}Pb(^{16}O,^{18}O)^{206}Pb (Bayman and Chen (1982)).

where v_{bB} is the interaction between the nuclei B and b, and U_β is the optical potential in the final channel. We make the assumption that v_{bB} can be decomposed into a term containing the interaction between the cores A and b and the potential describing the interaction between b and each of the transferred nucleons, namely

$$v_{bB} = v_{bA} + v_{b1} + v_{b2}, \tag{41}$$

where v_{b1} and v_{b2} is the same mean field potential we have used to define the single–particle wavefunctions of the neutrons in the nucleus a. The transition potential is

$$V_\beta = v_{bA} + v_{b1} + v_{b2} - U_\beta. \tag{42}$$

Assuming that $\langle\beta|v_{bA}|\alpha\rangle \simeq \langle\beta|U_\beta|\alpha\rangle$ (i.e, assuming that the matrix element of the core–core interaction between the initial and final states is very similar to the matrix element of the real part of the optical potential), one obtains the final expression of the transfer potential in the *post* representation,

$$V_\beta \simeq v_{b1} + v_{b2}. \tag{43}$$

This last approximation seems reasonable when dealing with heavy ion reactions in which there is no charge transfer, but more care have to be exerted when dealing with reactions in which light ions are involved. To obtain the total pair transfer amplitude a sum of the contributions associated with each mean field state j (weighted with the correspondent spectroscopic amplitude B_j) is to be carried out:

$$T_{2NT} = \sum_{j_f j_i} B_{j_f} B_{j_i} \left(T^{(1)}(j_i, j_f) + T^{(2)}_{succ}(j_i, j_f) - T^{(2)}_{NO}(j_i, j_f) \right). \tag{44}$$

In Table 3 we show the single–particle active configurations and the corresponding two–nucleon spectroscopic amplitudes associated with each single–particle level for the reaction under discussion.

7.2. Light ion reactions

We now turn our attention to two–particle transfer reactions induced with light ions. In this case, only a quantal calculation is possible. The calculation will be based on formulae similar to those reported in Eqs. (37a,37b,37c) (Bayman (1971)). In Fig. 16 the results for the ^{40}Ca$(t,p)^{42}$Ca reaction at 10.1 MeV, calculated in the *post* representation are shown in comparison with the experimental data (Bjerregaard et al. (1967)). Of notice that the choice between either representation may not be arbitrary in this case, since the approximate cancellation between the optical potential and the core–core potential is not equally well satisfied in each of the two representations. According to this consideration, in (t,p) and (p,t) reactions the representation corresponding to the proton–nucleus channel

	V	r_V	a_V	W	r_W	a_W
incoming channel	100	1.26	0.45	65.4	1.26	0.45
outgoing channel	65	1.35	0.34	45	1.34	0.33

Table 2: Parameters of the optical potentials associated with the reaction ^{208}Pb(^{16}O,^{18}O)^{206}Pb (Bayman and Chen (1982)), obtained by fitting elastic scattering data.

Nuclei	n, l, j	B
^{206}Pb	$2p_{1/2}$	-0.75
	$1f_{5/2}$	-0.47
	$2p_{3/2}$	-0.28
	$0i_{13/2}$	-0.28
	$1f_{7/2}$	-0.18
	$0h_{9/2}$	-0.14
^{18}O	$0d_{5/2}$	0.89
	$2p_{3/2}$	0.45

Table 3: Single–particle states and B–coefficients (two–particle spectroscopic amplitudes, see Broglia et al. (1973)) for the reaction ^{208}Pb(^{16}O,^{18}O)^{206}Pb (Maglione et al. (1985)).

seems to be better suited to satisfy the cancellation mentioned above. In keeping with this reasoning, in the case of the reaction ^{40}Ca(t, p)^{42}Ca, the *post* representation should be the preferred one.

The triton wave function used in this and the ^{110}Sn(p, t)^{112}Sn reaction can be written as (see Appendix A)

$$\Psi(\mathbf{r}_{1p}, \mathbf{r}_{2p}, \mathbf{r}_{12}) = \rho(r_{1p})\rho(r_{2p})\rho(r_{12})[\chi(\sigma_{n_1})\chi(\sigma_{n_2})]^0_0\chi_{m_t}(\sigma_p). \tag{45}$$

The corresponding central single–particle potentials used to calculate the two–particle transfer form factors are displayed in Fig. 17.

In Fig. 18 the results for the ^{112}Sn(p, t)^{110}Sn reaction at 26 MeV, calculated in the *prior* representation are displayed in comparison with the experimental data (Guazzoni et al. (2006)). Following the argument exposed in the discussion of the ^{40}Ca(t, p)^{42}Ca reaction, in this case we should prefer the *prior* representation. Of notice that in all the calculations of the absolute cross sections discussed above there are no free parameters adjusted to reproduce the data.

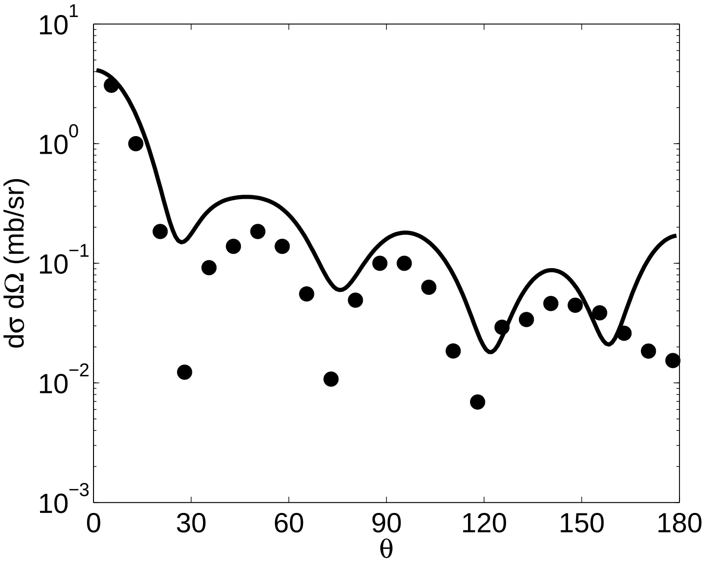

Figure 16: Total calculated differential transfer cross section for the ^{40}Ca(t, p)^{42}Ca reaction at 10.1 MeV in the *post* representation, in comparison with experimental data (Bjerregaard et al. (1967)).

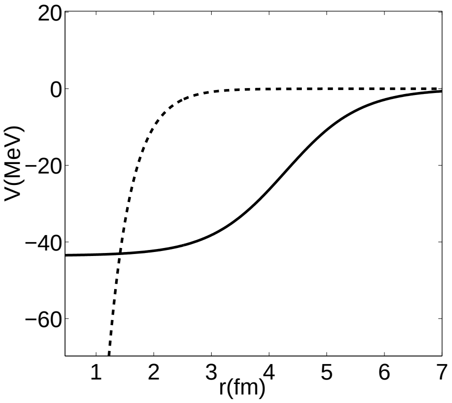

Figure 17: Central single–particle potentials of Ca (solid line) and t (dashed line) used in the quantal calculations shown in Fig. 16 (Bayman (1971)).

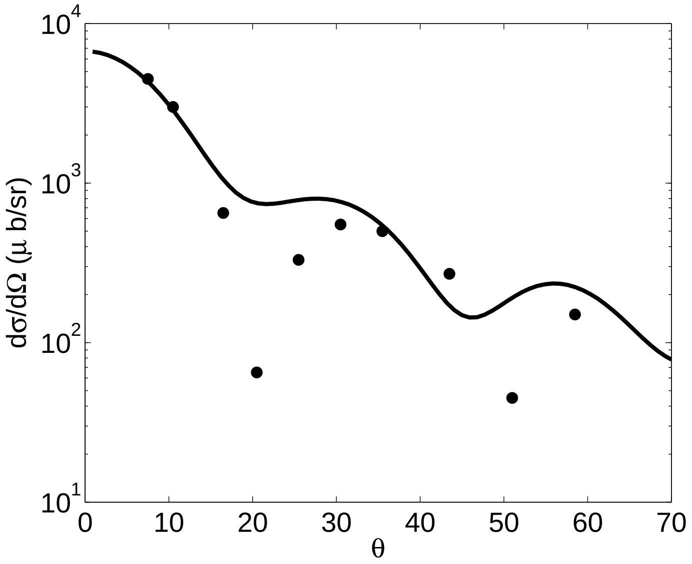

Figure 18: Differential cross section associated with the ^{112}Sn$(p,t)^{110}$Sn reaction in the *prior* representation in comparison with the experimental findings.

8. Conclusions

In a metal, the repulsion among the electrons compensates, to a large extent, the attraction generated by the positively charged ions. Such a system does not display the right cohesive energy. However, electrons being fermions, are described by an antisymmetric wavefunction. The associated exchange Coulomb interaction is attractive and adds to the cohesive energy an important contribution.

This system,being localized in space and displaying rigidity, violates translational invariance. One can observe it by shining a beam of light at it. Two outcomes are possible: a) electrons and ions oscillate rigidly together (Thomson scattering, center of mass oscillation), b) the system absorbs the photon which sets electrons and ions in oscillation against each other (photoabsorption, plasmon). The plasmon state (Higgs' boson of the system, Anderson (1994)), being orthogonal to the center of mass motion state -thus displaying $3N-3$ degrees of of freedom, N being the number of electrons of the system-, leads to restoration of translational (Galilean) invariance. The emission and absorption by the same electron, and the exchange between different electrons of virtual plasmons, gives rise to dressed particles which repel each other through a strongly screened Coulomb potential.

A crystal not only violates translational invariance globally (center of mass of the system), but also locally in each point of the crystal where an ion is localized. Lattice vibrations -so called phonons (Goldstone or, more precisely, Anderson–

Goldstone–Nambu modes)- lead to an overall (translational) symmetry restoration. The dressing of electrons by phonons -and plasmons- is central to account for the observed specific heat of metals, while the coupling of electrons and phonons is at the basis of electric resistivity.

The exchange of virtual phonons between electrons moving close to the Fermi energy gives rise to a tiny attraction, sufficient to overwhelm the tiny repulsion associated with the screened Coulomb field. The resulting overall attraction gives rise to pairs of electrons -Cooper pairs- of spin zero. At room temperature ($\approx$ 25 meV), these (quasi) bosons, being bound by an energy 2Δ of only a few meV, break as soon as they are formed. Eliminating thermal fluctuations by lowering the temperature of the crystal to few degrees K, allows for: a) condensation of strongly overlapping quasi bosons (Cooper pairs), b) distortion of the Fermi surface over an energy range 2Δ. This last effect selects a privileged orientation in gauge space and thus leads to a spontaneous breaking of gauge invariance (non–conservation of particle number). Symmetry restoration is obtained by fluctuations of the “deformed” nucleus orientation in gauge space. In fact, pairing rotational bands are the fingerprints of deformation in gauge space. These bands have been observed in the case of finite systems (atomic nuclei). However, in the case of a metallic superconductor, the moment of inertia associated with pairing rotational bands is so large that it is not possible to observe the individual states of these bands. On the other hand, setting two superconductors in weak contact with each other, with the help of a thin dioxide layer (through which electrons can tunnel) one observes, upon closing the circuit -that is, connecting among themselves the far edges of the superconductors opposite to the layer- a supercurrent (at zero bias). The carrier of this supercurrent has charge $2e$ (DC Josephson effect). This is a direct consequence of the coupling, through Cooper pair transfer, of the rotors in gauge space, associated with each of the two superconductors. In other words, Cooper pairs transfer gives rise to a coupling between the two superconductors. The detailed study of such processes have provided a complete picture of pairing correlation in metallic superconductors.

While in condensed matter the actual calculation of the intensity of the Josephson current meets the formidable difficulties of a microscopic description of the tunneling across a dioxide layer, absolute two–particle transfer cross sections induced in nuclear reactions can be calculated with good accuracy obtaining an overall account of the experimental findings. The study of two–particle transfer nuclear reactions not only is expected to be instrumental in shedding light into pairing correlations in atomic nuclei, but also to gain detailed information concerning the relative role successive, simultaneous and non–orthogonality transfer play in the transfer process, as well as the role hot orbitals have in such processes. Also, to provide information concerning pair correlation across the barrier as a function of the di–neutron separation energy, from tens of MeV in stable nuclei to hundreds of keV in halo nuclei.

RAB wants to acknowledge discussions, collaborations and suggestions throughout the years on the subject of this paper with and from Daniel Bès, Claus Riedel, Aage Bohr, Ben Mottelson, Phil Anderson, Bob Schrieffer, Aage Winther, and George Bertsch. Particularly inspiring has been the input coming from Peter Ring and Peter Schuck.

A. Simultaneous transfer

The appendixes A and B relate to light ion reactions and follow closely Bayman (1971) and Bayman and Chen (1982).

The simultaneous contribution to the (t, p) transfer cross section is

$$\frac{d\sigma}{d\Omega}(\hat{\mathbf{k}}_f) = \frac{k_f}{k_i}\frac{\mu_i\mu_f}{(2\pi\hbar^2)^2}\frac{1}{2}\sum_{m_t m_p}|\langle\Psi_f^{(-)}(\mathbf{k}_f)|V(r_{b1})|\Psi_i^{(+)}(k_i,\hat{\mathbf{z}})\rangle|^2, \tag{46}$$

where a summation is made over the spin orientations m_t, m_p of the incoming triton and the outgoing proton respectively, and the factor $1/2$ accounts for the two possible values of this orientation. The transfer potential $V(r_{b1})$ is the proton–neutron potential acting on neutron 1, so the above expression is written in the *post* representation.

For a $A(t, p)B$ reaction, the relative motion between the nucleus A and the triton is represented by an incoming wave. If the two transferred neutrons are in the $S = 0$ singlet state, the spin is entirely due to the spin of the proton. We can thus write the incoming distorted wave as

$$\psi_{m_t}^{(+)}(\mathbf{r}_{Aa},\mathbf{k}_i,\sigma_p) = \sum_{l_t}\exp\left(i\sigma_{l_t}^t\right)g_{l_t j_t}(r_{Aa})Y_0^{l_t}(\hat{\mathbf{r}}_{Aa})\frac{\sqrt{4\pi(2l_t+1)}}{k_i r_{Aa}}\chi_{m_t}(\sigma_p), \tag{47}$$

where $\mathbf{r}_{Aa}$ is the vector between A and the center of mass of the triton, $\mathbf{k}_i$ is the incident momentum, σ_p is the spin coordinate of the proton and l_t is the orbital angular momentum of the relative motion between the triton and the nucleus A. We have used $Y_0^{l_t}(\hat{\mathbf{k}}_i) = i^{l_t}\sqrt{\frac{2l_t+1}{4\pi}}\delta_{m_t,0}$, as $\mathbf{k}_i$ is oriented along the z–axis. Note that we have used the *time–reversal* phase convention, where the spherical harmonics are defined in terms of the associated Legendre polynomials as follows:

$$Y_m^l(\theta,\phi) = i^l\sqrt{\frac{2l+1}{4\pi}\frac{(l-m)!}{(l+m)!}}P_l^m(\cos\theta)e^{im\phi}. \tag{48}$$

If we write

$$Y_0^{l_t}(\hat{\mathbf{r}}_{Aa})\chi_{m_t}(\sigma_p) = \sum_{j_t}\langle l_t\ 0\ 1/2\ m_t|j_t\ m_t\rangle\left[Y^{l_t}(\hat{\mathbf{r}}_{Aa})\chi(\sigma_p)\right]_{m_t}^{j_t}, \tag{49}$$

we can express the incoming distorted wave in the form

$$\begin{aligned}\psi_{m_t}^{(+)}(\mathbf{r}_{Aa},\mathbf{k}_i,\sigma_p) = \sum_{l_t,j_t}\exp\left(i\sigma_{l_t}^t\right)\frac{\sqrt{4\pi(2l_t+1)}}{k_i r_{Aa}}g_{l_t j_t}(r_{Aa})\\ \times\langle l_t\ 0\ 1/2\ m_t|j_t\ m_t\rangle\left[Y^{l_t}(\hat{\mathbf{r}}_{Aa})\chi(\sigma_p)\right]_{m_t}^{j_t}.\end{aligned} \tag{50}$$

The outgoing proton distorted wave is

$$\psi^{(-)}_{m_p}(\mathbf{r}_{Bb},\mathbf{k}_f,\sigma_p) = \sum_{l_p j_p} \frac{4\pi}{k_f r_{Bb}} i^{l_p} \exp\left(-i\sigma^p_{l_p}\right) f^*_{l_p j_p}(r_{Bb}) \sum_m Y^{l_p}_m(\hat{\mathbf{r}}_{Bb}) Y^{l_p *}_m(\hat{\mathbf{k}}_f)\chi_{m_p}(\sigma_p), \tag{51}$$

where $\mathbf{r}_{Bb}$ is the position of the proton with respect to the nucleus B and σ_p is its spin coordinate. Now,

$$\begin{aligned}\sum_m Y^{l_p}_m(\hat{\mathbf{r}}_{Bb}) Y^{l_p *}_m(\hat{\mathbf{k}}_f)\chi_{m_p}(\sigma_p) &= \sum_{m,j_p} Y^{l_p *}_m(\hat{\mathbf{k}}_f)\langle l_p\; m\; 1/2\; m_p | j_p\; m+m_p\rangle \\ &\quad\times \left[Y^{l_p}(\hat{\mathbf{r}}_{Bb})\chi_{m_p}(\sigma_p)\right]^{j_p}_{m+m_p} \\ &= \sum_{m,j_p} Y^{l_p *}_{m-m_p}(\hat{\mathbf{k}}_f)\langle l_p\; m-m_p\; 1/2\; m_p | j_p\; m\rangle \left[Y^{l_p}(\hat{\mathbf{r}}_{Bb})\chi_{m_p}(\sigma_p)\right]^{j_p}_{m},\end{aligned} \tag{52}$$

and, finally,

$$\begin{aligned}\psi^{(-)}_{m_p}(\mathbf{r}_{Bb},\mathbf{k}_f,\sigma_p) &= \frac{4\pi}{k_f r_{Bb}} \sum_{l_p j_p, m} i^{l_p} \exp\left(-i\sigma^p_{l_p}\right) f^*_{l_p j_p}(r_{Bb}) Y^{l_p *}_{m-m_p}(\hat{\mathbf{k}}_f) \\ &\quad\times \langle l_p\; m-m_p\; 1/2\; m_p | j_p\; m\rangle \left[Y^{l_p}(\hat{\mathbf{r}}_{Bb})\chi(\sigma_p)\right]^{j_p}_{m}.\end{aligned} \tag{53}$$

We now turn our attention to the evaluation of the matrix element

$$\begin{aligned}\langle \Psi^{(-)}_f(\mathbf{k}_f)|V(r_{b1})|\Psi^{(+)}_i(k_i,\hat{\mathbf{z}})\rangle &= \frac{(4\pi)^{3/2}}{k_i k_f} \sum_{l_p l_t j_p j_t m} ((l_f \tfrac{1}{2})_{j_f}(l_f \tfrac{1}{2})_{j_f}|(l_f l_f)_0(\tfrac{1}{2}\tfrac{1}{2})_0)_0 \sqrt{2l_t+1} \\ &\quad\times \langle l_p\; m-m_p\; 1/2\; m_p | j_p\; m\rangle \langle l_t\; 0\; 1/2\; m_t | j_t\; m_t\rangle\, i^{-l_p} \exp[i(\sigma^p_{l_p}+\sigma^t_{l_t})] \\ &\quad\times 2Y^{l_p}_{m-m_p}(\hat{\mathbf{k}}_f) \sum_{\sigma_1\sigma_2\sigma_p} \int \frac{d\mathbf{r}_{Bb} d\mathbf{r} d\boldsymbol{\eta}}{r_{Bb} r_{Aa}} u_{l_f j_f}(r_{A1}) u_{l_f j_f}(r_{A2}) \left[Y^{l_f}(\hat{\mathbf{r}}_{A1}) Y^{l_f}(\hat{\mathbf{r}}_{A2})\right]^{0*}_0 \\ &\quad\times f_{l_p j_p}(r_{Bb}) g_{l_t j_t}(r_{Aa}) \Big[\chi(\sigma_1)\chi(\sigma_2)\Big]^{0*}_0 \left[Y^{l_p}(\hat{\mathbf{r}}_{Bb})\chi(\sigma_p)\right]^{j_p *}_m V(r_{b1}) \\ &\quad\times \theta^0_0(\mathbf{r},\mathbf{s}) \Big[\chi(\sigma_1)\chi(\sigma_2)\Big]^{0}_0 \left[Y^{l_t}(\hat{\mathbf{r}}_{Aa})\chi(\sigma_p)\right]^{j_t}_{m_t},\end{aligned} \tag{54}$$

with

$$\begin{aligned}\mathbf{r} &= \mathbf{r}_{A2} - \mathbf{r}_{A1} \\ \mathbf{s} &= \frac{1}{2}(\mathbf{r}_{A1} + \mathbf{r}_{A2}) - \mathbf{r}_p \\ \boldsymbol{\eta} &= \frac{1}{2}(\mathbf{r}_{A1} + \mathbf{r}_{A2}) \\ \mathbf{r}_{Bb} &= \mathbf{r}_p - \frac{\mathbf{r}_{A1} + \mathbf{r}_{A2}}{A+2},\end{aligned} \tag{55}$$

where $\mathbf{r}_{A1}, \mathbf{r}_{A2}, \mathbf{r}_p$ are the positions of the two neutrons and the proton with respect to nucleus A and σ_1, σ_2 the corresponding spin coordinates. The wavefunction

$$u_{l_f j_f}(r_{A1}) u_{l_f j_f}(r_{A2}) \left[Y^{l_f}(\hat{\mathbf{r}}_{A1}) Y^{l_f}(\hat{\mathbf{r}}_{A2}) \right]^{0*}_{0} \tag{56}$$

describes the two transferred neutrons in a final state with orbital angular momentum l_f and total angular momentum j_f, and $\theta^0_0(\mathbf{r}, \mathbf{s})$ is the spatial wavefunction of the triton.

The sum over σ_1, σ_2 in (54) is readily found to be 1. We will now simplify the term $\left[Y^{l_p}(\hat{\mathbf{r}}_{Bb}) \chi(\sigma_p) \right]^{j_p *}_{m} \left[Y^{l_t}(\hat{\mathbf{r}}_{Aa}) \chi(\sigma_p) \right]^{j_t}_{m_t}$, first noting that, with time–reversal phases,

$$\left[Y^{l_p}(\hat{\mathbf{r}}_{Bb}) \chi(\sigma_p) \right]^{j_p *}_{m} = (-1)^{1/2 - \sigma_p + j_p - m} \left[Y^{l_p}(\hat{\mathbf{r}}_{Bb}) \chi(-\sigma_p) \right]^{j_p}_{-m}. \tag{57}$$

On the other hand,

$$\begin{aligned} \left[Y^{l_p}(\hat{\mathbf{r}}_{Bb})\ \chi(-\sigma_p) \right]^{j_p}_{-m} \left[Y^{l_t}(\hat{\mathbf{r}}_{Aa}) \chi(\sigma_p) \right]^{j_t}_{m_t} &= \sum_{JM} \langle j_p \ -m \ j_t \ m_t | J \ M \rangle \\ &\times \left\{ \left[Y^{l_p}(\hat{\mathbf{r}}_{Bb}) \chi(-\sigma_p) \right]^{j_p} \left[Y^{l_t}(\hat{\mathbf{r}}_{Aa}) \chi(\sigma_p) \right]^{j_t} \right\}^{J}_{M} \end{aligned} \tag{58}$$

In order to survive the integration, the angular and spin functions must couple to $L = 0, S = 0, J = 0$, so the only term that remains is

$$\begin{aligned} &\langle j_p \ -m \ j_t \ m_t | 0 \ 0 \rangle \left\{ \left[Y^{l_p}(\hat{\mathbf{r}}_{Bb}) \chi(-\sigma_p) \right]^{j_p} \left[Y^{l_t}(\hat{\mathbf{r}}_{Aa}) \chi(\sigma_p) \right]^{j_t} \right\}^{0}_{0} \delta_{l_p l_t} \delta_{j_p j_t} \delta_{m m_t} \\ &= \frac{(-1)^{j_p + m_t}}{\sqrt{2 j_p + 1}} \left\{ \left[Y^{l_p}(\hat{\mathbf{r}}_{Bb}) \chi(-\sigma_p) \right]^{j_p} \left[Y^{l_t}(\hat{\mathbf{r}}_{Aa}) \chi(\sigma_p) \right]^{j_t} \right\}^{0}_{0} \delta_{l_p l_t} \delta_{j_p j_t} \delta_{m m_t}. \end{aligned} \tag{59}$$

We couple separately the spin and spatial functions:

$$\begin{aligned} &\left\{ \left[Y^{l}(\hat{\mathbf{r}}_{Bb}) \chi(-\sigma_p) \right]^{j} \ \left[Y^{l}(\hat{\mathbf{r}}_{Aa}) \chi(\sigma_p) \right]^{j} \right\}^{0}_{0} \\ &\qquad = ((l\tfrac{1}{2})_j (l\tfrac{1}{2})_j | (ll)_0 (\tfrac{1}{2}\tfrac{1}{2})_0)_0 \left[\chi(-\sigma_p) \chi(\sigma_p) \right]^{0}_{0} \left[Y^{l}(\hat{\mathbf{r}}_{Bb}) Y^{l}(\hat{\mathbf{r}}_{Aa}) \right]^{0}_{0}. \end{aligned} \tag{60}$$

We substitute (57),(59),(60) in (54) to obtain

$$\begin{aligned}\langle \Psi_f^{(-)}(\mathbf{k}_f)|V(r_{b1})|\Psi_i^{(+)}(k_i,\hat{\mathbf{z}})\rangle = {}& -\frac{(4\pi)^{3/2}}{k_ik_f}\sum_{lj}((l_f\tfrac{1}{2})_{j_f}(l_f\tfrac{1}{2})_{j_f}|(l_fl_f)_0(\tfrac{1}{2}\tfrac{1}{2})_0)_0\sqrt{\frac{2l+1}{2j+1}}\\ &\times\langle l\ m_t-m_p\ 1/2\ m_p|j\ m_t\rangle\langle l\ 0\ 1/2\ m_t|j\ m_t\rangle\, i^{-l}\exp[i(\sigma_l^p+\sigma_l^t)]\\ &\times 2Y^l_{m_t-m_p}(\hat{\mathbf{k}}_f)\int\frac{d\mathbf{r}_{Bb}d\mathbf{r}d\boldsymbol{\eta}}{r_{Bb}r_{Aa}}u_{l_fj_f}(r_{A1})u_{l_fj_f}(r_{A2})\left[Y^{l_f}(\hat{\mathbf{r}}_{A1})Y^{l_f}(\hat{\mathbf{r}}_{A2})\right]_0^{0*}\\ &\times f_{lj}(r_{Bb})g_{lj}(r_{Aa})\left[Y^l(\hat{\mathbf{r}}_{Bb})Y^l(\hat{\mathbf{r}}_{Aa})\right]_0^0 V(r_{b1})\theta_0^0(\mathbf{r},\mathbf{s})\\ &\times((l\tfrac{1}{2})_j(l\tfrac{1}{2})_j|(ll)_0(\tfrac{1}{2}\tfrac{1}{2})_0)_0\sum_{\sigma_p}(-1)^{1/2-\sigma_p}\left[\chi(-\sigma_p)\chi(\sigma_p)\right]_0^0.\end{aligned} \tag{61}$$

The last sum over σ_p is

$$\begin{aligned}\sum_{\sigma_p}(-1)^{1/2-\sigma_p}\left[\chi(-\sigma_p)\chi(\sigma_p)\right]_0^0 &= \sum_{\sigma_pm}(-1)^{1/2-\sigma_p}\langle 1/2\ m\ 1/2\ \ -m|0\ 0\rangle\\ &\quad\times\chi_m(-\sigma_p)\chi_{-m}(\sigma_p)\\ &= \frac{1}{\sqrt{2}}\sum_{\sigma_pm}(-1)^{1/2-\sigma_p}(-1)^{1/2-m}\delta_{m,-\sigma_p}\delta_{-m,\sigma_p} = -\sqrt{2}.\end{aligned} \tag{62}$$

The $9j$ symbols can be evaluated to find

$$\begin{aligned}((l_f\tfrac{1}{2})_{j_f}(l_f\tfrac{1}{2})_{j_f}|(l_fl_f)_0(\tfrac{1}{2}\tfrac{1}{2})_0)_0 &= \sqrt{\frac{2j_f+1}{2(2l_f+1)}}\\ ((l\tfrac{1}{2})_j(l\tfrac{1}{2})_j|(ll)_0(\tfrac{1}{2}\tfrac{1}{2})_0)_0 &= \sqrt{\frac{2j+1}{2(2l+1)}},\end{aligned} \tag{63}$$

so

$$\begin{aligned}\langle \Psi_f^{(-)}(\mathbf{k}_f)|V(r_{b1})|\Psi_i^{(+)}(k_i,\hat{\mathbf{z}})\rangle = {}& \frac{(4\pi)^{3/2}}{k_ik_f}\sum_{lj}\sqrt{\frac{2j_f+1}{2l_f+1}}\\ &\times\langle l\ m_t-m_p\ 1/2\ m_p|j\ m_t\rangle\langle l\ 0\ 1/2\ m_t|j\ m_t\rangle\, i^{-l}\exp[i(\sigma_l^p+\sigma_l^t)]\\ &\times\sqrt{2}Y^l_{m_t-m_p}(\hat{\mathbf{k}}_f)\int\frac{d\mathbf{r}_{Bb}d\mathbf{r}d\boldsymbol{\eta}}{r_{Bb}r_{Aa}}u_{l_fj_f}(r_{A1})u_{l_fj_f}(r_{A2})\left[Y^{l_f}(\hat{\mathbf{r}}_{A1})Y^{l_f}(\hat{\mathbf{r}}_{A2})\right]_0^{0*}\\ &\times f_{lj}(r_{Bb})g_{lj}(r_{Aa})\left[Y^l(\hat{\mathbf{r}}_{Bb})Y^l(\hat{\mathbf{r}}_{Aa})\right]_0^0 V(r_{b1})\theta_0^0(\mathbf{r},\mathbf{s}).\end{aligned} \tag{64}$$

We now check the possible values of the Clebsh–Gordan coefficients, finding, for $j = l - 1/2$:

$$\langle l\ m_t - m_p\ 1/2\ m_p | l - 1/2\ m_t\rangle\langle l\ 0\ 1/2\ m_t | l - 1/2\ m_t\rangle = \begin{cases} \dfrac{l}{2l+1} & \text{if } m_t = m_p \\ -\dfrac{\sqrt{l(l+1)}}{2l+1} & \text{if } m_t = -m_p \end{cases} \tag{65}$$

and, for $j = l + 1/2$:

$$\langle l\ m_t - m_p\ 1/2\ m_p | l + 1/2\ m_t\rangle\langle l\ 0\ 1/2\ m_t | l + 1/2\ m_t\rangle = \begin{cases} \dfrac{l+1}{2l+1} & \text{if } m_t = m_p \\ \dfrac{\sqrt{l(l+1)}}{2l+1} & \text{if } m_t = -m_p \end{cases} \tag{66}$$

Substituting, we get

$$\begin{aligned} \langle\Psi_f^{(-)}(\mathbf{k}_f)|V(r_{b1})|\Psi_i^{(+)}(k_i,\hat{\mathbf{z}})\rangle = {} & \frac{(4\pi)^{3/2}}{k_i k_f}\sum_l \frac{1}{(2l+1)}\sqrt{\frac{(2j_f+1)}{(2l_f+1)}}\exp[i(\sigma_l^p+\sigma_l^t)]i^{-l} \\ & \times \sqrt{2}Y^l_{m_t-m_p}(\hat{\mathbf{k}}_f)\int\frac{d\mathbf{r}_{Bb}d\mathbf{r}d\boldsymbol{\eta}}{r_{Bb}r_{Aa}}u_{l_f j_f}(r_{A1})u_{l_f j_f}(r_{A2})\left[Y^{l_f}(\hat{\mathbf{r}}_{A1})Y^{l_f}(\hat{\mathbf{r}}_{A2})\right]_0^{0*} \\ & \times V(r_{b1})\theta_0^0(\mathbf{r},\mathbf{s})\left[Y^l(\hat{\mathbf{r}}_{Bb})Y^l(\hat{\mathbf{r}}_{Aa})\right]_0^0 \\ & \times\Big[\Big(f_{ll+1/2}(r_{Bb})g_{ll+1/2}(r_{Aa})(l+1)+f_{ll-1/2}(r_{Bb})g_{ll-1/2}(r_{Aa})l\Big)\delta_{m_p,m_t} \\ & +\Big(f_{ll+1/2}(r_{Bb})g_{ll+1/2}(r_{Aa})\sqrt{l(l+1)}-f_{ll-1/2}(r_{Bb})g_{ll-1/2}(r_{Aa})\sqrt{l(l+1)}\Big)\delta_{m_p,-m_t}\Big]. \end{aligned} \tag{67}$$

We can further simplify this expression using

$$\begin{aligned} \left[Y^{l_f}(\hat{\mathbf{r}}_{A1})Y^{l_f}(\hat{\mathbf{r}}_{A2})\right]_0^{0*} &= \left[Y^{l_f}(\hat{\mathbf{r}}_{A1})Y^{l_f}(\hat{\mathbf{r}}_{A2})\right]_0^{0} = \sum_m\langle l_f\ m\ l_f\ -m|0\ 0\rangle Y_m^{l_f}(\hat{\mathbf{r}}_{A1})Y_{-m}^{l_f}(\hat{\mathbf{r}}_{A2}) \\ &= \sum_m(-1)^{l_f-m}\langle l_f\ m\ l_f\ -m|0\ 0\rangle Y_m^{l_f}(\hat{\mathbf{r}}_{A1})Y_m^{l_f*}(\hat{\mathbf{r}}_{A2}) \\ &= \frac{1}{\sqrt{2l_f+1}}\sum_m Y_m^{l_f}(\hat{\mathbf{r}}_{A1})Y_m^{l_f*}(\hat{\mathbf{r}}_{A2}) \\ &= \frac{\sqrt{(2l_f+1)}}{4\pi}P_{l_f}(\cos\theta_A), \end{aligned} \tag{68}$$

where θ_A is the angle between $\mathbf{r}_{A1}$ and $\mathbf{r}_{A2}$. Now,

$$\begin{aligned}\left[Y^l(\hat{\mathbf{r}}_{Bb})Y^l(\hat{\mathbf{r}}_{Aa})\right]^0_0 &= \sum_m \langle l\ m\ l\ -m|0\ 0\rangle Y^l_m(\hat{\mathbf{r}}_{Bb})Y^l_{-m}(\hat{\mathbf{r}}_{Aa}) \\ &= \frac{1}{\sqrt{(2l+1)}}\sum_m (-1)^{l+m} Y^l_m(\hat{\mathbf{r}}_{Bb})Y^l_{-m}(\hat{\mathbf{r}}_{Aa}).\end{aligned} \tag{69}$$

It can be easily shown that the integral of each one of terms in the above sum is independent of m, so we can drop the sum and multiply by $2l+1$ the $m=0$ term, leaving

$$\begin{aligned}\left[Y^l(\hat{\mathbf{r}}_{Bb})Y^l(\hat{\mathbf{r}}_{Aa})\right]^0_0 &\Rightarrow (-1)^l\sqrt{(2l+1)}\,Y^l_0(\hat{\mathbf{r}}_{Bb})Y^l_0(\hat{\mathbf{r}}_{Aa}) \\ &= \sqrt{(2l+1)}Y^l_0(\hat{\mathbf{r}}_{Bb})Y^{l*}_0(\hat{\mathbf{r}}_{Aa}).\end{aligned} \tag{70}$$

We now change the integration variables from $(\mathbf{r}_{Bb}, \mathbf{r}, \boldsymbol{\eta})$ to $(\mathbf{r}_{Aa}, \alpha, \beta, \gamma, r_{12}, r_{1p}, r_{2p})$ (see Fig. 19),

$$\left|\frac{\partial(\mathbf{r}, \boldsymbol{\eta}, \mathbf{r}_{Bb})}{\partial(\mathbf{r}_{Aa}, \alpha, \beta, \gamma, r_{12}, r_{1p}, r_{2p})}\right| = r_{12}r_{1p}r_{2p}\sin\beta \tag{71}$$

being the Jacobian of the transformation. Finally,

$$\begin{aligned}\langle\Psi^{(-)}_f(\mathbf{k}_f)|V(r_{b1})|\Psi^{(+)}_i(k_i,\hat{\mathbf{z}})\rangle = \frac{\sqrt{8\pi}}{k_ik_f}\sum_l\sqrt{\frac{2j_f+1}{2l+1}}\exp[i(\sigma^p_l+\sigma^t_l)]i^{-l} \\ \times Y^l_{m_t-m_p}(\hat{\mathbf{k}}_f)\int d\mathbf{r}_{Aa}Y^{l*}_0(\hat{\mathbf{r}}_{Aa})\int\frac{d\alpha\,d\beta\,d\gamma\,dr_{12}\,dr_{1p}\,dr_{2p}\ \sin\beta}{r_{Bb}r_{Aa}}Y^l_0(\hat{\mathbf{r}}_{Bb}) \\ \times u_{l_fj_f}(r_{A1})u_{l_fj_f}(r_{A2})V(r_{b1})\theta^0_0(\mathbf{r},\mathbf{s})P_{l_f}(\cos\theta_A)r_{12}r_{1p}r_{2p} \\ \times\Big[\Big(f_{ll+1/2}(r_{Bb})g_{ll+1/2}(r_{Aa})(l+1)+f_{ll-1/2}(r_{Bb})g_{ll-1/2}(r_{Aa})l\Big)\delta_{m_p,m_t} \\ +\Big(f_{ll+1/2}(r_{Bb})g_{ll+1/2}(r_{Aa})\sqrt{l(l+1)}-f_{ll-1/2}(r_{Bb})g_{ll-1/2}(r_{Aa})\sqrt{l(l+1)}\Big)\delta_{m_p,-m_t}\Big].\end{aligned} \tag{72}$$

We note that the inner integral is a function of $\mathbf{r}_{Aa}$ alone, and that it transforms as $Y^l_0(\hat{\mathbf{r}}_{Aa})$ under rotations, because all the dependence on the orientation of $\mathbf{r}_{Aa}$ is contained in the term $Y^l_0(\hat{\mathbf{r}}_{Bb})$. The inner integral can thus be cast into the form

$$\begin{aligned}A(r_{Aa})Y^l_0(\hat{\mathbf{r}}_{Aa}) = \int d\alpha\,d\beta\,d\gamma\,dr_{12}\,dr_{1p}\,dr_{2p}\ \sin\beta \\ \times F(\alpha,\beta,\gamma,r_{12},r_{1p},r_{2p},R_x,R_y,R_z).\end{aligned} \tag{73}$$

To evaluate $A(r_{Aa})$, we put $\mathbf{r}_{Aa}$ on the z–axis

$$\begin{aligned}A(r_{Aa}) = 2\pi i^{-l}\sqrt{\frac{4\pi}{2l+1}}\int d\beta\,d\gamma\,dr_{12}\,dr_{1p}\,dr_{2p}\ \sin\beta \\ \times F(\alpha,\beta,\gamma,r_{12},r_{1p},r_{2p},0,0,r_{Aa}),\end{aligned} \tag{74}$$

where a factor 2π has been included as the result of the integral over α, since the integrand clearly does not depend on α. We substitute (73) and (74) in (72), and after integrating over the angular variables of $\mathbf{r}_{Aa}$, we obtain

$$
\begin{aligned}
\langle \Psi_f^{(-)}(\mathbf{k}_f)|V(r_{b1})|\Psi_i^{(+)}(k_i,\hat{\mathbf{z}})\rangle &= 2\frac{(2\pi)^{3/2}}{k_i k_f}\sum_l \sqrt{\frac{2j_f+1}{2l+1}}\exp[i(\sigma_l^p+\sigma_l^t)]i^{-l} \\
&\times Y^l_{m_t-m_p}(\hat{\mathbf{k}}_f)\int dr_{Aa}\,d\beta\,d\gamma\,dr_{12}\,dr_{1p}\,dr_{2p}\,r_{Aa}\sin\beta\,r_{12}r_{1p}r_{2p} \\
&\times u_{l_f j_f}(r_{A1})u_{l_f j_f}(r_{A2})V(r_{b1})\theta_0^0(\mathbf{r},\mathbf{s})P_{l_f}(\cos\theta_A)P_l(\cos\theta_{if}) \\
&\times \Big[\Big(f_{ll+1/2}(r_{Bb})g_{ll+1/2}(r_{Aa})(l+1)+f_{ll-1/2}(r_{Bb})g_{ll-1/2}(r_{Aa})l\Big)\delta_{m_p,m_t} \\
&+\Big(f_{ll+1/2}(r_{Bb})g_{ll+1/2}(r_{Aa})\sqrt{l(l+1)}-f_{ll-1/2}(r_{Bb})g_{ll-1/2}(r_{Aa})\sqrt{l(l+1)}\Big)\delta_{m_p,-m_t}\Big]/r_{Bb},
\end{aligned}
\tag{75}
$$

where we have used

$$
Y^l_0(\hat{\mathbf{r}}_{Bb}) = i^l\sqrt{\frac{2l+1}{4\pi}}P_l(\cos\theta_{if}). \tag{76}
$$

The final expression of the differential cross section involves a sum over the spin orientations (see (46)). When $m_p = 1/2, m_t = 1/2$ or $m_p = -1/2, m_t = -1/2$, the terms proportional to δ_{m_p,m_t} will include the factor

$$
|Y^l_{m_t-m_p}(\hat{\mathbf{k}}_f)\delta_{m_p,m_t}| = |Y^l_0(\hat{\mathbf{k}}_f)| = \left| i^l\sqrt{\frac{2l+1}{4\pi}}P^0_l(\cos\theta)\right|, \tag{77}
$$

when $m_p = -1/2, m_t = 1/2$

$$
|Y^l_{m_t-m_p}(\hat{\mathbf{k}}_f)\delta_{m_p,-m_t}| = |Y^l_1(\hat{\mathbf{k}}_f)| = \left| i^l\sqrt{\frac{2l+1}{4\pi}\frac{1}{l(l+1)}}P^1_l(\cos\theta)\right|, \tag{78}
$$

and when $m_p = 1/2, m_t = -1/2$

$$
|Y^l_{m_t-m_p}(\hat{\mathbf{k}}_f)\delta_{m_p,-m_t}| = |Y^l_{-1}(\hat{\mathbf{k}}_f)| = |Y^l_1(\hat{\mathbf{k}}_f)| = \left| i^l\sqrt{\frac{2l+1}{4\pi}\frac{1}{l(l+1)}}P^1_l(\cos\theta)\right|. \tag{79}
$$

We use the tritium wavefunction

$$
\theta_0^0(\mathbf{r},\mathbf{s}) = \rho(r_{1p})\rho(r_{2p})\rho(r_{12}), \tag{80}
$$

$\rho(r)$ being a Tang–Herndon wave function (Tang and Herndon (1965)). We obtain

$$
\frac{d\sigma}{d\Omega}(\hat{\mathbf{k}}_f) = \frac{1}{2E_i^{3/2}E_f^{1/2}}\sqrt{\frac{\mu_f}{\mu_i}}\left(|I^{(0)}_{l_f j_f}(\theta)|^2+|I^{(1)}_{l_f j_f}(\theta)|^2\right), \tag{81}
$$

with

$$
\begin{aligned}
I^{(0)}_{l_f j_f}(\theta) = \sum_l & P^0_l(\cos\theta)\,\sqrt{2j_f+1}\,\exp[i(\sigma^p_l+\sigma^t_l)] \\
& \times \int dr_{Aa}\,d\beta\,d\gamma\,dr_{12}\,dr_{1p}\,dr_{2p}\,r_{Aa}\sin\beta\,\rho(r_{1p})\rho(r_{2p})\rho(r_{12}) \\
& \times u_{l_f j_f}(r_{A1})u_{l_f j_f}(r_{A2})V(r_{b1})P_{l_f}(\cos\theta_A)P_l(\cos\theta_{if})r_{12}r_{1p}r_{2p} \\
& \times \Big(f_{ll+1/2}(r_{Bb})g_{ll+1/2}(r_{Aa})\,(l+1) + f_{ll-1/2}(r_{Bb})g_{ll-1/2}(r_{Aa})\,l\Big)/r_{Bb},
\end{aligned}
\tag{82}
$$

and

$$
\begin{aligned}
I^{(1)}_{l_f j_f}(\theta) = \sum_l & P^1_l(\cos\theta)\,\sqrt{2j_f+1}\,\exp[i(\sigma^p_l+\sigma^t_l)] \\
& \times \int dr_{Aa}\,d\beta\,d\gamma\,dr_{12}\,dr_{1p}\,dr_{2p}\,r_{Aa}\sin\beta\,\rho(r_{1p})\rho(r_{2p})\rho(r_{12}) \\
& \times u_{l_f j_f}(r_{A1})u_{l_f j_f}(r_{A2})V(r_{b1})P_{l_f}(\cos\theta_A)P_l(\cos\theta_{if})r_{12}r_{1p}r_{2p} \\
& \times \Big(f_{ll+1/2}(r_{Bb})g_{ll+1/2}(r_{Aa}) - f_{ll-1/2}(r_{Bb})g_{ll-1/2}(r_{Aa})\Big)/r_{Bb}.
\end{aligned}
\tag{83}
$$

Note the absence of the $(-1)^l_f$ factor with respect to what can be found in Bayman (1971), due to the use of time–reversed phases instead of Condon–Shortley. This is compensated in the total result with the same difference in the expression of the spectroscopic factors. This ensures that, in either case, the contribution of all the single particle transitions tend to have the same phase for superfluid nuclei, adding coherently to enhance the transfer cross section.

The above expressions can easily be rewritten for a heavy–ion reaction between spinless nuclei, the distorted waves in entrance and exit channels being

$$
\psi^{(+)}(\mathbf{r}_{Aa},\mathbf{k}_{Aa}) = \sum_l \exp\left(i\sigma^i_l\right) g_l Y^l_0(\hat{\mathbf{r}}_{aA})\frac{\sqrt{4\pi(2l+1)}}{k_{aA}r_{aA}},
\tag{84}
$$

and

$$
\psi^{(-)}(\mathbf{r}_{bB},\mathbf{k}_{bB}) = \frac{4\pi}{k_{bB}r_{bB}}\sum_{\tilde{l}} i^{\tilde{l}}\exp\left(-i\sigma^f_{\tilde{l}}\right) f^*_{\tilde{l}}(r_{bB})\sum_m Y^{\tilde{l}*}_m(\hat{\mathbf{k}}_{bB})Y^{\tilde{l}}_m(\hat{\mathbf{r}}_{bB}).
\tag{85}
$$

If we are dealing with a heavy ion reaction, $\theta^0_0(\mathbf{r},\mathbf{s})$ must be replaced with the spatial part of the initial two–neutron wavefunction

$$
\Psi(\mathbf{r}_{b1},\mathbf{r}_{b2},\sigma_1,\sigma_2) = \left[\psi^{j_i}(\mathbf{r}_{b1},\sigma_1)\psi^{j_i}(\mathbf{r}_{b2},\sigma_2)\right]^0_0,
\tag{86}
$$

where $\mathbf{r}_{b1},\mathbf{r}_{b2}$ are the positions of the two neutrons with respect to the b core. It can be shown to be

$$
\frac{u_{l_i j_i}(r_{b1})u_{l_i j_i}(r_{b2})}{4\pi}\sqrt{\frac{2j_i+1}{2}}P_{l_i}(\cos\theta_b),
\tag{87}
$$

where θ_b is the angle between $\mathbf{r}_{b1}$ and $\mathbf{r}_{b2}$.

After doing the same simplifications as in the light–ion case, we find

$$\begin{aligned}\langle\Psi_f^{(-)}(\mathbf{k}_{bB})|V(r_{b1})|\Psi_i^{(+)}(k_{aA},\hat{\mathbf{z}})\rangle &= \frac{1}{2k_{aA}k_{bB}}\sum_l \sqrt{(2j_f+1)(2j_i+1)}\\ &\times i^{-l}\exp[i(\sigma_l^f+\sigma_l^i)]P_l(\cos\theta)(2l+1)\\ &\times\int dr_{aA}\,d\beta\,d\gamma\,dr_{12}\,dr_{b1}\,dr_{b2}\,r_{aA}\sin\beta\,r_{12}r_{b1}r_{b2}\\ &\times P_{l_f}(\cos\theta_A)P_{l_i}(\cos\theta_b)u_{l_f j_f}(r_{A1})u_{l_f j_f}(r_{A2})V(r_{b1})\\ &\times u_{l_i j_i}(r_{b1})u_{l_i j_i}(r_{b2})f_l(r_{bB})g_l(r_{aA})P_l(\cos\theta_{if})/r_{bB}.\end{aligned} \tag{88}$$

A.1. Coordinates used in the calculations

We must find the expression of the variables appearing in the integral as functions of the integration variables $r_{1p}, r_{2p}, r_{12}, r_{Aa}, \beta, \gamma$ as indicated in Fig. 19 (remember that $\mathbf{r}_{Aa} = r_{Aa}\,\hat{\mathbf{z}}$). $\mathbf{r}_{Aa}$ being the center of mass coordinate, we have

$$\mathbf{r}_{Aa} = \frac{1}{m_a}\left(\mathbf{r}_{A1}+\mathbf{r}_{A2}+m_b\mathbf{r}_{Ab}\right), \tag{89}$$

and

$$\mathbf{r}_{Aa} = \frac{1}{m_a}\left(\mathbf{r}_{A1}+\mathbf{r}_{A2}+m_b\mathbf{r}_{Ab}\right), \tag{90}$$

$$\mathbf{d}_1 = \frac{1}{m_a}\left(m_b\mathbf{r}_{b2}-(m_b+1)\mathbf{r}_{12}\right), \tag{91}$$

$$d_1 = \frac{1}{m_a}\sqrt{(m_b+1)r_{12}^2+m_b(m_b+1)r_{b1}^2-m_b r_{b2}^2}, \tag{92}$$

$$d_2 = \frac{1}{m_a}\sqrt{(m_b+1)r_{12}^2+m_b(m_b+1)r_{b2}^2-m_b r_{b1}^2}, \tag{93}$$

and

$$\mathbf{r}_{Bb} = \frac{m_a}{m_b}\mathbf{r}_{Aa} - \frac{m_B+m_b}{m_b m_B}(\mathbf{r}_{A1}+\mathbf{r}_{A2}). \tag{94}$$

The angle α between $\mathbf{d}_1$ and $\mathbf{r}_{12}$ is such that

$$\cos(\alpha) = \frac{d_1^2+r_{12}^2-d_2^2}{2r_{12}d_1}. \tag{95}$$

The complete determination of $\mathbf{r}_{A1}, \mathbf{r}_{A2}, \mathbf{r}_{12}$ can be obtained by writing their expression in a simple configuration, in which the triangle lies in the xz–plane with $\mathbf{d}_1$ pointing along the positive z–direction, and $\mathbf{r}_{Aa} = 0$. Then, a first rotation $\mathcal{R}_z(\gamma)$ of an angle γ around the z–axis, a second rotation $\mathcal{R}_y(\beta)$ of an angle β around the y–axis, and a translation along $\mathbf{r}_{Aa}$ will bring the vectors to the most general configuration. In other words,

$$\begin{aligned}\mathbf{r}_{A1} &= \mathbf{r}_{Aa} + \mathcal{R}_y(\beta)\mathcal{R}_z(\gamma)\mathbf{r}'_{A1},\\ \mathbf{r}_{12} &= \mathcal{R}_y(\beta)\mathcal{R}_z(\gamma)\mathbf{r}'_{12},\\ \mathbf{r}_{A2} &= \mathbf{r}_{A1} + \mathbf{r}_{12},\end{aligned} \tag{96}$$

with

$$\mathbf{r}'_{A1} = \begin{bmatrix} 0 \\ 0 \\ d_1 \end{bmatrix}, \tag{97}$$

$$\mathbf{r}'_{12} = r_{12}\begin{bmatrix} \sin(\alpha) \\ 0 \\ -\cos(\alpha) \end{bmatrix}, \tag{98}$$

and the rotation matrixes are

$$\mathcal{R}_y(\beta) = \begin{bmatrix} \cos(\beta) & 0 & \sin(\beta) \\ 0 & 1 & 0 \\ -\sin(\beta) & 0 & \cos(\beta) \end{bmatrix}, \tag{99}$$

and

$$\mathcal{R}_z(\gamma) = \begin{bmatrix} \cos(\gamma) & -\sin(\gamma) & 0 \\ \sin(\gamma) & \cos(\gamma) & 0 \\ 0 & 0 & 1 \end{bmatrix}. \tag{100}$$

$$\mathbf{r}_{A1} = \begin{bmatrix} d_1 \sin(\beta) \\ 0 \\ r_{Aa} + d_1 \cos(\beta) \end{bmatrix}, \tag{101}$$

$$\mathbf{r}_{A2} = \begin{bmatrix} d_1 \sin(\beta) + r_{12}\cos(\beta)\cos(\gamma)\sin(\alpha) - r_{12}\sin(\beta)\cos(\alpha) \\ r_{12}\sin(\gamma)\sin(\alpha) \\ r_{Aa} + d_1\cos(\beta) - r_{12}\sin(\beta)\cos(\gamma)\sin(\alpha) - r_{12}\cos(\alpha)\cos(\beta) \end{bmatrix}. \tag{102}$$

We we also find

$$\mathbf{r}_{b1} = \frac{1}{m_b}(\mathbf{r}_{A2} + (m_b + 1)\mathbf{r}_{A1} - m_a\mathbf{r}_{Aa}), \tag{103}$$

and

$$\mathbf{r}_{b2} = \frac{1}{m_b}(\mathbf{r}_{A1} + (m_b + 1)\mathbf{r}_{A2} - m_a\mathbf{r}_{Aa}). \tag{104}$$

We easily obtain

$$\cos\theta_A = \frac{r_{A1}^2 + r_{A2}^2 - r_{12}^2}{2r_{A1}r_{A2}}, \tag{105}$$

and

$$\cos\theta_b = \frac{r_{b1}^2 + r_{b2}^2 - r_{12}^2}{2r_{b1}r_{b2}}. \tag{106}$$

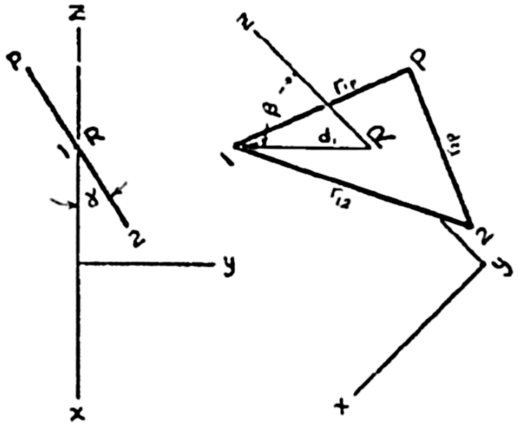

Figure 19: Coordinate system used for the simultaneous amplitude. The angle α (=0 in the figure) corresponds to the orientation about the z–axis. The origin is located in the center of mass of A, and R is the distance to the center of mass of the triton (from Bayman (1971)).

B. Successive and non–orthogonal contributions

We write the successive transition amplitude as (see Bayman and Chen (1982)):

$$\begin{aligned}
T^{VV}_{2NT} = & \frac{4\mu_{Cc}}{\hbar^2} \sum_{\substack{\sigma_1\sigma_2 \\ \sigma_1'\sigma_2' \\ KM}} \int d^3r_{Cc} d^3r_{b1} d^3r_{A2} d^3r'_{Cc} d^3r'_{b1} d^3r'_{A2} \chi^{(-)*}(\mathbf{k}_{Bb}, \mathbf{r}_{Bb}) \\
& \times \left[\psi^{j_f}(\mathbf{r}_{A1}, \sigma_1)\psi^{j_f}(\mathbf{r}_{A2}, \sigma_2)\right]^{0*}_0 v(r_{b1}) \left[\psi^{j_f}(\mathbf{r}_{A2}, \sigma_2)\psi^{j_i}(\mathbf{r}_{b1}, \sigma_1)\right]^K_M \\
& \times G(\mathbf{r}_{Cc}, \mathbf{r}'_{Cc}) \left[\psi^{j_f}(\mathbf{r}'_{A2}, \sigma'_2)\psi^{j_i}(\mathbf{r}'_{b1}, \sigma'_1)\right]^{K*}_M v(r'_{c2}) \\
& \times \left[\psi^{j_i}(\mathbf{r}'_{b1}, \sigma'_1)\psi^{j_i}(\mathbf{r}'_{b2}, \sigma'_2)\right]^0_0 \chi^{(+)}(\mathbf{r}'_{Aa}).
\end{aligned} \tag{107}$$

We expand the Green function and distorted waves in a basis of angular momentum eigenstates:

$$\chi^{(-)*}(\mathbf{k}_{Bb}, \mathbf{r}_{Bb}) = \sum_{\tilde{l}} \sqrt{2\tilde{l}+1} \frac{4\pi}{k_{Bb} r_{Bb}} i^{-\tilde{l}} e^{i\sigma^{\tilde{l}}_f} F_{\tilde{l}}(r_{Bb}) \left[Y^{\tilde{l}}(\hat{r}_{Bb}) Y^{\tilde{l}}(\hat{k}_{Bb})\right]^0_0, \tag{108}$$

$$\chi^{(+)}(\mathbf{r}'_{Aa}) = \sum_{l} i^l \sqrt{2l+1} \frac{4\pi}{k_{Aa} r'_{Aa}} e^{i\sigma^l_i} F_l(r'_{Aa}) \left[Y^l(\hat{r}'_{Aa}) Y^l(\hat{k}_{Aa})\right]^0_0, \tag{109}$$

where we have taken into account that $\hat{k}_{Aa} \equiv \hat{z}$. The Green function in the intermediate channel can be written as

$$G(\mathbf{r}_{Cc}, \mathbf{r}'_{Cc}) = i \sum_{l_c} \sqrt{2l_c + 1} \frac{f_{l_c}(k_{Cc}, r_<) P_{l_c}(k_{Cc}, r_>)}{k_{Cc} r_{Cc} r'_{Cc}} \left[Y^{l_c}(\hat{r}_{Cc}) Y^{l_c}(\hat{r}'_{Cc}) \right]^0_0 . \tag{110}$$

Finally

$$\begin{aligned}
T^{VV}_{2NT} = & \frac{4\mu_{Cc}(4\pi)^2 i}{\hbar^2 k_{Aa} k_{Bb} k_{Cc}} \sum_{l,l_c,\tilde{l}} e^{i(\sigma^l_i + \sigma^{\tilde{l}}_f)} i^{l-\tilde{l}} \sqrt{(2l+1)(2l_c+1)(2\tilde{l}+1)} \\
& \times \sum_{\substack{\sigma_1\sigma_2 \\ \sigma'_1\sigma'_2}} \int d^3r_{Cc} d^3r_{b1} d^3r_{A2} d^3r'_{Cc} d^3r'_{b1} d^3r'_{A2} v(r_{b1}) v(r'_{c2}) \left[Y^{\tilde{l}}(\hat{r}_{Bb}) Y^{\tilde{l}}(\hat{k}_{Bb}) \right]^0_0 \\
& \times \left[Y^l(\hat{r}'_{Aa}) Y^l(\hat{k}'_{Aa}) \right]^0_0 \left[Y^{l_c}(\hat{r}_{Cc}) Y^{l_c}(\hat{r}'_{Cc}) \right]^0_0 \frac{F_{\tilde{l}}(r_{Bb})}{r_{Bb}} \frac{F_l(r'_{Aa})}{r'_{Aa}} \\
& \times \frac{f_{l_c}(k_{Cc}, r_<) P_{l_c}(k_{Cc}, r_>)}{r_{Cc} r'_{Cc}} \left[\psi^{j_f}(\mathbf{r}_{A1}, \sigma_1) \psi^{j_f}(\mathbf{r}_{A2}, \sigma_2) \right]^{0*}_0 \\
& \times \left[\psi^{j_i}(\mathbf{r}'_{b1}, \sigma'_1) \psi^{j_i}(\mathbf{r}'_{b2}, \sigma'_2) \right]^0_0 \sum_{KM} \left[\psi^{j_f}(\mathbf{r}_{A2}, \sigma_2) \psi^{j_i}(\mathbf{r}_{b1}, \sigma_1) \right]^K_M \\
& \times \left[\psi^{j_f}(\mathbf{r}'_{A2}, \sigma'_2) \psi^{j_i}(\mathbf{r}'_{b1}, \sigma'_1) \right]^{K*}_M
\end{aligned} \tag{111}$$

Let us now perform the integration over $\mathbf{r}_{A2}$. If we do the approximation of considering $\mathbf{r}_{A1} \approx \mathbf{r}_{C1}$, $\mathbf{r}_{A1}$ becomes independent of $\mathbf{r}_{A2}$, so

$$\begin{aligned}
&\sum_{\sigma_1,\sigma_2}\int d\mathbf{r}_{A2}\left[\psi^{j_f}(\mathbf{r}_{A1},\sigma_1)\psi^{j_f}(\mathbf{r}_{A2},\sigma_2)\right]^{0*}_0\left[\psi^{j_f}(\mathbf{r}_{A2},\sigma_2)\psi^{j_i}(\mathbf{r}_{b1},\sigma_1)\right]^K_M\\
&\quad=\sum_{\sigma_1,\sigma_2}(-1)^{1/2-\sigma_1+1/2-\sigma_2}\int d\mathbf{r}_{A2}\left[\psi^{j_f}(\mathbf{r}_{A1},-\sigma_1)\psi^{j_f}(\mathbf{r}_{A2},-\sigma_2)\right]^{0}_0\left[\psi^{j_f}(\mathbf{r}_{A2},\sigma_2)\psi^{j_i}(\mathbf{r}_{b1},\sigma_1)\right]^K_M\\
&\quad=-\sum_{\sigma_1,\sigma_2}(-1)^{1/2-\sigma_1+1/2-\sigma_2}\int d\mathbf{r}_{A2}\left[\psi^{j_f}(\mathbf{r}_{A2},-\sigma_2)\psi^{j_f}(\mathbf{r}_{A1},-\sigma_1)\right]^{0}_0\left[\psi^{j_f}(\mathbf{r}_{A2},\sigma_2)\psi^{j_i}(\mathbf{r}_{b1},\sigma_1)\right]^K_M\\
&\quad=-((j_f\,j_f)_0(j_f\,j_i)_K|(j_f\,j_f)_0(j_f\,j_i)_K)_K\sum_{\sigma_1,\sigma_2}(-1)^{1/2-\sigma_1+1/2-\sigma_2}\\
&\quad\times\int d\mathbf{r}_{A2}\left[\psi^{j_f}(\mathbf{r}_{A2},-\sigma_2)\psi^{j_f}(\mathbf{r}_{A2},\sigma_2)\right]^{0}_0\left[\psi^{j_f}(\mathbf{r}_{A1},-\sigma_1)\psi^{j_i}(\mathbf{r}_{b1},\sigma_1)\right]^K_M\\
&\quad=\frac{1}{2j_f+1}\sqrt{2j_f+1}((l_f\tfrac{1}{2})_{j_f}(l_i\tfrac{1}{2})_{j_i}|(l_f l_i)_K(\tfrac{1}{2}\tfrac{1}{2})_0)_K\\
&\quad\times u_{l_f}(r_{A1})u_{l_i}(r_{b1})\left[Y^{l_f}(\hat{r}_{A1})Y^{l_i}(\hat{r}_{b1})\right]^K_M\sum_{\sigma_1}(-1)^{1/2-\sigma_1}\left[\chi^{1/2}(-\sigma_1)\chi^{1/2}(\sigma_1)\right]^0_0\\
&\quad=-\sqrt{\frac{2}{2j_f+1}}((l_f\tfrac{1}{2})_{j_f}(l_i\tfrac{1}{2})_{j_i}|(l_f l_i)_K(\tfrac{1}{2}\tfrac{1}{2})_0)_K\left[Y^{l_f}(\hat{r}_{A1})Y^{l_i}(\hat{r}_{b1})\right]^K_M u_{l_f}(r_{A1})u_{l_i}(r_{b1}),
\end{aligned}\tag{112}$$

where we have evaluated the $9j$ symbol

$$((j_f\,j_f)_0(j_f\,j_i)_K|(j_f\,j_f)_0(j_f\,j_i)_K)_K=\frac{1}{2j_f+1}. \tag{113}$$

We proceed in a similar way to evaluate the integral over $\mathbf{r}'_{b1}$, considering now $\mathbf{r}'_{b2} \approx \mathbf{r}'_{c2}$ so $\mathbf{r}'_{b2}$ becomes independent of $\mathbf{r}'_{b1}$:

$$\begin{aligned}
&\sum_{\sigma'_1,\sigma'_2} \int d\mathbf{r}'_{b1} \left[\psi^{j_i}(\mathbf{r}'_{b1},\sigma'_1)\psi^{j_i}(\mathbf{r}'_{b2},\sigma'_2)\right]^0_0 \left[\psi^{j_f}(\mathbf{r}'_{A2},\sigma'_2)\psi^{j_i}(\mathbf{r}'_{b1},\sigma'_1)\right]^{K*}_M \\
&\qquad = -(-1)^{K-M} \sum_{\sigma'_1,\sigma'_2} \int d\mathbf{r}'_{b1} \left[\psi^{j_f}(\mathbf{r}'_{A2},-\sigma'_2)\psi^{j_i}(\mathbf{r}'_{b1},-\sigma'_1)\right]^{K}_{-M} \\
&\qquad \times \left[\psi^{j_i}(\mathbf{r}'_{b2},\sigma'_2)\psi^{j_i}(\mathbf{r}'_{b1},\sigma'_1)\right]^0_0 (-1)^{1/2-\sigma'_1+1/2-\sigma'_2} \\
&\qquad = -(-1)^{K-M}((j_f\, j_i)_K(j_i\, j_i)_0|(j_f\, j_i)_K(j_i\, j_i)_0)_K(-\sqrt{2j_i+1}) \\
&\qquad \times ((l_f\tfrac{1}{2})_{j_f}(l_i\tfrac{1}{2})_{j_i}|(l_f\, l_i)_K(\tfrac{1}{2}\tfrac{1}{2})_0)_K(-\sqrt{2})u_{l_f}(r'_{A2})u_{l_i}(r'_{b2}) \left[Y^{l_f}(\hat{r}'_{A2})Y^{l_i}(\hat{r}'_{b2})\right]^K_{-M} \\
&\qquad = -\sqrt{\frac{2}{2j_i+1}}((l_f\tfrac{1}{2})_{j_f}(l_i\tfrac{1}{2})_{j_i}|(l_f\, l_i)_K(\tfrac{1}{2}\tfrac{1}{2})_0)_K \left[Y^{l_f}(\hat{r}'_{A2})Y^{l_i}(\hat{r}'_{b2})\right]^{K*}_M u_{l_f}(r'_{A2})u_{l_i}(r'_{b2}).
\end{aligned} \tag{114}$$

Putting all together

$$\begin{aligned}
T^{VV}_{2NT} =&\frac{4\mu_{Cc}(4\pi)^2 i}{\hbar^2 k_{Aa}k_{Bb}k_{Cc}} \frac{2}{\sqrt{(2j_i+1)(2j_f+1)}} \sum_{K,M}((l_f\tfrac{1}{2})_{j_f}(l_i\tfrac{1}{2})_{j_i}|(l_f\, l_i)_K(\tfrac{1}{2}\tfrac{1}{2})_0)^2_K \\
&\times \sum_{l_c,l,\tilde{l}} e^{i(\sigma^l_i+\sigma^{\tilde{l}}_f)} \sqrt{(2l_c+1)(2l+1)(2\tilde{l}+1)}\, i^{l-\tilde{l}} \\
&\times \int d^3r_{Cc}d^3r_{b1}d^3r'_{Cc}d^3r'_{A2}v(r_{b1})v(r'_{c2})u_{l_f}(r_{A1})u_{l_i}(r_{b1})u_{l_f}(r'_{A2})u_{l_i}(r'_{b2}) \\
&\times \left[Y^{l_f}(\hat{r}'_{A2})Y^{l_i}(\hat{r}'_{b2})\right]^{K*}_M \left[Y^{l_f}(\hat{r}_{A1})Y^{l_i}(\hat{r}_{b1})\right]^K_M \frac{F_l(r'_{Aa})F_{\tilde{l}}(r'_{Bb})\, f_{l_c}(k_{Cc},r_<)P_{l_c}(k_{Cc},r_>)}{r'_{Aa}r_{Bb}r_{Cc}r'_{Cc}} \\
&\times \left[Y^{\tilde{l}}(\hat{r}_{Bb})Y^{\tilde{l}}(\hat{k}_{Bb})\right]^0_0 \left[Y^{l}(\hat{r}'_{Aa})Y^{l}(\hat{k}_{Aa})\right]^0_0 \left[Y^{l_c}(\hat{r}_{Cc})Y^{l_c}(\hat{r}'_{Cc})\right]^0_0 .
\end{aligned} \tag{115}$$

We can write

$$\begin{aligned}
&\left[Y^{\tilde{l}}(\hat{r}_{Bb})Y^{\tilde{l}}(\hat{k}_{Bb})\right]^0_0 \left[Y^{l}(\hat{r}'_{Aa})Y^{l}(\hat{k}_{Aa})\right]^0_0 = \\
&\qquad ((l\, l)_0(\tilde{l}\,\tilde{l})_0|(l\,\tilde{l})_0(l\,\tilde{l})_0)_0 \left[Y^{\tilde{l}}(\hat{r}_{Bb})Y^{l}(\hat{r}'_{Aa})\right]^0_0 \left[Y^{\tilde{l}}(\hat{k}_{Bb})Y^{l}(\hat{k}_{Aa})\right]^0_0 \qquad (116) \\
&\qquad = \frac{\delta_{\tilde{l}\,l}}{2l+1} \left[Y^{l}(\hat{r}_{Bb})Y^{l}(\hat{r}'_{Aa})\right]^0_0 \left[Y^{l}(\hat{k}_{Bb})Y^{l}(\hat{k}_{Aa})\right]^0_0 .
\end{aligned}$$

Taking into account that

$$\left[Y^{l}(\hat{k}_{Bb})Y^{l}(\hat{k}_{Aa})\right]^0_0 = \frac{(-1)^l}{\sqrt{4\pi}} Y^l_0(\hat{k}_{Bb})i^l, \tag{117}$$

and

$$\begin{aligned}
&\left[Y^{l}(\hat{r}_{Bb})Y^{l}(\hat{r}'_{Aa})\right]^{0}_{0}\left[Y^{l_c}(\hat{r}_{Cc})Y^{l_c}(\hat{r}'_{Cc})\right]^{0}_{0} = \\
&\qquad ((l\,l)_0(l_c\,l_c)_0|(l\,l_c)_K(l\,l_c)_K)_0\left\{\left[Y^{l}(\hat{r}_{Bb})Y^{l_c}(\hat{r}_{Cc})\right]^{K}\left[Y^{l}(\hat{r}'_{Aa})Y^{l_c}(\hat{r}'_{Cc})\right]^{K}\right\}^{0}_{0} \\
&\qquad = \sqrt{\frac{2K+1}{(2l+1)(2l_c+1)}} \\
&\qquad \times \sum_{M'}\frac{(-1)^{K+M'}}{\sqrt{2K+1}}\left[Y^{l}(\hat{r}_{Bb})Y^{l_c}(\hat{r}_{Cc})\right]^{K}_{-M'}\left[Y^{l}(\hat{r}'_{Aa})Y^{l_c}(\hat{r}'_{Cc})\right]^{K}_{M'} \\
&\qquad = \sqrt{\frac{1}{(2l+1)(2l_c+1)}} \\
&\qquad \times \sum_{M'}\left[Y^{l}(\hat{r}_{Bb})Y^{l_c}(\hat{r}_{Cc})\right]^{K*}_{M'}\left[Y^{l}(\hat{r}'_{Aa})Y^{l_c}(\hat{r}'_{Cc})\right]^{K}_{M'}\,.
\end{aligned} \tag{118}$$

It is important to note that the integrals

$$\int d\hat{r}_{Cc}d\hat{r}_{b1}\left[Y^{l}(\hat{r}_{Bb})Y^{l_c}(\hat{r}_{Cc})\right]^{K*}_{M}\left[Y^{l_f}(\hat{r}_{A1})Y^{l_i}(\hat{r}_{b1})\right]^{K}_{M}, \tag{119}$$

and

$$\int d\hat{r}'_{Cc}d\hat{r}'_{A2}\left[Y^{l}(\hat{r}'_{Aa})Y^{l_c}(\hat{r}'_{Cc})\right]^{K}_{M}\left[Y^{l_f}(\hat{r}'_{A2})Y^{l_i}(\hat{r}'_{b2})\right]^{K*}_{M}, \tag{120}$$

over the angular variables do not depend on M. Let us see why with (119),

$$\begin{aligned}
&\left[Y^{l}(\hat{r}_{Bb})Y^{l_c}(\hat{r}_{Cc})\right]^{K*}_{M}\left[Y^{l_f}(\hat{r}_{A1})Y^{l_i}(\hat{r}_{b1})\right]^{K}_{M} = (-1)^{K-M}\left[Y^{l}(\hat{r}_{Bb})Y^{l_c}(\hat{r}_{Cc})\right]^{K}_{-M} \\
&\qquad \times\left[Y^{l_f}(\hat{r}_{A1})Y^{l_i}(\hat{r}_{b1})\right]^{K}_{M} = (-1)^{K-M}\sum_{J}\langle K\;K\;M\;-M|J\;0\rangle \\
&\qquad \times\left\{\left[Y^{l}(\hat{r}_{Bb})Y^{l_c}(\hat{r}_{Cc})\right]^{K}\left[Y^{l_f}(\hat{r}_{A1})Y^{l_i}(\hat{r}_{b1})\right]^{K}\right\}^{J}_{0}.
\end{aligned} \tag{121}$$

After integration, only the term

$$\begin{aligned}
&(-1)^{K-M}\langle K\;K\;M\;-M|0\;0\rangle\left\{\left[Y^{l}(\hat{r}_{Bb})Y^{l_c}(\hat{r}_{Cc})\right]^{K}\left[Y^{l_f}(\hat{r}_{A1})Y^{l_i}(\hat{r}_{b1})\right]^{K}\right\}^{0}_{0} = . \\
&\qquad \frac{1}{\sqrt{2K+1}}\left\{\left[Y^{l}(\hat{r}_{Bb})Y^{l_c}(\hat{r}_{Cc})\right]^{K}\left[Y^{l_f}(\hat{r}_{A1})Y^{l_i}(\hat{r}_{b1})\right]^{K}\right\}^{0}_{0}
\end{aligned} \tag{122}$$

corresponding to $J = 0$ survives, which is indeed independent of M. We can thus omit the sum over M and multiply by $(2K + 1)$, obtaining

$$\begin{aligned} T^{VV}_{2NT} =& \frac{64\mu_{Cc}(\pi)^{3/2} i}{\hbar^2 k_{Aa} k_{Bb} k_{Cc}} \frac{i^{-l}}{\sqrt{(2j_i + 1)(2j_f + 1)}} \\ & \times \sum_K (2K + 1)((l_f \tfrac{1}{2})_{j_f} (l_i \tfrac{1}{2})_{j_i} | (l_f l_i)_K (\tfrac{1}{2} \tfrac{1}{2})_0)^2_K \\ & \times \sum_{l_c, l} \frac{e^{i(\sigma^l_i + \sigma^l_f)}}{\sqrt{(2l + 1)}} Y^l_0(\hat{k}_{Bb}) S_{K,l,l_c}, \end{aligned} \tag{123}$$

with

$$\begin{aligned} S_{K,l,l_c} =& \int d^3 r_{Cc} d^3 r_{b1} v(r_{b1}) u_{l_f}(r_{A1}) u_{l_i}(r_{b1}) \frac{s_{K,l,l_c}(r_{Cc})}{r_{Cc}} \frac{F_l(r_{Bb})}{r_{Bb}} \\ & \times \left[Y^{l_f}(\hat{r}_{A1}) Y^{l_i}(\hat{r}_{b1}) \right]^K_M \left[Y^{l_c}(\hat{r}_{Cc}) Y^l(\hat{r}_{Bb}) \right]^{K*}_M , \end{aligned} \tag{124}$$

and

$$\begin{aligned} s_{K,l,l_c}(r_{Cc}) = & \int_{r_{Cc}\, fixed} d^3 r'_{Cc} d^3 r'_{A2} v(r'_{c2}) u_{l_f}(r'_{A2}) u_{l_i}(r'_{b2}) \frac{F_l(r'_{Aa})}{r'_{Aa}} \frac{f_{l_c}(k_{Cc}, r_<) P_{l_c}(k_{Cc}, r_>)}{r'_{Cc}} \\ & \times \left[Y^{l_f}(\hat{r}'_{A2}) Y^{l_i}(\hat{r}'_{b2}) \right]^{K*}_M \left[Y^{l_c}(\hat{r}'_{Cc}) Y^l(\hat{r}'_{Aa}) \right]^K_M . \end{aligned} \tag{125}$$

The integrand in (124) can easily seen to be independent of M, so we can sum over M and divide by $(2K + 1)$, to get the integrand

$$\begin{aligned} & \frac{1}{2K + 1} v(r_{b1}) u_{l_f}(r_{A1}) u_{l_i}(r_{b1}) \frac{s_{K,l,l_c}(r_{Cc})}{r_{Cc}} \frac{F_l(r_{Bb})}{r_{Bb}} \\ & \qquad \times \sum_M \left[Y^{l_f}(\hat{r}_{A1}) Y^{l_i}(\hat{r}_{b1}) \right]^K_M \left[Y^{l_c}(\hat{r}_{Cc}) Y^l(\hat{r}_{Bb}) \right]^{K*}_M . \end{aligned} \tag{126}$$

This integrand is rotationally invariant (it is proportional to a T^L_M spherical tensor with $L = 0$, $M = 0$), so we can just evaluate it in the “standard” configuration in which $\mathbf{r}_{Cc}$ is directed along the z–axis and multiply by $8\pi^2$ (see Fig. 20), obtaining the final expression for S_{K,l,l_c}:

$$\begin{aligned} S_{K,l,l_c} =& \frac{4\pi^{3/2} \sqrt{2l_c + 1}}{2K + 1} i^{-l_c} \\ & \times \int r^2_{Cc}\, dr_{Cc}\, r^2_{b1}\, dr_{b1}\, \sin\theta\, d\theta\, v(r_{b1}) u_{l_f}(r_{A1}) u_{l_i}(r_{b1}) \\ & \times \frac{s_{K,l,l_c}(r_{Cc})}{r_{Cc}} \frac{F_l(r_{Bb})}{r_{Bb}} \\ & \times \sum_M \langle l_c\ 0\ l\ M | K\ M \rangle \left[Y^{l_f}(\hat{r}_{A1}) Y^{l_i}(\theta + \pi, 0) \right]^K_M Y^{l*}_M(\hat{r}_{Bb}). \end{aligned} \tag{127}$$

Similarly, we have

$$\begin{aligned}
s_{K,l,l_c}(r_{Cc}) =& \frac{4\pi^{3/2}\sqrt{2l_c+1}}{2K+1} i^{l_c} \\
&\times \int r_{Cc}^{\prime 2}\, dr'_{Cc}\, r_{A2}^{\prime 2}\, dr'_{A2}\ \sin\theta'\, d\theta'\, v(r'_{c2}) u_{l_f}(r'_{A2}) u_{l_i}(r'_{b2}) \\
&\times \frac{F_l(r'_{Aa})}{r'_{Aa}} \frac{f_{l_c}(k_{Cc}, r_<) P_{l_c}(k_{Cc}, r_>)}{r'_{Cc}} \\
&\times \sum_M \langle l_c\ 0\ l\ M | K\ M\rangle \left[Y^{l_f}(\hat{r}'_{A2}) Y^{l_i}(\hat{r}'_{b2}) \right]_M^{K*} Y_M^l(\hat{r}'_{Aa}).
\end{aligned} \tag{128}$$

We obtain the final expression

$$\begin{aligned}
T_{2NT}^{VV} =& \frac{1024\mu_{Cc}\pi^{9/2} i}{\hbar^2 k_{Aa} k_{Bb} k_{Cc}} \frac{1}{\sqrt{(2j_i+1)(2j_f+1)}} \\
&\times \sum_K \frac{1}{2K+1} ((l_f \tfrac{1}{2})_{j_f} (l_i \tfrac{1}{2})_{j_i} | (l_f l_i)_K (\tfrac{1}{2} \tfrac{1}{2})_0)_K^2 \\
&\times \sum_{l_c, l} e^{i(\sigma_i^l + \sigma_f^l)} \frac{(2l_c+1)}{\sqrt{2l+1}} Y_0^l(\hat{k}_{Bb}) S_{K,l,l_c},
\end{aligned} \tag{129}$$

with

$$\begin{aligned}
S_{K,l,l_c} =& \int r_{Cc}^2\, dr_{Cc}\, r_{b1}^2\, dr_{b1}\ \sin\theta\, d\theta\, v(r_{b1}) u_{l_f}(r_{C1}) u_{l_i}(r_{b1}) \\
&\times \frac{s_{K,l,l_c}(r_{Cc})}{r_{Cc}} \frac{F_l(r_{Bb})}{r_{Bb}} \\
&\times \sum_M \langle l_c\ 0\ l\ M | K\ M\rangle \left[Y^{l_f}(\hat{r}_{C1}) Y^{l_i}(\theta+\pi, 0) \right]_M^K Y_M^{l*}(\hat{r}_{Bb}),
\end{aligned} \tag{130}$$

and

$$\begin{aligned}
s_{K,l,l_c}(r_{Cc}) =& \int r_{Cc}^{\prime 2}\, dr'_{Cc}\, r_{A2}^{\prime 2}\, dr'_{A2}\ \sin\theta'\, d\theta'\, v(r'_{c2}) u_{l_f}(r'_{A2}) u_{l_i}(r'_{c2}) \\
&\times \frac{F_l(r'_{Aa})}{r'_{Aa}} \frac{f_{l_c}(k_{Cc}, r_<) P_{l_c}(k_{Cc}, r_>)}{r'_{Cc}} \\
&\times \sum_M \langle l_c\ 0\ l\ M | K\ M\rangle \left[Y^{l_f}(\hat{r}'_{A2}) Y^{l_i}(\hat{r}'_{c2}) \right]_M^{K*} Y_M^l(\hat{r}'_{Aa}).
\end{aligned} \tag{131}$$

If we are dealing with light ion reactions with spin–orbit terms in the optical potentials, the amplitudes for different values of the total angular momentum j of the relative motion of the nuclei are combined in the same way as for the simultaneous amplitude.

B.1. Non–orthogonality term

We write the non–orthogonality contribution to the transition amplitude (see Bayman and Chen (1982)):

$$\begin{aligned} T^{NO}_{2NT} =& 2\sum_{\substack{\sigma_1\sigma_2\\ \sigma'_1\sigma'_2\\ KM}} \int d^3r_{Cc}d^3r_{b1}d^3r_{A2}d^3r'_{b1}d^3r'_{A2}\,\chi^{(-)*}(\mathbf{k}_{Bb},\mathbf{r}_{Bb}) \\ &\times\left[\psi^{j_f}(\mathbf{r}_{A1},\sigma_1)\psi^{j_f}(\mathbf{r}_{A2},\sigma_2)\right]^{0*}_{0} v(r_{b1})\left[\psi^{j_f}(\mathbf{r}_{A2},\sigma_2)\psi^{j_i}(\mathbf{r}_{b1},\sigma_1)\right]^{K}_{M} \\ &\times\left[\psi^{j_f}(\mathbf{r}'_{A2},\sigma'_2)\psi^{j_i}(\mathbf{r}'_{b1},\sigma'_1)\right]^{K*}_{M}\left[\psi^{j_i}(\mathbf{r}'_{b1},\sigma'_1)\psi^{j_i}(\mathbf{r}'_{b2},\sigma'_2)\right]^{0}_{0}\chi^{(+)}(\mathbf{r}'_{Aa}). \end{aligned} \tag{132}$$

This expression is equivalent to (107) if we make the replacement

$$\frac{2\mu_{Cc}}{\hbar^2}G(\mathbf{r}_{Cc},\mathbf{r}'_{Cc})v(r'_{c2}) \rightarrow \delta(\mathbf{r}_{Cc}-\mathbf{r}'_{Cc}). \tag{133}$$

Looking at the partial–wave expansions of $G(\mathbf{r}_{Cc},\mathbf{r}'_{Cc})$ and $\delta(\mathbf{r}_{Cc}-\mathbf{r}'_{Cc})$, we find that we can use the above expressions for the successive transfer with the replacement

$$i\frac{2\mu_{Cc}}{\hbar^2}\frac{f_{l_c}(k_{Cc},r_<)P_{l_c}(k_{Cc},r_>)}{k_{Cc}}v(r'_{c2}) \rightarrow \delta(r_{Cc}-r'_{Cc}). \tag{134}$$

We thus have

$$\begin{aligned} T^{NO}_{2NT} =& \frac{512\pi^{9/2}}{k_{Aa}k_{Bb}}\frac{1}{\sqrt{(2j_i+1)(2j_f+1)}} \\ &\times\sum_K((l_f\tfrac{1}{2})_{j_f}(l_i\tfrac{1}{2})_{j_i}|(l_f l_i)_K(\tfrac{1}{2}\tfrac{1}{2})_0)^2_K \\ &\times\sum_{l_c,l} e^{i(\sigma^l_i+\sigma^l_f)}\frac{(2l_c+1)}{\sqrt{2l+1}}Y^l_0(\hat{k}_{Bb})S_{K,l,l_c}, \end{aligned} \tag{135}$$

with

$$\begin{aligned} S_{K,l,l_c} =& \int r^2_{Cc}\,dr_{Cc}\,r^2_{b1}\,dr_{b1}\ \sin\theta\,d\theta\,v(r_{b1})u_{l_f}(r_{C1})u_{l_i}(r_{b1}) \\ &\times\frac{s_{K,l,l_c}(r_{Cc})}{r_{Cc}}\frac{F_l(r_{Bb})}{r_{Bb}} \\ &\times\sum_M\langle l_c\ 0\ l\ M|K\ M\rangle\left[Y^{l_f}(\hat{r}_{C1})Y^{l_i}(\theta+\pi,0)\right]^K_M Y^{l*}_M(\hat{r}_{Bb}), \end{aligned} \tag{136}$$

and

$$\begin{aligned} s_{K,l,l_c}(r_{Cc}) =& r_{Cc}\int dr'_{A2}\,r'^2_{A2}\ \sin\theta'\,d\theta'\,u_{l_f}(r'_{A2})u_{l_i}(r'_{c2})\frac{F_l(r'_{Aa})}{r'_{Aa}} \\ &\times\sum_M\langle l_c\ 0\ l\ M|K\ M\rangle\left[Y^{l_f}(\hat{r}'_{A2})Y^{l_i}(\hat{r}'_{c2})\right]^{K*}_M Y^l_M(\hat{r}'_{Aa}). \end{aligned} \tag{137}$$

B.2. Coordinates used in the calculation of successive transfer

In the standard configuration in which the integrals (130) and (131) are to be evaluated (see Fig. 20) , we have

$$\mathbf{r}_{Cc} = r_{Cc}\,\hat{\mathbf{z}}\,, \qquad \mathbf{r}_{b1} = r_{b1}(-\cos\theta\,\hat{\mathbf{z}} - \sin\theta\,\hat{\mathbf{x}}). \tag{138}$$

Now,

$$\begin{aligned}\mathbf{r}_{C1} &= \mathbf{r}_{Cc} + \mathbf{r}_{c1} = \mathbf{r}_{Cc} + \frac{m_b}{m_b+1}\mathbf{r}_{b1} \\ &= \left(r_{Cc} - \frac{m_b}{m_b+1} r_{b1}\cos\theta\right)\hat{\mathbf{z}} - \frac{m_b}{m_b+1} r_{b1}\sin\theta\hat{\mathbf{x}},\end{aligned} \tag{139}$$

and

$$\mathbf{r}_{Bb} = \mathbf{r}_{BC} + \mathbf{r}_{Cb} = -\frac{1}{m_B}\mathbf{r}_{C1} + \mathbf{r}_{Cb}. \tag{140}$$

But

$$\mathbf{r}_{Cb} = \mathbf{r}_{Cc} + \mathbf{r}_{cb} = \mathbf{r}_{Cc} - \frac{1}{m_b+1}\mathbf{r}_{b1}, \tag{141}$$

so, substituting in (140) we get

$$\mathbf{r}_{Bb} = \left(\frac{m_B-1}{m_B} r_{Cc} + \frac{m_b+m_B}{m_B(m_b+1)} r_{b1}\cos\theta\right)\hat{\mathbf{z}} + \frac{m_b+m_B}{m_B(m_b+1)} r_{b1}\sin\theta\hat{\mathbf{x}}. \tag{142}$$

The primed variables are arranged in a similar fashion,

$$\mathbf{r}'_{Cc} = r'_{Cc}\,\hat{\mathbf{z}}\,, \qquad \mathbf{r}'_{A2} = r'_{A2}(-\cos\theta'\,\hat{\mathbf{z}} - \sin\theta'\,\hat{\mathbf{x}}). \tag{143}$$

And we get

$$\mathbf{r}'_{c2} = \left(-r'_{Cc} - \frac{m_A}{m_A+1} r'_{A2}\cos\theta'\right)\hat{\mathbf{z}} - \frac{m_A}{m_A+1} r'_{A2}\sin\theta'\hat{\mathbf{x}}, \tag{144}$$

and

$$\mathbf{r}'_{Aa} = \left(\frac{m_a-1}{m_a} r'_{Cc} - \frac{m_A+m_a}{m_a(m_A+1)} r'_{A2}\cos\theta'\right)\hat{\mathbf{z}} - \frac{m_A+m_a}{m_a(m_A+1)} r'_{A2}\sin\theta'\hat{\mathbf{x}}. \tag{145}$$

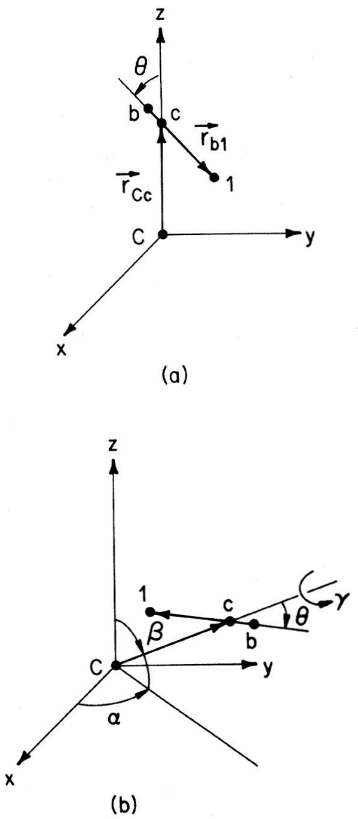

(a)

(b)

Figure 20: (a) “Standard” configuration, with $\mathbf{r}_{Cc}$ along the z–axis, $\mathbf{r}_{b1}$ in the $x - z$ plane and $(\mathbf{r}_{b1})_x < 0$. (b) The result of applying a rigid–body rotation (α, β, γ) to the configuration of (a) (from Bayman and Chen (1982)).

References

Anderson, P. W., 1958. Random–phase approximation in the theory of superconductivity. Physical Review Letters 112, 1900.

Anderson, P. W., 1959. Theory of dirty superconductors. Journal of Physics and Chemistry of Solids 11, 26.

Anderson, P. W., 1964. Superconductivity. Science 144, 373.

Anderson, P. W., 1969. Superconductivity in the past and in the future. In: Parks, R. (Ed.), Superconductivity. Vol. 2. Marcel Dekker, Inc., New York, p. 1343.

Anderson, P. W., 1972. More is different. Science 177, 393.

Anderson, P. W., 1984. Basic notions of condensed matter physics. Benjamin, Menlo Park, California.

Anderson, P. W., 1994. A career in theoretical physics. World Scientific, Singapore.

Aprahamian, A., Brenner, D., Casten, R., Gill, R., Piotrowski, A., 1987. First observation of a near harmonic vibrational nucleus. Physical Review Letters 59, 535.

Ascuitto, R. J., Glendenning, N. K., Sørensen, B., 1971. Confirmation of strong second order processes in (p, t) reactions on deformed nuclei. Physics Letters B 34, 17.

Bardeen, J., 1962. Tunneling into superconductors. Physical Review Letters 9, 147.

Bardeen, J., Cooper, L. N., Schrieffer, J. R., 1957a. Microscopic theory of superconductivity. Physical Review 106, 162.

Bardeen, J., Cooper, L. N., Schrieffer, J. R., 1957b. Theory of superconductivity. Physical Review 108, 1175.

Barranco, F., Bortignon, P., Broglia, R., Colò, G., Vigezzi, E., 2001. The halo of the exotic nucleus ^{11}Li: a single Cooper pair. European Physical Journal A 11, 385.

Barranco, F., Broglia, R. A., Colò, G., Gori, G., Vigezzi, E., Bortignon, P. F., 2004. Many-body effects in nuclear structure. European Physical Journal A 21, 57.

Bayman, B., 1960a. A derivation of the pairing-correlation method. Nuclear Physics 15, 33.

Bayman, B., 1960b. Seniority, Quasiparticles and Collective Vibrations, Lecture notes at the Palmer Physical Laboratory, Princeton University. Unpublished.

Bayman, B. F., 1971. Finite–range calculation of the two–neutron transfer reaction. Nuclear Physics A 168, 1.

Bayman, B. F., Chen, J., 1982. One-step and two-step contributions to two-nucleon transfer reactions. Physical Review C 26, 1509.

Belyaev, S. T., 1959. Kgl. Danske Videnskab. Selskab, Mat.-fys. Medd. 31, No11.

Bengtsson, R., Schuck, P., 1980. Semiclassical treatment of nuclear pairing properties. Physics Letters B 89, 321.

Bès, D., Broglia, R., 1977. In: Bohr, A., Broglia, R. (Eds.), International School of Physics “Enrico Fermi” Course LXIX, Elementary Modes of Excitation in Nuclei. North Holland, Amsterdam, p. 55.

Bès, D. R., 1963. Beta–vibrations in even nuclei. Nuclear Physics 49, 544 – 565.

Bès, D. R., Broglia, R. A., 1966. Pairing vibrations. Nuclear Physics 80, 289.

Bès, D. R., Broglia, R. A., 1979. Nuclear Field Theory treatment of the interacting Boson Model. In: Iachello, F. (Ed.), Procs. of the Workshop on interacting Bosons in Nuclear Physics. Plenum Press, New York, p. 151.

Bès, D. R., Sorensen, R. A., 1969. The pairing–plus–quadrupole model. Advances in Nuclear Physics 2, 129.

Bjerregaard, J. H., Hansen, O., Nathan, O., Chapman, R., Hinds, S., 1969. (t, p) reactions on ^{112,124}Sn and the pairing model. Nuclear Physics A 131, 481.

Bjerregaard, J. H., Hansen, O., Nathan, O., Chapman, R., Hinds, S., Middleton, R., 1967. The (t, p) reaction with the even isotopes of Ca. Nuclear Physics A 103, 33.

Bjerregaard, J. H., Hansen, O., Nathan, O., Hinds, S., 1966. The (t, p) reaction with the even isotopes of Sm. Nuclear Physics 86, 145.

Bjerregaard, J. H., Hansen, O., Nathan, O., Vistisen, L., Chapman, R., Hinds, S., 1968. The reactions ^{116,118}Sn$(t, p)^{118,120}$Sn. Nuclear Physics A 110, 1.

Bohr, A., 1964. In: Comptes Rendus du Congrès International de Physique Nucléaire. Vol. 1. Centre National de la Recherche Scientifique, p. 487.

Bohr, A., Mottelson, B. R., 1974. Some current themes in nuclear research. Physica Scripta 10 A, 13.

Bohr, A., Mottelson, B. R., 1975. Nuclear Structure, Vol.II. Benjamin, New York.

Bohr, A., Mottelson, B. R., Pines, D., 1958. Possible analogy between the excitation spectra of nuclei and those of the superconducting metallic state. Physical Review 110, 936.

Bortignon, P. F., Broglia, R. A., Bès, D. R., Liotta, R., 1977. Nuclear field theory. Physics Reports 30, 305.

Brink, D., Broglia, R. A., 2005. Nuclear Superfluidity. Cambridge University Press, Cambridge.

Broglia, R., January 1985. Pairing vibrations and sub–Coulomb fussion cross sections. In: Feldmeier, H. (Ed.), Procs. of the Int. Workshop on Gross Properties of Nuclei and Nuclear Excitations, Hirh egg, Austria. p. 221.

Broglia, R., Coló, G., Onida, G., Roman, H., 2004. Solid State Physics of Finite Systems: metal clusters, fullerenes, atomic wires. Springer Verlag, Berlin, Heidelberg.

Broglia, R., Dasso, C., Winther, A., 1981. Coherent surface excitation model of heavy–ion reactions. In: Bohr, A., Broglia, R. (Eds.), Proceedings of the International School of Physics “Enrico Fermi” Course LXXVII , Nuclear Structure and Heavy–Ion collisions. North Holland, Amsterdam, p. 327.

Broglia, R., Terasaki, J., Giovanardi, N., 2000. The Anderson–Goldstone–Nambu mode in finite and in infinite systems. Physics Reports 335, 1.

Broglia, R., Winther, A., 2004. Heavy Ion Reactions. Westview Press, Cambridge, MA.

Broglia, R. A., 1973. The pairing model. Annals of Physics 80, 60.

Broglia, R. A., 2002. From nuclei to proteins. La Rivista del Nuovo Cimento 25 (2), 1.

Broglia, R. A., 2005. From phase transitions in finite systems to protein folding and non–conventional drug design. La Rivista del Nuovo Cimento 28 (1), 1.

Broglia, R. A., 2009a. Learning to design resistance proof drugs from folding. European Physical Journal D 51, 137.

Broglia, R. A., 2009b. A remarkable emergent property of spontaneous (amino acid content) symmetry breaking. (to be published).

Broglia, R. A., Barranco, F., Coló, G., Vigezzi, E., Bortignon, P. F., Gori, G., Terasaki, J., 2002. Nuclear field theory description of the three-body system ^{11}Li. In: Norman, E., Schroeder, L., Wozniak, G., Smith, A. M. (Eds.), Proceedings of the Nuclear Physics Conference INPC 2001. Vol. 610. AIP, Berkeley. California (USA), p. 746.

Broglia, R. A., Clivio, A., Tiana, G., 2009. Foldless s.r.l. University of Milan and Rottapharm Madaus Pharmaceutical firm created to develop non–conventional (folding) inhibitors (operative since 7/05/2009).

Broglia, R. A., Dasso, C. H., Landowne, S., Nilsson, B. S., Winther, A., 1978. Multi-pair transfer reactions between superfluid heavy ions. Physics Letters B 73, 401.

Broglia, R. A., Dasso, C. H., Landowne, S., Winther, A., 1983. Possible effect of transfer reactions on heavy ion fusion at sub-barrier energies. Phys. Rev. C 27 (5), 2433.

Broglia, R. A., Hansen, O., Riedel, C., 1973. Two–neutron transfer reactions and the pairing model. Advances in Nuclear Physics 6, 287.

Broglia, R. A., Maqueda, E. E., 1966. Exact calculations in the d-s nuclear shell. Nuclear Physics 86 (2), 457.

Broglia, R. A., Riedel, C., Udagawa, T., 1972. Sum rules and two-particle units in the analysis of two-neutron transfer reactions. Nuclear Physics A 184, 23.

Charlton, L., 1976. Finite–range evaluation of $(p-d,d-t)$ with momentum space techniques. Physical Review C 14, 506.

Chatterjee, A., Navin, A., Shrivastava, A., Bhattacharyya, S., Rejmund, M., Keeley, N., Nanal, V., Nyberg, J., Pillay, R. G., Ramachandran, K., Stefan, I., Bazin, D., Beaumel, D., Blumenfeld, Y., de France, G., Gupta, D., Labiche, M., Lemasson, A., Lemmon, R., Raabe, R., Scarpaci, J. A., Simenel, C., Timis, C., 2008. 1n and 2n transfer with the borromean nucleus ^{6}He near the coulomb barrier. Physical Review Letters 101, 032701.

Cohen, M. H., Falicov, L. M., Phillips, J. C., 1962. Superconductive tunneling. Physical Review Letters 8, 316.

Dasso, C. H., Døssing, T., Landowne, S., Broglia, R. A., Winther, A., 1982. Exploring the surface of deformed nuclei with heavy ion reactions: Classical treatment. Nuclear Physics A 389, 191.

Dasso, C. H., Landowne, S., Broglia, R. A., Winther, A., 1984. Investigating the pairing phase transition in rapidly rotating deformed nuclei with heavy ion two-nucleon transfer reactions. Zeitschrift fr Physik A 317, 187.

Dasso, C. H., Landowne, S., Winther, A., 1983. A study of q-value effects on barrier penetration. Nuclear Physics A 407, 221.

Dietrich, K., Hara, K., 1973. On the semi-classical description of heavy-ion reactions. Nuclear Physics A 211, 349.

Dietrich, K., Hara, K., Weller, F., 1971. Multiple pair transfer in reactions between heavy nuclei. Physics Letters B 35, 201.

Dobaczewski, J., Nazarewicz, W., Werner, T. R., Berger, J. F., Chinn, C. R., Dechargé, J., 1996. Mean-field description of ground-state properties of drip-line nuclei: Pairing and continuum effects. Phys. Rev. C 53 (6), 2809.

Elliot, J. P., 1958a. Collective Motion in the Nuclear Shell Model. I. Classification Schemes for States of Mixed Configurations. Proceedings of the Royal Society of London A 245 (1240), 128.

Elliot, J. P., 1958b. Collective Motion in the Nuclear Shell Model. II. The Introduction of Intrinsic Wave–Functions. Proceedings of the Royal Society of London A 245 (1243), 562.

Elliot, J. P., 1962. *Escuela Latinoamericana de Fsica Mexico 1962*, Universidad de Mexico, lecture notes. unpublished.

Elliot, J. P., Harvey, M., 1963. Collective Motion in the Nuclear Shell Model. III. The Calculation of Spectra. Proceedings of the Royal Society of London A 272 (1351), 557.

Esaki, L., 1973. Long journey into tunneling. In: Norstedt, P., Söner (Eds.), Le Prix Nobel en 1973. p. 64.

Esbensen, H., Bertsch, G. F., Hencken, K., 1997. Application of contact interactions to Borromean halos. Phys. Rev. C 56, 3054.

Farine, M., Schuck, P., 1999. Surface properties of nuclear pairing with the gogny force in a simplified model. Physics Letters B 459, 444.

Farine, M., Schuck, P., 2002. Size dependence of pairing in finite fermi systems. In: Nazarewicz, W., Vretenar, D. (Eds.), The Nuclear Many–Body Problem. Kluwer, Amsterdam, p. 189.

Ferramosca, S., Lo Cicero, M., Laface, A., Sivianni, F., Cesana, E., Provasi, D., Tiana, G., Galli, M., Moroni, M., Clivio, A., Broglia, R., Rusconi, S., 2008. The non–conventional (folding) protease inhibitor blocks the human immudeficiency virus type–1 replication without evidence of resistence during in vitro passage. ANTIVIRAL TEHRAPY 13, A34.

Fleming, D. G., Blann, M., Fulbright, H. W., Robbins, J. A., 1970. (p,t) reactions on the even tin isotopes. Nuclear Physics A 157, 1.

Flynn, E. R., Beery, J. G., Blair, A. G., 1970. The ^{122,124}Sn$(t,p)^{124,126}$Sn reaction at 20 MeV. Nuclear Physics A 154, 225.

Giaver, I., 1973. Electron tunneling and superconductivity. In: Norstedt, P., Söner (Eds.), Le Prix Nobel en 1973. p. 84.

Glendenning, N. K., 1963. Nuclear stripping reactions. Annual Review of Nuclear Science 13, 191.

Glendenning, N. K., 1965. Nuclear Spectroscopy with Two–Nucleon Transfer Reactions. Phys. Rev., B102.

Glendenning, N. K., 1968. Tables of structure Amplitudes for (p,t) Reaction. Lawrence Radiation Laboratory Report.

Goldstone, J., 1961. Field theories with “superconductor” solutions. Nuovo Cimento 19, 155.

Golovkov, M., Grigorenko, L., Ter-Akopian, G., Fomichev, A., Oganessian, Y., Gorshkov, V., Krupko, S., Rodin, A., Sidorchuk, S., Slepnev, R., Stepantsov, S., Wolski, R., Pang, D., Chudoba, V., Korsheninnikov, A., Kuzmin, E., Nikolskii, E., Novatskii, B., Stepanov, D., Roussel-Chomaz, P., Mittig, W., Ninane, A., Hanappe, F., Stuttge, L., Yukhimchuk, A., Perevozchikov, V., Vinogradov, Y., Grishechkin, S., Zlatoustovskiy, S., 2008. The ^{8}He and ^{10}He spectra studied in the (t,p) reaction. arXiv:0804.0310 [nucl-ex].

Gori, G., Barranco, F., Vigezzi, E., Broglia, R. A., 2004. Parity inversion and breakdown of shell closure in Be isotopes. Phys. Rev. C 69, 041302.

Guazzoni, P., Zetta, L., Covello, A., Gargano, A., Bayman, B. F., Graw, G., Hertenberger, R., Wirth, H.-F., Jaskola, M., 2006. Spectroscopy of ^{110}Sn via the high-resolution ^{112}Sn$(p,t)\,^{110}$Sn reaction. Physical Review C 74, 054605.

Gunnarsson, O., 1997. Superconductivity in fullerides. Review of Modern Physics 69, 575.

Gunnarsson, O., 2004. Alkali-doped Fullerides: Narrow-band Solids with Unusual Properties. World Scientific, Singapore.

Hansen, P., Tostevin, J., 2003. Direct reactions with exotic nuclei. Annual Review of Nuclear and Particle Science 53, 219.

Hashimoto, N., Kawai, M., 1978. The (p, d) (d, t) process in strong (p, t) reactions. Progress of Theoretical Physics 59, 1245.

Heyde, K., 1998. From Nucleons to the Atomic Nucleus. Springer, Heidelberg.

Iachello, F., Arima, A., 1988. The Interacting Boson Model. University Press, Cambridge.

Igarashi, M., Kubo, K., Yagi, K., 1991. Two–nucleon transfer mechanisms. Physics Reports 199, 1.

Jacobs, P. M., Smilansky, U., 1983. Comments on the description of sub-barrier fusion in terms of dissipative tunneling. Physics Letters B 127, 313.

Josephson, B., 1969. Weakly coupled superconductors. In: Parks, R. (Ed.), Superconductivity. Vol. 1. Marcel Dekker, Inc., New York, p. 423.

Josephson, B., 1973. The discovery of tunneling supercurrents. In: Norstedt, P., Söner (Eds.), Le Prix Nobel en 1973. p. 104.

Josephson, B. D., 1962. Possible new effects in superconductive tunnelling. Physics Letters 1, 251.

Keeley, N., Skaza, F., Lapoux, V., Alamanos, N., Auger, F., Beaumel, D., Becheva, E., Blumenfeld, Y., Delaunay, F., Drouart, A., Gillibert, A., Giot, L., Kemper, K., Nalpas, L., Pakou, A., Pollacco, E., Raabe, R., Roussel-Chomaz, P., Rusek, K., Scarpaci, J.-A., Sida, J.-L., Stepantsov, S., Wolski, R., 2007. Probing the ^{8}He ground state via the $^{8}\mathrm{He}(p, t)^{6}\mathrm{He}$ reaction. Physics Letters B 646, 222.

Khan, E., Sandulescu, N., Giai, N. V., Grasso, M., 2004. Two-neutron transfer in nuclei close to the drip line. Physical Review C 69, 014314.

Kisslinger, L. S., Sorensen, R. A., 1963. Spherical nuclei with simple residual forces. Review of Modern Physics 35, 853.

Klimt, S., Lutz, M., Vogl, U., Weise, W., 1990. Generalized SU(3) Nambu–Jona–Lasinio model: (I). Mesonic modes. Nuclear Physics A 516, 429.

Kucharek, H., Ring, P., Schuk, P., Bengtsson, R., Girod, M., 1989. Pairing properties of nuclear matter from the gogny force. Physics Letters B 216, 249.

Laughlin, R., 2006. A different Universe. Basic Books, Cambridge, MA.

Lauritzen, B., Anselmino, A., Bortignon, P. F., Broglia, R. A., 1993. Pairing phase transition in small particles. Annals of Physics 223, 216.

Lenske, H., Schrieder, G., 1998. Probing the structure of exotic nuclei by transfer reactions. The European Physical Journal A 2, 41.

Lo Cicero, M., Laface, A., S., F., Sivianni, F., Cesana, E., Provasi, D., Tiana, G., Galli, M., Moroni, M., Clivio, A., Broglia, R., Rusconi, S., 2007. In vitro activity of a non–conventional (folding) inhibitor on human immunodeficiency virus type–1 replication. ANTIVIRAL TEHRAPY 12, S19.

Lotti, P., Vitturi, A., Broglia, R. A., Sørensen, J. H., Winther, A., 1991. Collective description of two-nucleon transfer reactions in heavy-ion collisions. Nuclear Physics A 524, 95.

Maglione, E., Pollarolo, G., Vitturi, A., Broglia, R. A., Winther, A., 1985. Absolute cross sections of two–nucleon transfer reactions induced by heavy ions. Physics Letters B 162, 59.

Mc Millan, W., Rowell, J., 1969. Tunneling and strong–coupling superconductivity. In: Parks, R. (Ed.), Superconductivity. Vol. 1. Marcel Dekker, Inc., New York, p. 561.

Nambu, Y., 1960. Quasi–particles and gauge invariance in the theory of superconductivity. Physical Review 117, 648.

Nambu, Y., 1991. Dynamical symmetry breaking. In: Eguchi, T., Nishigama, K. (Eds.), Broken Symmetry, Selected papers of Y. Nambu (1995). World Scientific, Singapore, p. 436.

Nambu, Y., Jona-Lasinio, G., 1961. Dynamical model of elementary particles based on an analogy with superconductivity. i. Phys. Rev. 122, 345.

Navin, A., Anthony, D. W., Aumann, T., Baumann, T., Bazin, D., Blumenfeld, Y., Brown, B. A., Glasmacher, T., Hansen, P. G., Ibbotson, R. W., Lofy, P. A., Maddalena, V., Miller, K., Nakamura, T., Pritychenko, B. V., Sherrill, B. M., Spears, E., Steiner, M., Tostevin, J. A., Yurkon, J., Wagner, A., 2000. Direct

Evidence for the Breakdown of the $N = 8$ Shell Closure in ^{12}Be. Phys. Rev. Lett. 85, 266.

Nikam, R. S., Ring, P., 1987. Manifestation of the berry phase in diabolic pair transfer in rotating nuclei. Phys. Rev. Lett. 58, 980.

Nikam, R. S., Ring, P., Canto, L. F., 1986. Diabolic pair transfer and oscillating behavior of backbending in rotating nuclei. Zeitschrift fr Physik A 324, 241.

Nikam, R. S., Ring, P., Canto, L. F., 1987. A nuclear squid: Diabolic pair transfer in rotating nuclei. Physics Letters B 185, 269.

Nolan, P. J., Twin, P. J., 1988. Superdeformed shapes at high angular momentum. Annual Review of Nuclear and Particle Science 38, 533.

Perenboom, J. A. A. J., Wyder, P., Meier, F., 1981. Electronic properties of small metallic particles. Physics Reports 78, 173.

Pethick, C., Smith, H., 2008. Bose–Einstein Condensation in Dilute Gases. Cambridge University Press, Cambridge.

Ramanathan, S., Shakhnovich, E., 1994. Statistical mechanics of proteins with ‘‘evolutionary selected’’ sequences. Phys. Rev. E 50, 1303.

Richter, A., 1993. Trends in nuclear physics. Nuclear Physics A 553, 417c.

Ring, P., Schuck, P., 1980. The Nuclear Many–Body Problem. Springer, Berlin.

Rowe, D. J., 1970. Nuclear Collective Motion. Models and Theory. Methuen & Co., London.

Sagawa, H., Brown, B., Esbensen, H., 1993. Parity inversion in the N=7 isotones and the pairing blocking effect. Physics Letters B 309, 1.

Scalapino, D., 1969. The electron–phonon interaction and strong coupling superconductors. In: Parks, R. (Ed.), Superconductivity. Vol. 1. Marcel Dekker, Inc., New York, p. 449.

Shakhnovich, E. I., Gutin, A. M., 1993. Engineering of stable and fast–folding sequences of model proteins. PNAS 90, 7195.

Soloviev, V. G., 1965. Quasi–particle and collective structure of the states of even, strongly-deformed nuclei. Nuclear Physics 69 (1), 1.

Stephens, F. S., Simon, R. S., 1972. Coriolis effects in the yrast states. Nuclear Physics A 183, 257.

Takemasa, T., Tamura, T., Udagawa, T., 1979. Exact finite range calculations of light–ion induced two–neutron transfer reactions. Nuclear Physics A 321, 269.

Tang, Y. C., Herndon, R. C., 1965. Form factors of ^{3}H and ^{4}He with repulsive–core potentials. Physics Letters 18, 42.

Tanihata, I., Alcorta, M., Bandyopadhyay, D., Bieri, R., Buchmann, L., Davids, B., Galinski, N., Howell, D., Mills, W., Mythili, S., Openshaw, R., Padilla-Rodal, E., Ruprecht, G., Sheffer, G., Shotter, A. C., Trinczek, M., Walden, P., Savajols, H., Roger, T., Caamano, M., Mittig, W., Roussel-Chomaz, P., Kanungo, R., Gallant, A., Notani, M., Savard, G., Thompson, I. J., 2008. Measurement of the two-halo neutron transfer reaction ^{1}H(^{11}Li,^{9}Li)^{3}H at 3A MeV. Physical Review Letters 100, 192502.

Tostevin, J., 2007. Nuclear reactions used to probe the structure of nuclei far from stability. Acta Physica Polonica B 38, 1195.

Tostevin, J. A., Podolyák, G. Brown, B. A., Hansen, P. G., 2004. Correlated two-nucleon stripping reactions. Physical Review C 70, 064602.

Vigezzi, E., Bes, D. R., Broglia, R. A., Frauendorf, S., 1988. Semiclassical description of the pairing force matrix elements at finite rotational frequencies. Phys. Rev. C 38, 1448.

Vinh Mau, N., 1995. Particle-vibration coupling in one neutron halo nuclei. Nuclear Physics A 592, 33.

Vogl, U., Lutz, M., Klimt, S., Weise, W., 1990. Generalized SU(3) Nambu-Jona-Lasinio model: (II). From current to constituent quarks. Nuclear Physics A 516, 469.

Vogl, U., Weise, W., 1991. The Nambu and Jona–Lasinio model: Its implications for Hadrons and Nuclei. Progress in Particle and Nuclear Physics 27, 195.

von Oertzen, W., Vitturi, A., 2001. Pairing correlations of nucleons and multi–nucleon transfer between heavy nuclei. Reports on Progress in Physics 64, 1247.

Wapstra, A., Gove, N., 1971. Nuclear Data Table 9, 265.

Weil, A., 1966. Sur la Science. Gallimard, Paris.

Weil, A., 1999. Oeuvres. Gallimard, Paris.

Weinberg, S., 1996. The Quantum Theory of Fields. Vol. 2. Cambridge University Press, Cambridge.

Weise, W., 1994. Chiral dynamics and hadrons in dense matter. In: Broglia, R. A., Kienle, P., Bortignon, P. F. (Eds.), Procs. International School of Heavy Ion Physics, 3rd Course. World Scientific, Singapore, p. 436.

Wu, C. Y., Oertzen, W. V., Cline, D., Guidry, M. W., 1990. Pairing correlations and two-nucleon transfer between heavy nuclei. Annual Review of Nuclear and Particle Science 40, 285.

Yoshida, S., 1962. Note on the two-nucleon stripping reaction. Nuclear Physics 33, 685.